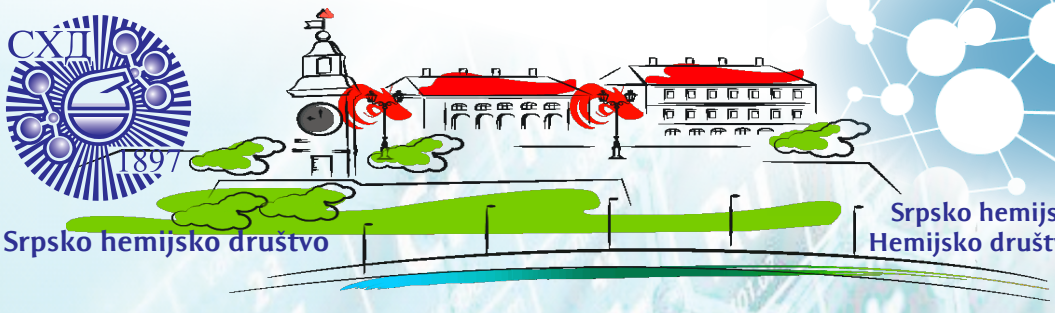

Srpsko hemijsko društvo

Srpsko hemijsko društvo
Hemijsko društvo Vojvodine

55. savetovanje Srpskog hemijskog društva

KNJIGA RADOVA

55th Meeting of the Serbian Chemical Society

PROCEEDINGS

Novi Sad 8. i 9. juni 2018.
Novi Sad, Serbia, June 8-9, 2018

ISBN 978-86-7132-070-2

Srpsko hemijsko društvo

Serbian Chemical Society

Srpsko hemijsko društvo
Hemijsko društvo Vojvodine

Serbian Chemical Society
Chemical Society of Vojvodina

55. SAVETOVANJE SRPSKOG HEMIJSKOG DRUŠTVA

KNJIGA RADOVA

55th MEETING OF THE SERBIAN CHEMICAL SOCIETY

Proceedings

Novi Sad 8. i 9. juni 2018.

Novi Sad, Serbia, June 8-9, 2018

55. SAVETOVANJE SRPSKOG HEMIJSKOG DRUŠTVA
Novi Sad, 8 i 9. juni 2018.
KNJIGA RADOVA

55th MEETING OF THE SERBIAN CHEMICAL SOCIETY
Novi Sad, Serbia, June 8-9 , 2018
PROCEEDINGS

***Izdaje** / Published by*
***Srpsko hemijsko društvo** / Serbian Chemical Society*
Karnegijeva 4/III, 11000 Beograd, Srbija
tel./fax: +381 11 3370 467; www.shd.org.rs, E-mail: Office@shd.org.rs

***Za izdavača** / For Publisher*
***Vesna Mišković STANKOVIĆ**, predsednik Društva*

***Urednici** / Editors*
Janoš ČANADI
Sanja Panić
Aleksandar DEKANSKI

Dizajn korica, slog i kompjuterska obrada teksta
Cover Design, Page Making and Computer Layout
Aleksandar DEKANSKI

***OnLine publikacija** / OnLine publication*

*ISBN **978-86-7132-070-2***

Naučni Odbor
Scientific Committee

Prof. Dr. János Csanádi, predsednik/chair
Dr Biljana Abramović
Dr Goran Bošković
Dr Daniela Šojić Merkulov
Dr Suzana Jovanović-Šanta
Dr Vladimir Srdić
Dr Lidija Jevrić
Dr Branislav Šojić
Dr Vesna Despotović
Dr Vladislava Jovanović
Dr Mirjana Kostić
Dr Tamara Premović
Dr Dragica Trivić
Dr Marija Nikolić
Dr Maja Gruden-Pavlović

Organizacioni Odbor
Organising Committee

Dr. Sanja Panić, predsednik/chair
Dr Aleksandar Dekanski
Dr Daniela Šojić Merkulov
Kristian Pastor
Nina Finčur
Dr Zorica Stojanović
Dr Arpad Kiralj
Dr Tamara Ivetić
Dr Vesna Despotović
Dr Nemanja Banić
Marina Lazarević
Maria Uzelac

Savetovanje su podržali / *Supported by*

Ministarstvo prosvete, nauke i tehnološkog razvoja Republike Srbije
Ministry of Education, Science and Technological Development of Republic of Serbia

Покрајински секретаријат за високо образовање и научноистраживачку делатност АП Војводина
Provincial Secretariat for Higher Education and Scientific Research of Autonomous Province of Vojvodina

*Ova knjiga sadrži **19 radova***
(obima od najmanje četiri stranice)
pojedinih saopštenja prezentovanih na
55. savetovanju Srpskog hemijskog društva.

*This book contains **19 Proceedings***
of some of the contributions presented at
the 55th Meeting of the Serbian Chemical Society.

SADRŽAJ : : CONTENTS

Plenarna predavanja / Plenary Lectures **5**

Intensification of bulk crystal growth by magnetic fields: from lab-scale to commercial size equipment 6
Natasha Dropka, Christiane Frank-Rotsch, Frank M. Kiessling and Peter Rudolph
Intenziviranje rasta kristala iz rastopa pomoću magnetnih polja: od laboratorijskog nivoa do industrijskog postrojenja

Saopštenja / Contributions **12**

Analitička hemija / Analytical Chemistry **13**

HPLC određivanje herbicida u vodi nakon degradacije sa hlor-dioksidom 14
Igor D. Kodranov, Marija V. Pergal, Dragana M. Kuč, Dragan D. Manojlović
HPLC determination of herbicides in water after degradation by chlorine dioxide

Optimizacija postupka ekstrakcije polifenola iz pogače konzumnog suncokreta 19
Zorica Stojanović, Snežana Kravić, Nada Grahovac, Ranko Romanić, Ana Đurović, Nada Hladni, Ana Marjanović Jeromela
Optimization of extraction process of polyphenols from sunflower cake

Tečno-čvrsta ekstrakcija izabranih pesticida na bazi jonskih tečnosti za direktnu analizu zemljišta i sedimenata 24
Jelena S. Milićević, Aleksandra N. Dimitrijević, Nikola Zdolšek, Tatjana M. Trtić-Petrović
Liquid-solid extraction of the selected pesticides based on ionic liquids for direct analzsis of soil and sedimets samples 28

Fizička hemija / Physical Chemistry **30**

Influence of the low frequency 10-1000 Hz magnetic field on Saccharomyces cerevisiae respiration activity 31
Marija Lješević, Branka Lončarević, Itana Nuša Bubanja, Vladimir Beškoski, Gordana Gojgić-Cvijović, Zoran Velikić, Dragomir Stanisavljev
Uticaj niskofrekventnog magnetnog polja (10-1000 Hz) na respiracionu aktivnost ćelija kvasca Saccharomyces cerevisiae

Elektrohemija / Electrochemistry **36**

Elektrohemijsko ponašanje bakra u prisustvu macerata hmelja
Vesna J. Grekulović, Mirjana M. Rajčić Vujasinović, Aleksandra M. Mitovski, Zoran M. Stević
Electrochemical behaviour of copper in the presence of hops macerate

Hemijsko inženjerstvo / Chemical Engineering **42**

Experimental determination and modeling of the sunflower oil ozonization process 43
Maja Z. Milošević, Mirjana Lj. Kijevčanin, Ivona R. Radović, Jelena M. Vuksanović
Eksperimentalno određivanje i modelovanje procesa ozonizacije suncokretovog ulja

Modeling of mixture densities using PC-SAFT equation of state 47
Mirko Z. Stijepović, Nikola D. Grozdanić, Gorica R. Ivaniš, Mirjana. LJ. Kijevčanin
Modelovanje gustina binarnih smeša korišćenjem PC-SAFT jednačine stanja

Viscosity modeling of binary mixtures ethyl butyrate + n-alcohol..... 52
Divna M. Majstorović, Emila M. Živković, Jovan D. Jovanović, Mirjana Lj. Kijevčanin
Modelovanje viskoznosti binarnih smeša etilbutirat + n-alkohol

Tekstilno inženjerstvo / Textile Engineering **58**

The influence of the content of hemicelluloses on moisture sorption and effective relative dielectric permeability of alkali modified jute woven fabrics 59
Aleksandra Ivanovska, Mirjana Kostic, Dragana Cerovic, Koviljka Asanovic
Uticaj sadržaja hemiceluloza na sorpciju vlage i efektivnu relativnu dielektričnu propustljivost alkalno modifikovane tkanine od jute

Protein-repellent and antioxidative properties of bioactive coatings based on TEMPO oxidized cellulose nanofibrils and chitosan..... 66
Matea Korica, Lidija Fras Zemljič, Matej Bračič, Rupert Kargl, Mirjana Kostić
Protein-odbijajuća i antioksidativna svojstva bioaktivnih prevlaka na bazi TEMPO oksidisanih celuloznih nanofibrila i hitozana

Antibacterial activity of Cu-based nanoparticles synthesized on the cotton fabrics previously modified with succinic and citric acids..... 77
Darka Marković, Tim Nunney, Christopher Deeks, Željko Radovanović, Marija Radoičić, Maja Radetić
Antibakterijska aktivnost nanočestica na bazi Cu sintetisanih na pamučnim tkaninama prethodno modifikovanim ćilibarnom i limunskom kiselinom

The influence of 1,2,3,4-butantetracarboxylic acid on in situ synthesis of Cu_2O/CuO nanoparticles on the cotton fabric and its antibacterial activty..... 82
Darka Marković, Natalija Jocić, Tim Nunney, Christopher Deeks, Željko Radovanović, Zoran Šaponjić, Maja Radetić
Uticaj koncentracije 1,2,3,4-butantetrakarboksilne kiseline na *in situ* sintezu nanočestica Cu_2O/CuO na pamučnoj tkanini i njenu antibakterijsku aktivnost

Nauka o materijalima / Material Science **88**

Homogenization effect on microstructure Al-Mg-Si alloy containing low-melting point elements 89
Tamara Radetić, Bojan Gligorijević, Mirjana Filipović, Miljana Popović, Endre Romhanji
Effekat homogenizacije na mikrostrukturu Al-Mg-Si legure koja sadrži nisko-topive elemente

Hemija životne sredine / Environmental Chemistry **95**

Uticaj pH na vezivanje jona teških metala na površinu lignoceluloznih biosorbenata 96
Dragana Kukić, Marina Šćiban, Vesna Vasić, Jelena Prodanović
The influence of pH on the binding of heavy metal ions to the surface of lignocellulosic biosorbents

Simultaneous removal of selected pesticides from aqueos solutions by coconut shell activated carbon 102
Ksenija Kumrić, Marija Egerić, Radojka Vujasin, Đorđe Petrović, Aleksandar Devečerski, Ljiljana Matović
Istovremeno uklanjanje odabranih pesticida iz vode primenom ugljeničnog materijala dobijenog iz kokosove ljuske

Biohemija / Biochemistry **108**

Metaboličke promene tokom životnog ciklusa kukuruznog plamenca Ostrinia nubilalis (Hübner, 1796) – aktivnost citrat sintaze i laktat dehidrogenaze..... 109
Iva Uzelac, Miloš Avramov, Nikola Krivokuća, Snežana Gošić-Dondo, Filip Franeta, Elvira Vukašinović, Jelena Purać, Danijela Kojić, Željko D. Popović
Metabolic changes during the life cycle of the European corn borer Ostrinia nubilalis (Hübner, 1796) – the activity of citrate synthase and lactate dehydrogenase

Hemija i tehnologija makromolekula
Chemistry and Technology of Macromolecules **117**

Chitosan-based films for application in food industry 118
Marija Lučić Škorić, Melina Kalagasidis Krušić, Aleksandra Nešić, Sanja Šešlija, Gabriella Santagata, Mario Malinconico
Primena filmova na bazi hitozana u prehrambenoj industriji

Glucose-sensitive chitosan/PVA microbeads with the potential application for the controlled release of insulin 124
Marija Lučić Škorić, Nikola Pavlović, Antonije Mitrović, Melina Kalagasidis Krušić
Mikrogelovi hitozana i PVA osetljivi na glukozu sa potencijalnom primenom za kontrolisano otpuštanje insulina

Plenarna predavanja

Plenary Lectures

Intensification of bulk crystal growth by magnetic fields: from lab-scale to commercial size equipment

Natasha Dropka, Christiane Frank-Rotsch, Frank M. Kiessling and Peter Rudolph*
Leibniz Institute for Crystal Growth, Max Born Str.2, 12489 Berlin
**Crystal Technology Consulting (CTC), Helga Hahnemann Str. 57, 12529 Schönefeld*

Introduction

The rapidly rising computing power in the last decades opens up entirely new options for numerical simulations of crystal growth. Particularly bulk crystal growth with its large furnaces and grown crystals (*e.g.* multicrystalline (mc) silicon ingot weighting up to 1600kg, single crystalline silicon ingot of 300 mm diameter, few meters long), several simultaneously acting driving forces (*e.g.* buoyancy, rotational force, Lorentz force, surface tension, viscous force *etc.*), long transient processes (*e.g.* mc Si crystal growth lasts ca. 1 week) with numerous temporally changing process parameters (e.g. heating power, gas flow *etc.*), high operating temperatures (*e.g.* melting temperatures T_m(Si) = 1683 K, T_m(GaAs) = 1512 K, T_m(Ge) = 1211 K) and contamination restrictions can be hardly studied by costly plant trials. On lab scale setups, not all similarity numbers can be fulfilled. The real alternative for deeper insight into the complex transport phenomena taking place in bulk crystal growth and guidance/assistance in development of novel processes can be obtained only by CFD simulations.

In the bulk crystal growth, there is a strong need for a cost-effective technology that can improve the ingot quality and increase the yield. For a successful process, it is important *i.a.* to control the level of impurities and thermal stress in the crystal. The later is a challenging task bearing in mind that semiconductors are bad heat conductors (*e.g.* λ_s(GaAs)=0.071 W / (cm/K) at T_m) with high latent heat (*e.g.* $\Delta H_{l,s}$ (GaAs)=7.26·10^5 J/kg) on the solid/liquid interface which is difficult to remove. As a consequence, interface shape easily becomes concave causing thermal stress within a crystal and an occurrence of dislocations. The low critical shear stress (*e.g.* τ_c(GaAs)=0.587 MPa at 1472 K) induces high dislocation density under lower thermal stress and thus degrades the crystal quality.

One way to enhance the yield and improve the crystal quality is to perform process intensification by application of external fields (*e.g.* magnetic fields, vibration and ultrasound), by scale up and numbering up of the crucibles. Particularly non-steady traveling magnetic fields (TMFs) with their Lorentz forces (F_L) proved to be very useful for contactless melt stirring and interface shaping. Unfortunately, the conventional techniques based on TMF coils placed outside the furnace and supplied by ac, suffer from strong shielding effects and therefore high magnetic induction requirements. Moreover, magnitude, direction and distribution of Lorentz forces are firmly determined by heat requirements.

More efficient approach was proposed within the framework of KRIST*MAG*® project (2005-2008), where Leibniz Institute for Crystal Growth with several partners developed the first internal heater magnet module (HMM) for simultaneous generation of heat and magnetic field in the hot zone.

Up to now, KRIST*MAG*® concept has been successfully further developed and applied on 10 furnaces for the growth of various semiconductors: Si, Ge, GaAs, (Hg,Cd)Te *etc.,* by

various crystal growth techniques: directional solidification (DS), vertical gradient freeze (VGF), Czochralski (Cz), **liquid phase epitaxy (Fig. 1.)**, from lab scale up to the industrial size equipment[1-6] (Fig. 2.). It is guarded by 18 patents (*i.a.*[7-13]) and honored by two innovation prizes[14].
The overview of very encouraging 3D numerical results will be presented and the **strengths and the bottlenecks** of the KRIST*MAG*® technology will be discussed.

Results and discussions
The main idea of KRIST*MAG*® concept is to generate Lorentz forces in the melt with intensity, direction and spatial distribution as required. Such volume force can be used for contactless tailoring of the melt flow pattern and consequently temperature and concentration distributions with an aim to e.g. stir the melt, reduce the turbulences in the melt, flatten solid/liquid (s/l) interface, homogenize dopand distribution, remove impurities from the (s/l) interface etc. Such adjustable volume force is generated by specially shaped graphite heating coils that are simultaneously supplied with a combination of dc and out-of-phase ac. Both currents are generated heat, while ac generates stronger dynamic magnetic field than dc. Decoupling of thermal from magnetic fields and finally generation of customizable Lorentz force in the melt is possible by variation of ac/dc ratio, frequency and phase shift among the heating coils. Design of HMM, its position relative to the melt: top, bottom or side (Fig. 1.), the choice of electro-magnetic parameter: frequency, phase shift and ac magnitude depend on the application.

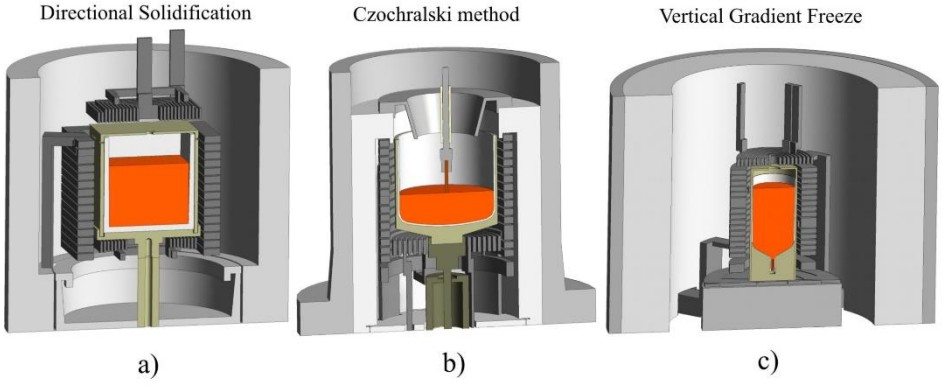

Fig.1. *Bulk crystal growth furnaces equipped with KRISTMAG® HMM for: a) directional solidification of Si, b) Czochralski growth of Si and c) Vertical Gradient Freeze growth of GaAs.*

Bearing in mind that Lorentz force magnitude is exponentially decreasing with a distance from the HMM coil, side HMM is more favorable for the interface flatting during the first VGF and DS growth phase[15-17], while top HMM is more efficient towards the end of the growth, particularly by the long ingots [13] (Fig. 3- and 4.).
Superposition of two opposite travelling TMFs with different frequency and therewith different penetration depths in the melt enables shifting of maximum of the Lorentz force magnitude away from the crucible wall towards the melt bulk (Fig. 5). This double-frequency TMF is beneficial for the melt stirring if a crucible coating needs protection[12,18] or contamination from the coating should be hampered[19].

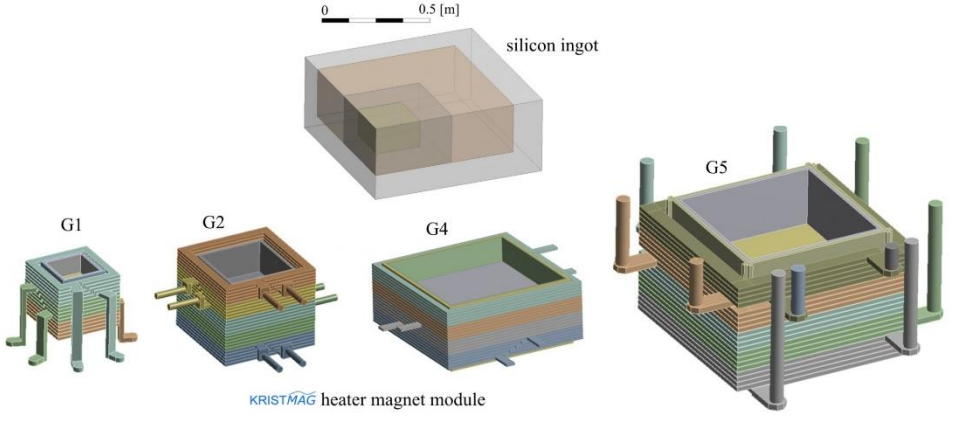

Fig. 2. *Si ingots and KRISTMAG® HMMs for directional solidification of Si from the lab scale G1 (14kg Si) up to the industrial scale G5 (640kg Si).*

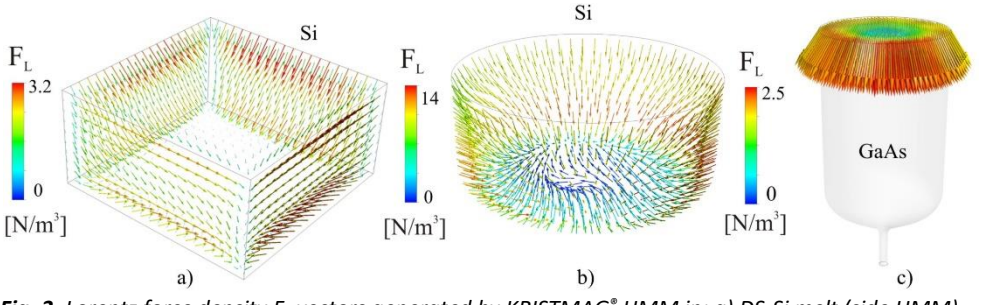

Fig. 3. *Lorentz force density F_L vectors generated by KRISTMAG® HMM in: a) DS-Si melt (side HMM), b) Cz-Si melt (side HMM), c) VGF-GaAs melt (top HMM).*

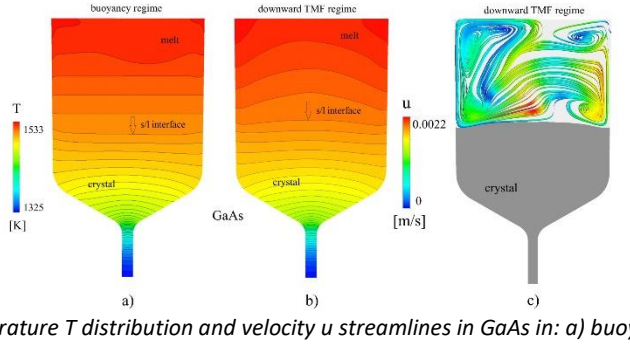

Fig. 4. *Temperature T distribution and velocity u streamlines in GaAs in: a) buoyancy regime with concave s/l interface and b,c) TMF driven flow with slightly convex s/l interface.*

Additionally, magnitude of ac current can be modulated in time that give rise to pulsing Lorentz forces, combining benefits of vibrations and magnetic fields[20].

Numbering up of crucibles imposed the severe requirements on the HMM design with respect to thermal and magnetic homogeneity among all melts/ingots[21]. An example of HMM design for 4 crucibles and corresponding T-fields in VGF-GaAs growth are shown in Fig. 6.

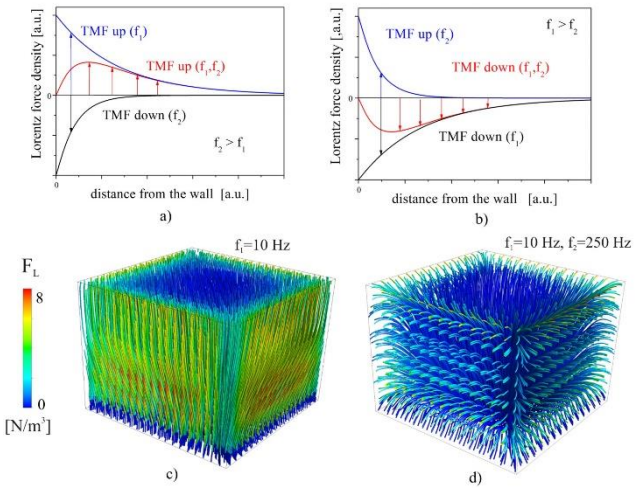

Fig. 5. *Lorentz force density F_L in Si melt exposed to single and double-frequency TMF: a,b) superposition concept; c,d) streamlines for downwards TMF.*

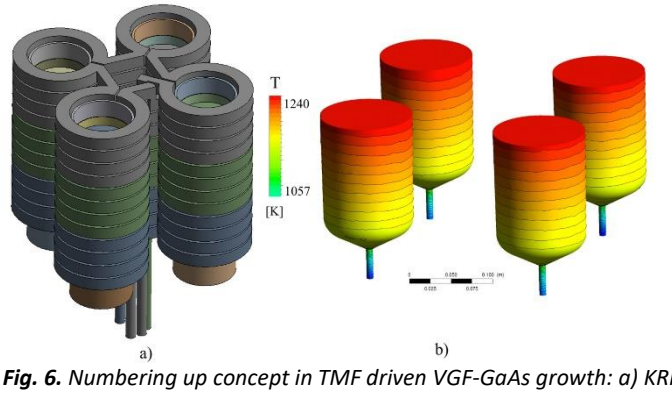

Fig. 6. *Numbering up concept in TMF driven VGF-GaAs growth: a) KRISTMAG® HMM for four crucibles, b) temperature T distribution in four GaAs ingots grown in HMM.*

Scale up of KRIST*MAG*® concept from the lab scale to the industrial size equipment was studied by 3D CFD simulations for DS-Si (Fig. 2.) and Cz-Si growths[22], using commercial software Ansys. Based on the similitude analyses, transfer of technology between different scales for cases where 2 or 3 driving forces exist (buoyancy, Lorentz and rotational force) is possible if Shielding number S and various ratios of dimensionless numbers Grashof Gr, Stephan Ste, Reynolds Re and magnetic forcing number F are kept constant.

Finally, it is important to mention that KRIST*MAG*® technology is not only applicable to the good electrical conducting melts, but also to the materials with low electrical conductivity (*e.g.* from to $1.7 \cdot 10^7$ S/m down to $5 \cdot 10^1$ S/m), as it was shown in Ge, Si, CdTe, BaF_2 and YAG growth[23]. For materials with low electrical conductivity, higher ac frequencies should be used for generation of TMF, in order to keep the required total electrical current in a range attractive for commercial applications.

Conclusion

Presented results pointed out the inevitable role of combined 3D CFD and electro-magnetic simulations for understanding and further optimization of bulk crystal growth processes. Favorable melt flow distributions for the faster bulk growth of upscaled high quality crystals can be reached using various TMFs generated inside the hot zone. The optimal TMF parameters and corresponding Lorentz force density distribution represents an intrinsic property of each set-up, *i.e.* its size, design and selected process parameters.

Acknowledgments: *Construction of furnaces by Peter Lange and proof reading the article by Karolina Giziewicz are gratefully acknowledged. The KRISTMAG® project was partially co-financed by the European Regional Developments Fund (EFRE), "Zukunftsfonds" Berlin and "Zukunftsagentur" of the State Brandenburg.*

Intenziviranje rasta kristala iz rastopa pomoću magnetnih polja: od laboratorijskog nivoa do industrijskog postrojenja

U oblasti proizvodnje kristala iz rastopa postoji kontinuirana potreba za razvojem efikasne tehnologije za poboljšanje prinosa i kvaliteta kristala. Za uspešan proces rasta, neophodno je kontrolisati nivo nečistoća i termalna naprezanja u kristalu. Jedan od mogućih pristupa je intenziviranje procesa rasta primenom magnetnih polja. U okviru KRISTMAG® projekta (2005-2008), Leibniz Institute for Crystal Growth sa nekoliko partnera razvio je prvi interni grejno-magnetni modul za simultanu proizvodnju toplote i putujućeg magnetnog polja u zoni rasta kristala. Do sada, ovaj koncept je praktično realizovan u 10 postrojenja za rast različitih kristala (npr. Si, Ge, GaAs, (Hg,Cd)Te), od laboratorijskog nivoa do postrojenja industrijske veličine. Tehnologija je zaštićena sa 18 patenata uz osvojene dve nagrade za inovaciju. Osnovna karakteristika KRISTMAG® koncepta je mogućnost generisanja Lorencovih sila u rastopu sa željenim intenzitetom, pravcem i prostornom raspodelom. Takve sile se mogu koristiti za npr. bezkontaktno mešanje i smanjenje turbulencija u rastopu, ravnanje kristalizacionog fronta, homogenizaciju raspodele primesa, odnošenje nečistoca sa kristalizacionog fronta itd. U ovom radu biće predstavljen pregled vrlo ohrabrujućih numeričkih rezultata uz diskusiju prednosti i ograničenja KRISTMAG® tehnologije.

References

1. P. Rudolph, J. Cryst. Growth **310** (2008)1298
2. Ch. Kudla, A.T. Blumenau, F.Büllesfeld; N. Dropka, Ch. Frank-Rotsch, F. Kiessling, O. Klein, P. Lange, W. Miller, U. Rehse, U. Sahr, M. Schellhorn, G. Weidemann, M. Ziem, G. Bethin, R. Fornari, M. Müller, J. Sprekels, V. Trautmann, P. Rudolph, J. Cryst. Growth **365** (2013) 54
3. F.-M. Kiessling, F. Büllesfeld, N. Dropka, Ch. Frank-Rotsch, M. Müller, P. Rudolph, J. Cryst. Growth **360** (2012) 81
4. Ch. Frank-Rotsch, P. Rudolph, J. Cryst. Growth **311**(2009) 2294
5. H. Bitterlich, Ch. Frank-Rotsch, W. Miller, U. Rehse, P. Rudolph, J. Cryst. Growth **318**(2011)1034
6. N. Dropka, W. Miller, R. Menzel, U. Rehse, J. Cryst. Growth 312 (2010) 1407
7. P. Rudolph and KRIST*MAG*®-Team from IKZ, WIAS, Steremat, Auteam, Markenanmeldung der Bezeichnung KRIST*MAG*®, AZ 307 27 628.7; European Application 09. 06. 2008 brand label protection.
8. R.-P. Lange, P. Rudolph, M. Ziem, Patent DE 10 2007 020 239 B4
9. N. Dropka, Ch. Frank-Rotsch, P. Rudolph, R.-P. Lange, U. Rehse, Patent DE 10 2010 041 061B4, PCT/EP2011/066332, WO2012/038432 A1

10. N. Dropka, Ch. Frank-Rotsch, M. Ziem, P. Lange, Patent DE 10 2012 204 313 B3
11. N. Dropka, P. Rudolph, U. Rehse, Patent DE 10 2010 028173B4
12. F. Büllesfeld, U. Sahr, W. Miller, P. Rudolph, U. Rehse, N. Dropka, Patent DE 10 2008 059 521 B4
13. N. Dropka, Ch. Frank-Rotsch, P. Lange, P. Krause, Patent DE 10 2013 211 769A1, WO2014/202284A1.
14. www.innovationspreis.de/preisträger-und-finalisten/preisträger/2008/leibniz-institut-fuer-kristallzuechtung-steremat-gmbh-auteam-gmbh.html
15. N. Dropka, Ch. Frank-Rotsch, W. Miller, P. Rudolph, J. Cryst. Growth **338** (2012) 208
16. N. Dropka, Ch. Frank-Rotsch, P. Rudolph, J. Cryst. Growth **365** (2013) 64
17. N. Dropka, Ch. Frank-Rotsch, J. Cryst. Growth **367** (2013) 1
18. N. Dropka, W. Miller, U. Rehse, P. Rudolph, F. Buellesfeld, U. Sahr, O. Klein, D. Reinhardt, J. Cryst. Growth **318** (2011) 275
19. N. Dropka, Ch. Frank-Rotsch, P. Rudolph, Cryst. Res. Technol. 47 (2012) 299
20. N. Dropka, Ch. Frank-Rotsch, J. Cryst. Growth **386** (2014) 146
21. N. Dropka, A. Glacki, Ch. Frank-Rotsch, Cryst. Growth Des. **14** (2014) 5122
22. N. Dropka, T. Ervik, M. Czupalla, F.M. Kiessling, J. Cryst. Growth **451**(2016) 95
23. N. Dropka, Ch. Frank-Rotsch, W. Miller, P. Rudolph, J. Cryst. Growth **338** (2012) 208

Saopštenja
Contributions

Analitička hemija

Analytical Chemistry

HPLC određivanje herbicida u vodi nakon degradacije sa hlor-dioksidom

Igor D. Kodranov, Marija V. Pergal*, Dragana M. Kuč, Dragan D. Manojlović
Univerzitet u Beogradu, Hemijski fakultet, Studentski trg 12-16, Beograd, Srbija
**Univerzitet u Beogradu, Institut za Hemiju, Tehnologiju i Metalurgiju, Njegoševa 12, Beograd, Srbija (E-mail: marijav@chem.bg.ac.rs)*

Uvod

Herbicidi su jedna od najviše korišćenih grupa pesticida, prvenstveno za tretiranje u agro- i hortikulturi.[1] Koriste se za suzbijanje korova u usevima. Korov smanjuje prinos, povećava cenu poljoprivredne proizvodnje i može smanjiti kvalitet useva.[2] Široko rasprostranjena upotreba herbicida, a i pesticida uopšte u poljoprivredne i nepoljoprivredne svrhe, rezultirala je i prisustvo njihovih ostataka u različitim ekološkim matriksima.[3] Zemljište biva kontaminirano usled korišćenja herbicida, koji su dobro rastvorni u vodi. Oni, kao i njihovi produkti degradacije, spiraju se i dospevaju u podzemne vode, čime ih zagađuju.[4,5] Herbicidi triazinske grupe koriste se za suzbijanje jednogodišnjih trava i širokolisnih korova u različitim zasadima tako što inhibiraju proces fotosinteze. Njihovo prisustvo u hrani se kontroliše, jer izazivaju kancer, defekte kod još nerođene dece i poremećaje u funkciji hormona.[6]

U cilju smanjenja štetnosti ostataka pesticida, primenjuju se različiti postupci za njihovu degradaciju i uklanjanje. Jedan od načina je pomoću hlor-dioksida (ClO_2).[7]

Hlor-dioksid je veoma moćno sredstvo za dezinfekciju i izuzetno selektivan oksidans (E_0 = 0,936 V), tako da može selektivno da oksiduje specifične funkcionalne grupe kao što su fenolne grupe i tercijarni amini.[8,9] Pogodan je za tretiranje jabuka, zelene salate i mlevenog mesa u cilju smanjenja mikrobiološke aktivnosti, za degradaciju nekih lekova, kao i za uklanjanje pesticida na svežem voću i povrću.[10,11] Koristi se kao dezinfekciono/oksidaciono sredstvo u tretmanu pijaće vode. U poređenju sa hlorom, ima jače antimikrobno dejstvo, dok u poređenju sa ozonom i hlorom ne daje toksične proizvode kao što su trihalogeno-metani, halogene kiseline i ketoni.[9,12,13] Mana hlor-dioksida ogleda se u tome što hlor-dioksid tokom tretiranja prelazi u hloritni i hloratni anjon, koji imaju negativne efekte na ljudsko zdravlje, jer dovode do promena na crvenim krvnim zrncima.[14]

Cilj ovog istraživanja bio je da se optimizuju uslovi za degradaciju herbicida triazinske grupe, kao što su atrazin, terbutilazin i prometrin, sa hlor-dioksidom u dejonizovanoj vodi i primena istih uslova na realni sistem (voda iz reke Save).

Eksperimentalni deo

Kao uzorci za ovo proučavanje korišćeni su herbicidi atrazin (ATR; 98,2 %; Sigma Aldrich), terbutilazin (TBA; 99,0 %; Sigma Aldrich) i prometrin (PRM; 97,7 %; Sigma Aldrich) (strukture prikazane na Slici 1). Hlor-dioksid napravljen je kao rastvor rastvaranjem natrijum-hlorita (Superior Water Disinfection Power, TwinOxide®) i natrijum-sulfata monohidrata ((Superior Water Disinfection Power, TwinOxide®) u 1 L vode HPLC čistoće (Ultra pure water, Thermofisher TKA MicroPure water purification system, 0,055 µS/cm). Ovakav rastvor hlor-dioksida standardizovan je pomoću standardnog rastvora natrijum-tiosulfata prema 4500-ClO2 DPD, Standard Method. Vrednost pH određivana je na instrumentu Orion Star A221, Thermo Scientific, pH/mV – metrom sa staklenom elektrodom. Za podešavanje pH-vrednosti korišćeni su sumporna kiselina (98 %, Sigma Aldrich) i natrijum-hidroksid (*p.a.*,

Sigma Aldrich). Kao eluenti za HPLC-DAD analizu korišćeni su acetonitril (>99,9 %, Sigma Aldrich) i 0,1 % rastvor mravlje kiseline (HPLC, Fluka analytical) u ultra – čistoj vodi. Uzorci su profiltrirani kroz filtere (Econofilter PTFE 25 mm 0,45 µm, Agilent Technologies).

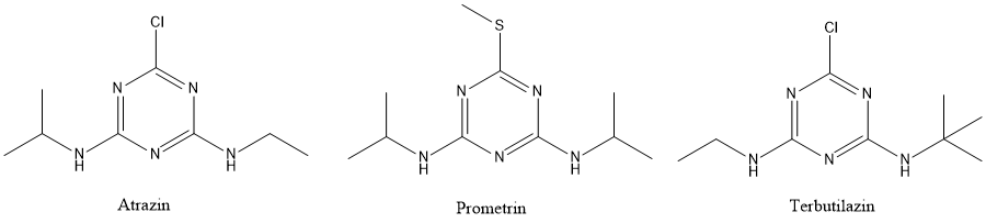

Slika 1. *Strukture odabranih herbicida iz grupe triazina*

Pre analize na HPLC-u, uzorci su rastvoreni u acetonitrilu tako da im koncentracija bude oko 1000 ppm (interni standard). Interni standard je zatim razblažen ultra – čistom vodom do željene koncentracije od 10 ppm. Ova koncentracija herbicida je bila ista u svim uzorcima koji su analizirani u ovom istraživanju. U rastvore herbicida dodat je hlor-dioksid kao degradaciono sredstvo. U jednu seriju uzoraka dodat je u koncentraciji od 5 ppm, dok je u drugu dodat u koncentraciji od 10 ppm. Reakcija je prekidana pomoću 0,1 M rastvora natrijum-tiosulfata (~0,3 mL $Na_2S_2O_3$ u 10 mL uzorka) nakon određenih vremenskih intervala: 30 min, 1 h, 2 h, 3 h, 6 h i 24 h. U cilju optimizacije uslova degradacije, reakcija je praćena u uslovima mraka i na svetlu, kao i pri različitim pH-vrednostima (3,00, 7,00 i 9,00).

Nakon izvršenih optimizacija uslova degradacija, uslovi najefikasnijih degradacija primenjeni su na realnom uzorku. Uzorkovana je voda iz reke Sava, u blizini vodozahvata JKP Beogradski vodovod i kanalizacija "Makiš". Voda je uzorkovana na 15 m od obale sa dubine od oko 1 m. U uzorak vode dodat je pesticid (jedna serija uzoraka sa herbicidom PRM, druga serija uzoraka TBA) u koncentraciji od 10 ppm i zatim su primenjeni uslovi pri kojima su postignute najefikasnije degradacije. Efikasnost degradacije u realnom uzorku ispitivana je takođe pomoću HPLC-DAD analize.

Na prethodno opisan način pripremljeni uzorci su profiltrirani i uspešnost degradacije je određivana na HPLC-DAD. Korišćen je hromatograf Thermo UltiMate 3000 sa DAD detektorom. Korišćena je kolona Hypersil Gold aQ (150 mm x 3 mm x 3µm). Eluiranje je bilo gradijentno: propuštena je smeša eluenata A i B, 0-0,5 min 5 % B, 0,5-6 min 5-45 % B, 6-8 min 45-95 % B, 8-9 min 95 % B, 9-9,01 min 95-5 % B, 9,01-14 min 5 % B, uz protok eluenata od 0,6 mL/min i pri temperaturi kolone od 40 °C. Kao eluent A korišćn je 0,1 % rastvor mravlje kiseline, a kao eluent B korišćen je acetonitril. Injektovano je 20 µL uzorka. Detektor je bio podešen na sledeće talasne dužine: 197 nm, 220 nm i 240 nm.

Efikasnost degradacije izračunata je prema sledećoj formuli:

$$\eta = \frac{P_0 - P_t}{P_0} 100$$

gde je η efikasnost degradacije, %; P_0 / mAU min^{-1} površina pika herbicida pre degradacije; Pt / mAU min^{-1} površina pika herbicida nakon degradacije.

Rezultati i diskusija

Procenat degradacije praćen je pomoću HPLC analize na osnovu smanjenja površine pika na osnovu jednačine 1), a najefikasnije degradacije prikazane su grafički na Slici 2.

Analiza uzorka ATR pokazala je da se ni u mraku ni na svetlu, za obe koncentracije dodatog hlor-dioksida, ne postižu zadovoljavajuće efikasnosti degradacije (mrak: 5 ppm ClO_2 1 h 5,43 %, 10 ppm ClO_2 1 h 10,20 %; svetlo: 5 ppm ClO_2 24 h 16,85 %, 10 ppm ClO_2 2 h 25,27 %). Na različitim pH-vrednostima dobra vrednost degradacije postiže se pri uslovima pH 3,00 za obe koncentracije hlor-dioksida (5 ppm ClO_2 6 h 46,32 %, 10 ppm ClO_2 6 h 47,24 % - najefikasnija degradacija), dok se pri uslovima pH 7,00 i 9,00 ne postižu zadovoljavajuće efikasnosti degradacija (pH 7,00: 5 ppm ClO_2 24 h 12,54 %, 10 ppm ClO_2 24 h 17,71 %; pH 9,00: 5 ppm ClO_2 24 h 11,22 %, 10 ppm ClO_2 24 h 18,25 %).
Analiza uzorka PRM pokazala je da se pri uslovima mraka, za obe koncentracije dodatog hlor-dioksida ne postižu zadovoljavajuće efikasnosti degradacija (5 ppm ClO_2 6 h 24,56 %, 10 ppm ClO_2 24 h 28,13 %). Pri svim ostalim uslovima (svetlo, pH 3,00, pH 7,00 i pH 9,00) za koncentracije 5 ppm hlor-dioksida postižu se dobre efikasnosti degradacija (svetlo 24 h 52,78 %, pH 3,00 24 h 46,77 %, pH 7,00 24 h 51,93 %, pH 9,00 24 h 46,79 %), dok se pri koncentraciji od 10 ppm postižu veoma dobre efikasnosti degradacija (svetlo 24 h 78,13 % - najefikasnija degradacija, pH 3,00 24 h 72,95 %, pH 7,00 24 h 51,93 %, pH 9,00 24 h 72,90 %).

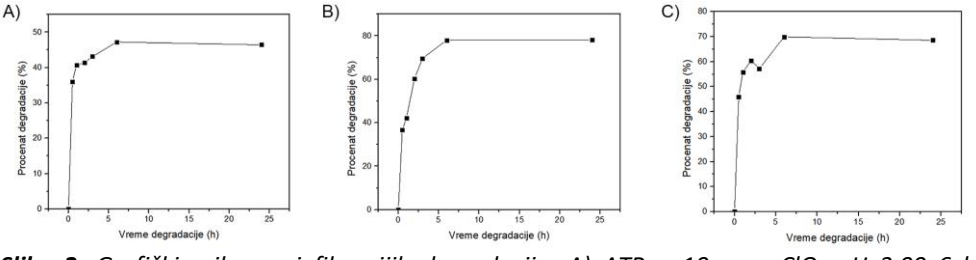

Slika 2. *Grafički prikaz najefikasnijih degradacija: A) ATR – 10 ppm ClO_2 pH 3,00 6 h; B) PRM – 10 ppm ClO_2 svetlo 24 h; C) TBA – 10 ppm ClO_2 pH 3,00 6 h*

Analiza uzorka TBA pokazala je da pri uslovima mraka ne dolazi gotovo ni do kakve degradacije za obe koncentracije hlor-dioksida (5 ppm ClO_2 6 h 1,32 %, 10 ppm ClO_2 1 h 0,80 %). Pri uslovima svetla, na pH 7,00 i pH 9,00 ne postižu se zadovoljavajuće efikasnosti degradacija za obe koncentracije dodatog hlor-dioksida (svetlo: 5 ppm ClO_2 24 h 13,11 %, 10 ppm ClO_2 6 h 23,36 %; pH 7.00: 5 ppm ClO_2 24 h 26,0 %, 10 ppm ClO_2 3 h 30,21 %; pH 9,00: 5 ppm ClO_2 3 h 23,52 %, 10 ppm ClO_2 2 h 36,15 %). Pri uslovima pH 3,00 sa 5 ppm hlor-dioksida postiže se dobra efikasnost degradacije nakon 24 h i iznosi 51,70 %, dok se sa 10 ppm hlor-dioksida postiže veoma dobra efikasnost degradacije nakon 6 h i iznosi 69,92 % - najefikasnija degradacija.
Analiza realnog uzorka sa herbicidom PRM pokazala je da se najefikasnija degradacija postiže nakon 24 h sa 10 ppm ClO_2 na svetlu i iznosi 74 %, dok sa herbicidom TBA najefikasnija degradacija postiže nakon 6 h na pH 3,00 sa 10 ppm ClO_2 i iznosi 4 %. Rezultati su pokazali da u vodi iz reke Save, koristeći hlor-dioksid koncentracije 10 ppm, postignuta je manja efikasnost u poređenju sa degradacijom u dejonizovanoj vodi usled prisustva organskih supstanci u rečnoj vodi.

Zaključak

Degradacija triazin grupe herbicida, ATR, PRM i TBA (10 ppm), proučavana je u dejonizovanoj vodi pri uslovima svetla i mraka, kao i na različitim pH-vrednostima (3,00,

7,00 i 9,00). Takođe, ispitana je i degradacija u realnom sistemu, savskoj vodi. Utvrđeno je da se degradacija sva tri herbicida dešava na svim pH-vrednostima i pri svim uslovima, izuzev uzorka TBA kod koga u mraku gotovo i da ne dolazi do degradacije. Najefikasija degradacija za uzorak ATR postiže se sa 10 ppm ClO_2 na pH 3,00 nakon 6 h i iznosi 47 %, za uzorak PRM sa 10 ppm ClO_2 na svetlu nakon 24 h i iznosi 78 % i za uzorak TBA sa 10 ppm ClO_2 na pH 3,00 nakon 6 h i iznosi 70 %. Analiza efikasnosti degradacije u realnom uzorku, savskoj vodi, pokazala je da se najefikasnija degradacija za uzorak PRM postiže sa 10 ppm ClO_2 na svetlu nakon 24 h i iznosi 74 %, a za uzorak TBA se postiže sa 10 ppm ClO_2 nakon 6 h na pH 3,00 i iznosi 4 %. Efikasnosti degradacije za oba uzorka su manje u realnom uzorku nego u dejonizovanoj vodi, jer se hlor-dioksid troši na oksidaciju organskih supstanci koje su prisutne u savskoj vodi.

Zahvalnica: *Ovaj rad je finansiran od strane Ministarstva prosvete, nauke i tehnološkog razvoja Republike Srbije. Zahvaljujemo se i TwinOxide RS d.o.o za dostupnost preparata* ***"TWINS".***

HPLC determination of herbicides in water after degradation by chlorine dioxide

The degradation of triazine herbicides (atrazine, terbuthylazine and prometrine) by chlorine dioxide was investigated in this paper. Optimization of degradation was first studied in deionized water and then in real water system (Sava river water). Optimization was performed under light and dark conditions, with different concentration of chlorine dioxide, at different periods of degradation and at different pH values of solutions. Degradation efficiency of herbicides was followed using HPLC with photodiode array detection (DAD). Percent of degradation and time of degradation were increased with increasing of chlorine dioxide concentration. The best degradation efficiency of prometrine with yield of 78 % was achieved by treatment with 10 ppm of chlorine dioxide, after 24 h of initial treatment under light condition. In the case of atrazine and terbuthylazine, the best efficiency of degradation yielded 47 and 58 % and was achieved by treatment with 10 ppm of chlorine dioxide, after 6 h of initial treatment and at pH of 3.00. Degradation of herbicides prometrine and terbuthylazine, in Sava river water, using concentration of chlorine dioxide of 10 ppm, had smaller efficiency in comparison with degradation in deionized water due to presence of organic substances in river water.

Literatura

1. J. Park, M. T. Brown, S. Depuydt, J. K. Kim, DS. Won, T. Han, *Environ. Pollut.* **220** (2017) 818.
2. G. W. A Milne, Handbook of pesticides, *CRC Press LLC, Florida* (1998).
3. K. Konstantinou, D. G. Hela, T. A. Albanis, *Environ. Pollut.* **141** (2006) 555.
4. M. Davezza, D. Fabbri, E. Pramauro, A. Bianco Prevot, *Chemosphere* **86** (2012) 335.
5. Z. Liu, X. Yan, M. Drikas, D. Zhou, D. Wang, M. Yang, J. Qu, *J. Environ. Sci.* **23** (2011) 381.
6. F. Tian, Z. Qiang, C. Liu, T. Zhang, B. Dong, *Chemosphere* **79** (2010) 646.
7. Y. Wang, H. Liu, G. Liu, Y. Xie, *Sci. Total Environ.* **473–474** (2014) 437.
8. M.Hörsing, T. Kosjek, H. R. Andersen, E. Heath, A. Ledin, *Chemosphere* **89** (2012) 129.
9. Q. Zhao, H. Lia, Y. Xu, F. Zhang, J. Zhao, L. Wang, J. Hou, H. Ding, Y. Li, H. Jin, L. Ding, *J. Chromatogr. A* **1376** (2015) 26.
10. Q. Chen, Y. Wang, F. Chen, Y. Zhang, X. Liao, *Food Control* **40** (2014) 106.

11. V. K. Sharma, *Chemosphere* **73** (2008) 1379.
12. L. Shi, N. Li, C. Wang, C. Wang, *J. Haz. Mat.* **178** (2010) 1137.
13. U. Raczyk-Stanisawiak, J. Swietlik, A. Dabrowska, J. Nawrocki, *Water Res.* **38** (2004) 1044.
14. S. Sorlini, F. Gialdini, M. Biasibetti, C. Collivignarelli, *Water Res.* **54** (2014) 44.

Optimizacija postupka ekstrakcije polifenola iz pogače konzumnog suncokreta

Zorica Stojanović, Snežana Kravić, Nada Grahovac*, Ranko Romanić, Ana Đurović, Nada Hladni*, Ana Marjanović Jeromela*
Univerzitet u Novom Sadu, Tehnološki fakultet Novi Sad, Bulevar cara Lazara 1, Novi Sad
**Institut za ratarstvo i povrtarstvo, Maksima Gorkog 30, Novi Sad*

Uvod

Seme suncokreta se odavnina koristi u ljudskoj ishrani i u današnje vreme predstavlja jednu od najviše gajenih uljanih kultura u svetu. Razlikuju se dva tipa suncokreta koji se gaje, uljani tip i konzumni tip. Uljani tip suncokreta se proizvodi za dobijanje jestivog biljnog ulja, dok se konzumni suncokret odlikuje manjim sadržajem ulja i visokim sadržajem proteina i drugih biološki aktivnih jedinjenja, i koristi se pretežno za ljudsku ishranu usled visoke hranljive vrednosti. U poslednje vreme, mogućnost proizvodnje ulja od konzumnog suncokreta je predmet interesovanja kako u naučnim krugovima, tako i u krugovima proizvođača i prerađivača. Ulja iz konzumnog suncokreta dobijaju se ceđenjem, tj. primenom mehaničkih presa i delovanjem sile na seme. Nerafinisano, hladno ceđeno ulje poseduje karakteristična senzorna svojstva i sadrži očuvane bioaktivne komponente koje potiču iz semena suncokreta. Usled odsustva rafinacije, ova ulja su specifična po svom izgledu, boji, mirisu i ukusu, hemijskom sastavu, nutritivnoj vrednosti i održivosti. Nakon mehaničkog izdvajanja ulja presovanjem semena zaostaje pogača koja praktično predstavlja otpad iz prehrambene industrije i najčešće se koristi za ishranu životinja. Pored visokog sadržaja proteina, pogača sadrži značajne količine biološki aktivnih jedinjenja,[1] te može predstavljati polaznu sirovinu za dobijanje ekstrakata koji sadrže visoko vredna jedinjenja i koji bi dalje mogli da se koriste za obogaćivanje prehrambenih proizvoda ili kao dodaci u farmaceutskim proizvodima.

Polifenoli, pored ostalih važnih jedinjenja, predstavljaju veoma značajnu grupu supstanci koje se nalaze u konzumnom suncokretu. Unošenje ove vrste jedinjenja hranom ima višestruke efekte na ljudsko zdravlje, prvenstveno povezanih sa njihovom izraženom antioksidativnom aktivnošću i sposobnosti eliminacije slobodnih radikala. Konzumacija hrane bogate antioksidantima smanjuje inflamaciju i nivo oksidativnog stresa kod čoveka.[2,3] Takođe oni pozitivno utiču na celokupan kardiovaskularni sistem i proces starenja.[4] Istraživanja su potvrdila pozitivnu ulogu polifenolnih jedinjenja u prevenciji razvoja raka, kardiovaskularnih bolesti, dijabetesa, osteoporoze i neurodegenerativnih bolesti.[5] S obzirom na pozitivno dejstvo na zdravlje ljudi, otuda i veliko interesovanje za proučavanje ovih prirodnih jedinjenja, kao i ispitivanje njihovih novih potencijalnih izvora unosa.

Za ekstrakciju polifenola iz različitih biljnih materijala mogu se koristiti različite tehnike ekstrakcije. Uobičajeni postupci ekstrakcije su nedovoljno efikasni i ne omogućavaju visoko iskorišćenje biljnog materijala, zahtevaju upotrebu značajno većih količina organiskih rastvarača, uz istovremeni veliki utrošak energije usled dugotrajnih procesa ekstrakcije, neophodnosti zagrevanje i mešanja. U poslednje vreme se mnogo češće koriste moderne tehnike kao što su mikrotalasna i ultrazvučna ekstrakcija koje se ubrajaju u metode „zelene ekstrakcije“ i imaju za cilj zaštitu životne sredine i opšteg zdravlja ljudi. Generalno, koncept zelenih tehnika podrazumeva smanjenje ili eliminaciju primene toksičnih rastvarača za ekstrakciju uz istovremeno povećanje iskorišćenja procesa kroz manji utrošak energije, manje generisanje otpada, kraće vreme trajanja procesa i manje angažovanje operatera.[6]

Mikrotalasna i ultrazvučna ekstrakcija su u odnosu na tradicionalne tehnike znatno efikasnije po pitanju prinosa ekstrahovanih bioaktivnih jedinjenja, vreme trajanja ekstrakcije je kraće i smanjena je količina upotrebljenog rastvarača za ekstrakciju.
U cilju valorizacije pogače konzumnog suncokreta kao nusproizvoda dobijenog nakon izdvajanja hladno-ceđenog ulja i povećanja prinosa ekstrahovanih polifenolnih jedinjenja iz pogače, u radu je ispitana efikasnost različitih tehnika ekstrakcije, uključujući maceraciju, ekstrakciju uz intenzivno mešanje, ultrazvučnu i mikrotalasnu ekstrakciju. Primenjene tehnike su upoređene i defisana je najbolja ekstrakciona tehnika za posmatranu grupu jedinjenja. Pored toga, ispitana je efikasnost različitih ekstragenasa i izabran optimalan za izdvajanje polifenola. Na kraju je određen prinos ekstrakta i sadržaj polifenola u pogačama konzumnog sunockreta u cilju procene potencijala ovog sporednog proizvoda kao alternativnog izvora antioksidanata.

Materijal i metode

Sve hemikalije korišćene u radu su čistoće p.a., dobavljača Aldrich Chemical Co. (Steineheim, Germany), Merck (Darmstadt,Germany) i Centrohem (Stara Pazova, Srbija). Kao rastvarači korišćeni su metanol (40, 60 i 80 % rastvor), etanol (40, 60 i 80 % rastvor) i aceton (40, 60 i 80 % rastvor). Za određivanje ukupnog sadržaja polifenola korišćene su sledeće hemikalije: Folin-Ciocalteu reagens, natrijum-karbonat i galna kiselina.
Preliminarna istraživanja izvedena u cilju optimizacije uslova postupka ekstrakcije polifenola su obuhvatila analizu reprezentativnog uzorka pogače konzumnog suncokreta koji je dobijen mešanjem većeg broja pogača.
Nakon odabira ekstrakcione tehnike i izbora optimalnih uslova za ekstrakciju, analizirano je pet uzoraka pogača konzumnog suncokreta. Suncokreti su gajeni na istom lokalitetu, pri istim agro-tehničkim uslovima i u isto vreme. Uzorkovanje semena suncokreta je izvedeno neposredno posle žetve, dok je sušenje izvedeno pri atmosferskim uslovima. Svi uzorci semena suncokreta su bili celog jezgra bez oštećenja i čuvani su u zatvorenim plastičnim kesama u mraku. Nakon izdvajanja ulja hladnim presovanjem, pogače konzumnih suncokreta su usitnjavane u električnom mlinu. Za ekstrakciju je uzimano oko 5 g uzorka, dok je za ekstrakciju korišćeno 25 mL ekstragensa. Ekstrakcione tehnike koje su primenjene su uključile maceraciju, ekstraciju uz intenzivno mešanje, mikrotalasnu (MT) i ultrazvučnu (UZ) ekstrakciju. Maceracija je izvođena na temperaturi od 25°C u trajanju od 24 h. Za ekstrakciju uz intenzivno mešanje je korišćen Ultra-turrax® homogenizer, a vreme ekstrakcije je iznosilo 10 min. Ultrazvučna ekstrakcija je izvođena u ultrazvučnom kupatilu u trajanju od 60 min na 30°C uz korišćenje povratnog hladnjaka. Mikrotalasna ekstrakcija je izvođena pri snazi mikrotalasa od 320 W u trajanju od 10 min. Nakon završenog procesa ekstrakcije, ekstrakti su od biljnog materijala odvajani filtriranjem uz ispiranje rastvaračem za ekstrakciju. Dobijeni ekstrakti su koncentrovani na rotacionom vakuum uparivaču do suva i određivan je prinos ekstrakta.

Određivanje sadržaja ukupnih polifenola

Sadržaj ukupnih polifenola u ekstraktima je određen po proceduri Folin-Ciocalteu-a uz određene modifikacije.[7] Suvi ekstrakti su rastvoreni u 5 mL metanola. U 100 µL rastvorenog ekstrakta je dodato 500 µL Folin–Ciocalteu reagensa i 6 mL destilovane vode. Nakon intenzivnog mešanja u trajanju od 60 s, dodato je 2 mL 15 % rastvora Na2CO3 i rastvor je mućkan još 30 s nakon čega je dopunjen do 10 mL destilovanom vodom. Apsorbancija je

merena nakon 2 h na 750 nm na spektrofotometru (UV-2100, Cole Parmer, USA). Za definisanje kalibracione krive korišćen je rastvor galne kiseline i sadržaj ukupnih polifenola je izražavan kao mg ekvivalenta galne kiseline po kg suve mase biljnog materijala (mg GAE/kg SM).

Statistička analiza

Statistička analiza je izvedena korišćenjem programa Origin Pro 8. Svi rezultati su predstavljeni kao srednja vrednost ± standardna devijacija tri nezavisna merenja.

Rezultati i diskusija

Optimizacija postupka ekstrakcije polifenola iz uzoraka pogača konzumnog suncokreta je obuhvatila odabir ekstragensa i ekstrakcione tehnike koja obezbeđuje najviši prinos ekstrakta i sadržaj polifenola.

Pri ispitivanju ekstrakcione moći ekstragensa, poređeni su različiti rastvarači, a ekstrakcija je izvedena primenom ultrazvučne tehnike. Nezavisno od primenjene koncentracije rastvarača za ekstrakciju, prinosi ekstrahovanih materija dobijeni korišćenjem acetona i metanola kao ekstragensa su bili značajno manji u odnosu na prinose dobijene etanolom. Dodatno je utvrđeno da je sadržaj polifenolnih jedinjenja znatno veći u ekstraktima dobijenim primenom 60 % i 80 % etanolnih rastvora, uz najviši određen sadržaj primenom 80 % etanolnog rastvora (Slika 1). Pored toga, etanolni ekstrakt je bilo veoma jednostavno upariti do suva, te je stoga 80% etanol izabran kao odgovarajući rastvarač za ekstrakciju.

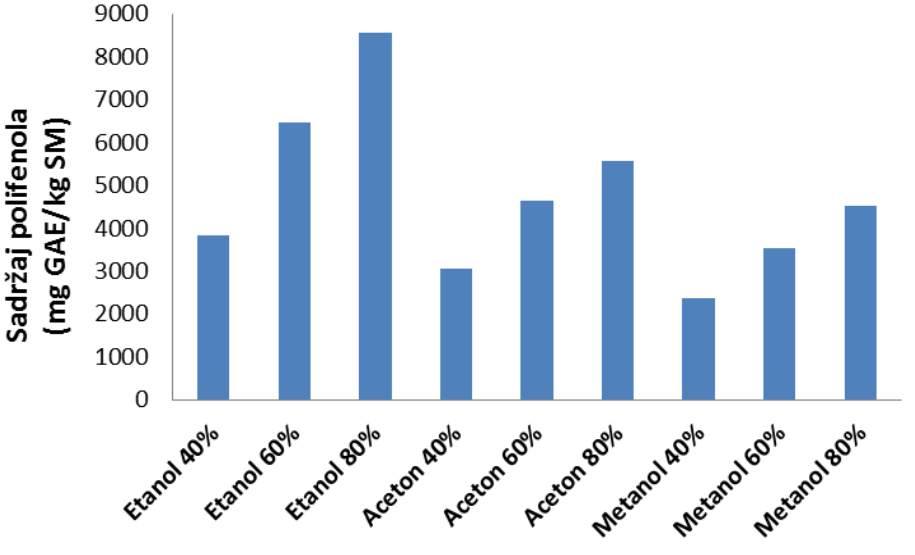

Slika 1. *Poređenje efikasnosti različitih rastvarača za izolovanje polifenola iz pogače konzumnog sunokreta*

U tabeli 1 prikazani su prinosi ekstrakta i sadržaj polifenola dobijeni primenom različitih ekstrakcionih tehnika, uz primenu 80 % etanolnog rastvora kao ekstragensa. Rezultati

ispitivanja su pokazali da je maceracija pokazala najmanju efikasnost. Primenom savremenih ekstrakcionih tehnika, ultrazvučne i mikrotalasne ekstrakcije, dobijeni su značajno veći prinosi i sadržaji polifenolnih jedinjenja u odnosu na konvencionalnu ekstrakciju.
Prinosi ekstrakta se nisu značajno razlikovali primenom ultrazvučne i mikrotalasne ekstrakcije, dok je u ekstraktu dobijenom primenom ultrazvučne ekstrakcije dobijen najveći sadržaj polifenola. Prednost ultrazvučne ekstrakcije se ogledala I u znatno reproduktivnijim rezultatima određivanja sadržaja polifenola, tj. relativna standardna devijacija dobijenih rezultata je bila mnogo manja u poređenju sa ostalim ekstrakcionim tehnikama. Za dalja određivanja posmatranih parametara odabrana je ultrazvučna ekstrakcija sa 80% etanolom kao ekstragensom.

***Tabala 1**. Rezultati prinosa ekstrahovanih supstanci i sadržaja polifenola u pogačama konzumnog suncokreta dobijeni primenom različitih ekstrakcionih tehnika*

Tip ekstrakcije	Prinos ekstrakta, %	Sadržaj polifenola, mg GAE/kg SM
Maceracija	3,64±0,14	5063,24±232,10
Ekstrakcija uz intenzivno mešanje	3,99±0,02	5605,58±538,41
Ultrazvučna ekstrakcija	5,78±0,25	8548,53±303,63
Mikrotalasna ekstrakcija	5,02±0,44	6085,82±630,18

Nakon odabira optimalnog rastvarača za ekstrakciju i izbora najefikasnije ekstrakcione tehnike, dalje su analizirani uzorci. Rezultati određivanja prinosa i sadržaja polifenola u dobijenim ekstraktima pogača konzumnih suncokreta su prikazani u Tabeli 2. Prinosi ekstrakta uzoraka su bili u intervalu od 3,93% do 5,46%, dok se sadržaj ukupnih polifenola u dobijenim uzorcima kretao u intervalu od 4041,48 do 4868,03 mg GAE/kg SM. Kao što se može videti, sadržaj polifenolnih jedinjenja nije zanemarljiv, te bi se ovi sporedni produkti prehrambene industrije mogli iskoristiti za dobijanje visokovrednih ekstrakata i obogaćivanje prehrambenih i farmaceutrskih proizvoda.

***Tabala 2 .** Rezultati analiza esktrakta pogača konzumnog suncokreta*

Uzorci	Prinos ekstrakta, %	Sadržaj polifenola, mg GAE/kg SM
1	5,32±0,18	4646,86±325,70
2	4,46±0,06	4041,48±212,65
3	3,93±0,02	4868,03±256,22
4	5,46±0,14	4201,00±346,57
5	4,75±0,08	4653,78±235,94

Zaključak

Na osnovu prikazanih rezultata može se zaključiti da su primenom ultrazvučne tehnike ekstrakcije dobijeni veći prinosi ekstrahovanih supstanci, kao i najviši sadržaji ukupnih polifenola. Najveću efikasnost ekstrakcije je pokazao 80% etanolni rastvor. Zbog toga se ova tehnika preporučuje za ekstrakciju polifenola iz pogača konzumnog suncokreta. U svim uzorcima pogača konzumnog suncokreta utvrđeno je prisustvo značajne količine polifenola, te one predstavljaju značajan izvor ovih visokovrednih jedinjenja.

***Zahvalnica:** Ovaj rad je nastao kao rezultat istraživanja u okviru projekata III 46009 i TR 31014 finansiranih od strane Ministarstva prosvete, nauke i tehnološkog razvoja Republike Srbije.*

Optimization of extraction process of polyphenols from sunflower cake

The paper examines the efficiency of various extraction techniques for isolating polyphenol compounds from sunflower cake. Maceration, extraction with intense mixing, ultrasonic and microwave extraction were compared. The extraction efficiency of different solvents for isolation of polyphenolic compounds, including acetone, ethanol and methanol at concentrations of 40, 60 and 80%, were also compared. It has been found that the highest yield is obtained by using the ultrasonic extraction for 60 min at 30°C with the application of 80% ethanol solution as extragens.

Literatura:

1. B.A. Bohm, T.F. Stuessy, *Flavonoids of the Sunflower Family (Asteraceae)*, Springer, Austria, 2001.
2. B. Halliwell, *Cardiovascular Research*, **73** (2007) 341.
3. W. Guo, E.H. Kong, M. Meydany, *Nutrition and Cancer*, **61** (2009) 807.
4. S. Khurana, K. Venkataraman, A. Hollingsworth, M. Piche, T.C. Tai, *Nutrients*, **5** (2013) 3779.
5. K.B. Pandey, S.I. Rizvi, Oxidative Medicine and Cellular Longevity, **2** (2009) 270.
6. A. Scalbert, C. Morand, C. Manach, C. Rémésy, *Biomedicine and Pharmacotherapy*, **56** (2002) 276
7. J. Švarc-Gajić, Z. Stojanović, A. Segura Carretero, D. Arráez Román, I. Borrás, I. Vasiljević, *Journal of Food Engineering*, **119** (2013) 525.

Tečno-čvrsta ekstrakcija izabranih pesticida na bazi jonskih tečnosti za direktnu analizu zemljišta i sedimenata

Jelena S. Milićević, Aleksandra N. Dimitrijević, Nikola Zdolšek, Tatjana M. Trtić-Petrović
Laboratorija za fiziku, Institut za nukelarne nauke Vinča, Univerzitet u Beogradu, P. P. 522, 11001 Beograd, Srbija, e-mail: jdjordjevic@vinca.rs

Uvod

Savremena poljoprivredna proizvodnja direktno je povezana sa upotrebom pesticida.[1] Prisustvo pesticida u svim delovima životne sredine je potvrđeno, a za neke pesticide postoje zakonske regulative za praćenje.[2] Analiza pesticida u uzorcima zemlje je složena zbog njihove hemijske raznovrsnosti i niskih koncentracija, kao i složenog sastava zemlje. Tako da je priprema uzorka sastavni deo analitičke metode u kome se analit izdvaja iz kompleksnog matriksa i koncentruje.

Ekstrakcija je metoda izbora za izdvajanje pesticida iz zemljišta u procesu pripreme uzorka. Različite ekstrakcione tehnike kao što su superkritična tečna ekstrakcija,[3] ekstrakcija na čvrstoj fazi,[4] ekstrakcija po Soxhletu[5] i mnoge druge se koriste kao metode za pripremu uzorka pre analitičkih metoda za kvantifikaciju. S obzirom da klasične ekstrakcione metode pripreme uzoraka zemljišta dugo traju i uglavnom koriste velike količine toksičnih organskih rastvarača, nova istraživanja su usmerena ka razvoju mikrometoda sa netoksičnim ili manje toksičnim rastvaračima.

Poslednjih godina se jonske tečnosti (JT) nameću kao potencijalna alternativa organskim rastvaračima zbog njihovih jedinstvenih osobina kao što su zanemarljiv napon pare, nezapaljivost, visoka hemijska i termalna stabilnost.[6] Naročito je značajna mogućnost dizajniranja i sinteze JT sa podesivim osobinama (rastvorljivost u vodi, hidrofobnost/hidrofilnost, selektivnost, itd.) koja se postiže kombinovanjem katjona i anjona koji čine jonsku tečnost. Formiranje dvofaznih vodenih sistema (DVS) na bazi jonskih tečnosti predstavlja alternativni ekstrakcioni metod bez korišćenja organskih rastvarača. Hidrofilne jonske tečnosti mogu biti isoljene iz vodenih rastvora dodatkom neorganskih ili organskih soli, pri čemu se formiraju dve vodene faze: faza bogata JT (JT-faza) i faza bogata soli (so-faza). Tečno-tečna ekstrakcija primenom DVS na bazi jonskih tečnosti pokazala se primenljiva za izdvajanje različitih toksičnih supstanci iz vodenih rastvora kao npr. tekstilnih boja i pesticida.[7,8]

Cilj ovog rada je ispitivanje direktne tečno-čvrste ekstrakcije pesticida različite polarnosti (imidakloprid (IMI), acetamiprid (ACE), linuron (LIN) i tebufenozid (TBF)) iz čvrstih uzoraka (zemlja i sedimenti) primenom dvofaznih vodenih sistema na bazi dve jonske tečnosti (1-metil-3-oktilimidazolium-hloridom [omim][Cl] i 1-butil-3-metilpirolidinium-dicijanamidom [bmpyr][DCA]), kao alternativne metode za pripremu uzorka pre hromatografskog određivanja pesticida.

Materijal i metode

Jonske tečnosti [omim][Cl] i [bmpyr][DCA] su dobijene od Iolitec GmbH (Denylingen, Nemačka) i Sigma Aldrich (St. Louis, MO, USA), redom. Pesticidi: linuron (3-(3,4-dihlorofenil)-1-metoksi-1-metilurea), tebufenozid (*N*-terc-butil-*N*′-(4-etilbenzoil)-3,5 dimetilbenzohidrazid), imidakloprid (*N*-[1-[(6-hloro-3-piridil)metil]-4,5-dihidroimidazol-2-il]nitramid) i acetamiprid (*N*-[(6-hloro-3-piridil)metil]-*N*′-cijano-*N*-metil-acetamidin) su dobijeni od Galenike-Fitofarmacija A.D. (Zemun, Srbija). Polazni rastvori pesticida (1000 mg

dm^{-3}) su pripremani u metanolu i čuvani na -20°C. Sve hemikalije su p.a. čistoće i svi rastvori su pripremani sa Milli-Q vodom (Millipore Corporation, SAD).
Tri čvrsta uzorka su korišćena u ovom radu: uzorak 1 je nekultivisano zemljište sakupljeno u Vinči (Beograd, Srbija) sa dubine od 0 – 15 cm, uzorci 2 i 3 su površinski rečni sedimenti (reka Sava na 5 km od ušća i reka Dunav na 1059 km od ušća). Svi uzorci su sušeni na 100 °C do konstantne mase.
Ispitivani uzorci su pripremani za ekstrakciju tako što je u 1 g uzorka dodato 1 cm^3 rastvora pesticida (koncentracije pojedinačnog pesticida 0.1 - 30 mg dm^{-3}) i 4 cm^3 metanola, i mešano na laboratorijskom šejkeru 8 sati pri brzini od 300 obrtaja/min. Nakon toga uzorci su sušeni 24 h na sobnoj temperaturi pre ekstrakcije.[6]
Ekstrakcija pesticida se sastojala iz sledećih faza: u 0,1 g pripremljenog čvrstog uzorka dodat je vodeni rastvor JT (50% [omim][Cl] ili 60% [bmpyr][DCA]), smeša je mućkana 2 min pomoću vorteksa i 60 min u ultrazvučnoj kadi. Tečna faza je nakon centrifugiranja odvojena i dodat je 50% rastvor K_3PO_4 tako da je sastav DVS bio: 22 % JT, 17 % K_3PO_4 i 61 % H_2O. DVS je izmešan pomoću vorteksa i centrifugiran 10 min na 10000 obrtaja/min nakon čega su odvojene faze, izmerena im je masa i određena koncentracija pesticida tečnom hromatografijom.[8]

Rezultati i diskusija

Fazni dijagrami i vezne linije

U cilju ispitivanja uslova za ekstrakciju, prvo su određeni i okarakterisani fazni dijagrami za ispitivane DVS {JT + K_3PO_4 + H_2O} na bazi jonskih tečnosti: [omim][Cl] i [bmpyr][DCA]. Eksperimentalni rezultati su fitovani primenom Merchuk-ove jednačine[9] i prikazani na slici 1. Rezultati pokazuju da [bmpyr][DCA] lakše gradi DVS nego [omim][Cl] tj. za isoljavanje je potrebna manja količina soli. Takođe su određene i vezne linije i njihove dužine (Tabela 1) koje daju informaciju o sastavu faza u ravnotežnom stanju. DVS na bazi [bmpyr][DCA] ima značajno dužu veznu liniju i niži udeo JT u so-fazi u poređenju sa DVS na bazi[omim][Cl] što implicira da će imati i bolje ekstrakcione osobine. Na osnovu ispitanih osobina DVS, određeni su eksperimentalni uslovi za ekstrakciju pesticida, tako da DVS na bazi obe ispitivane JT imaju isti sastav {22% JT + 17% K_3PO_4 + 61% vode}.
Za ispitivanje direktne ekstrakcije pesticida iz čvrstog uzorka (zemlja ili sedimenti), izabrana su četiri pesticida čije osnovne karakteristike su date u Tabeli 2.

Tabela 1. *Eksperimentalne vrednosti masenih udela u polaznoj smeši DVS {JT (Y) + K_3PO_4 (X)+ H_2O} DVS, JT-fazi i so-fazi, i dužine veznih linija (DVL)*

IL		[omim][Cl]	[bmpyr][DCA]
Sastav DVS	100X	17,25	17,11
	100Y	22,58	22,71
JT-faza	100X	6,55	0,19
	100Y	27,35	50,15
So-faza	100X	27,74	12,47
	100Y	12,24	2,62
100 DVL		25,94	50,92

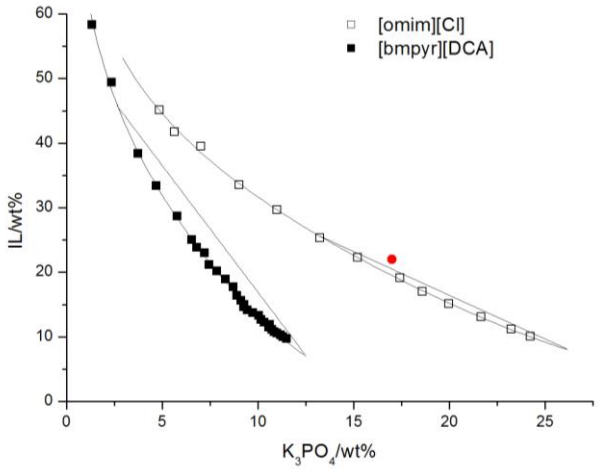

Slika 1. *Fazni dijagrami i vezne linije sistema {JT + K_3PO_4 + H_2O} na T = 296 K i (p = 0,1 MPa).*
● *– tačka na kojoj je rađena ekstrakcija.*

Izabrani pesticidi pripadaju različitim hemijskim grupama, imaju različitu rastvorljivost u vodi (od veoma hidrofilnih do hidrofobnih), kao i različite koeficijente raspodele u sistemu oktanol-voda (log $P_{o/w}$) na pH 13 (pH ispitivanih DVS na bazi JT i K_3PO_4). Na osnovu log $P_{o/w}$ ispitivani pesticidi se mogu podeliti u tri grupe: polarni (log $P_{o/w} < 1$), srednje polarni ($1 <$ log $P_{o/w} < 2$) i nepolarni (log $P_{o/w} > 2$).

Tabela 2. Rastvorljivost u vodi, kiselinsko bazne konstante (pKa) i koeficijenti raspodele pesticida u sistemu oktanol-voda (log $P_{o/w}$).

Pesticidi	Rastvorljivost u vodi, mg dm^{-3}	pK_a[a]	DT_{50} (dani, lab. na 20 °C)[b]	log $P_{o/w}$ na 20 °C[a]
IMI	610	11,2	187	0,46
ACE	4200	0,7	1,6	1,55
LIN	75	12,3	57,6	3,12
TBF	0,83	10,89	26,2	4,33

[a]Izračunati pomoću ACS/Labs 12 programa
[b]Preuzeto iz baza pesticida EU projekta FP6-SSP-022704)

U daljem radu ispitani su uslovi ekstrakcije izabranih pesticida iz vodenog rastvora i to: uticaj koncentracije soli (Slika 2a) i vremena ekstrakcije (Slika 2b). S obzirom da su rezultati ispitivanja DVS pokazali da [bmpyr][DCA] ima bolje osobine u građenju ovih sistema u poređenju sa [omim][Cl], i da će biti i bolji ekstragens, optimizacija parametara ekstrakcije je rađena sa DVS na bazi [omim][Cl]. Sa slike 2a se jasno vidi da je stepen ekstrakcija (E) za sve pesticide veći od 90 % i u slučaju najmanje moguće koncentracije K_3PO_4 (16 %) i da se sa malim povećanjem koncentracije (17 %) dostiže se maksimalan E za LIN, ACE i IMI, dok se za TEB potrebno 26 % soli. Takođe sa ove slike se vidi, da ekstrakcija u DVS na bazi [omim][Cl] nije određena hidrofobno/hidrofilnim osobinama pesticida, npr. ACE i IMI (umereno polarni i polarni pesticidi) imaju viši E nego nepolarni TEB. Sa slike 2b se vidi da je potrebno 60 min da se uspostave ravnotežni uslovi i dostigne maksimalni stepen ekstrakcije za sve ispitivane pesticide.

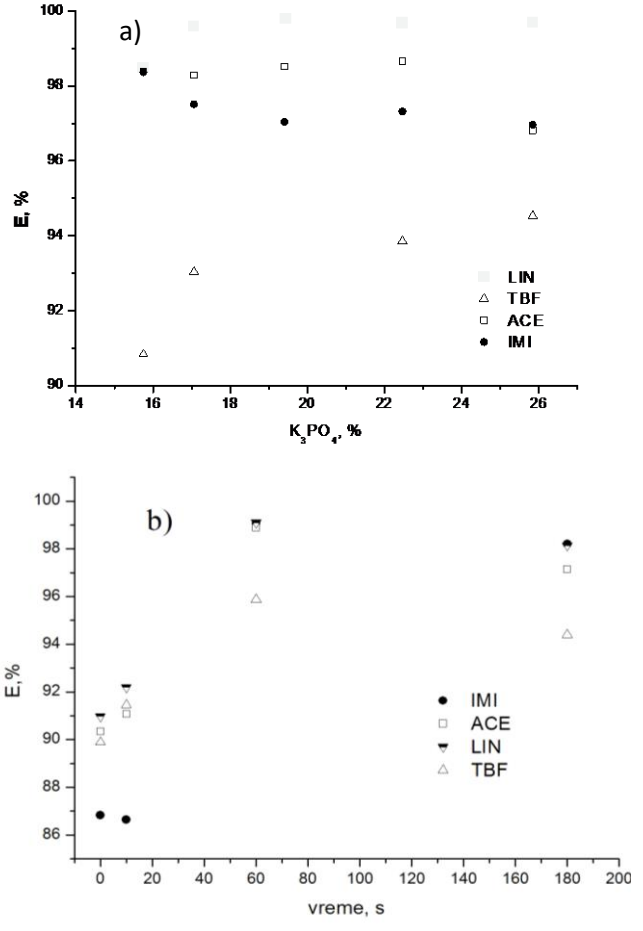

Slika 2. *a) Uticaj udela soli K_3PO_4 i b) vremena ekstrakcije na stepen ekstrakcije ispitivanih pesticide u DVS {JT + K3PO4 + H2O} na bazi [omim][Cl].*

Zatim su izabrani pesticidi ekstrahovani direktno iz čvrstih uzoraka (zemlja i sedimeti), tako što je u pripremljeni uzorak zemlje (sa dodatim pesticidima) dodavan vodeni rastvor JT ([omim][Cl] i [bmpyr][DCA]), nakon uspostavljene ravnoteže, čvrsti ostatak je odvojen centrifugiranjem, a u vodenom rastvoru je formiran DVS dodatkom rastvora K_3PO_4. U Tabeli 3 prikazane su vrednosti za *Recovery* za sve ispitivane pesticide i za sva tri čvrsta uzorka. *Recovery* veći od 80,7 % je zadovoljavajući s obzirom na kompleksan matriks i u skladu je sa rezultatima drugih autora.[10,11] Analiza sastava zemljišta je pokazala najveći procenat humusa i ukupnog organskog ugljenika za uzorak Z3 što je i razlog nižeg *Recovery*-ja. Određeni analitički parametri ekstrakcije izabranih pesticida u DVS na bazi [omim][Cl] su sledeći: linearni opseg 5-300 μg/g, LOD u opsegu od 1,13 μg/g do 1,69 μg/g, a za [bmpyr][DCA] opseg linarnosti od 0,5-300 μg/g i LOD od 0,2 μg/g do 0,51 μg/g.

Tabela 3. Recovery (R, %, n=3) i relativne standardne devijacije (RSDs, %) za pesticide u proučavanom zemljištu.

Pesticid	Z 1		Z 2		Z 3	
	R, %	RSD, %	R, %	RSD, %	R, %	RSD, %
IMI	98,33	4,54	92,13	5,32	86,22	7,85
ACE	95,12	3,42	89,51	4,25	80,68	6,12
LIN	97,56	4,15	90,25	5,34	83,31	7,05
TBF	96,11	2,86	91,73	3,87	84,04	5,91

Zaključak

S obzirom da su posmatrana tri različita tipa zemljišta, na osnovu svega izloženog može se zaključiti da je razvijena metoda ekstrakcije smeše pesticida (imidakloprida, acetamiprida, linurona i tebufenozida) dvofaznim vodenim sistemima na bazi jonskih tečnosti dobra alternativa za tradicionalne metode pripreme uzoraka zemljišta pre HPLC/DAD. Efikasnost ekstrakcije je veća za DVS {JT + K_3PO4 + H_2O} na bazi [bmpyr][DCA] u poređenju sa [omim][Cl]. Metoda je brza, pokazuje dobru linearnost i selektivnost, ne zahteva veliku potrošnju ekstragensa, potrebne su male količine uzoraka za rad pa se može očekivati potecijalna implementacija metode za rutinska ispitivanja.

Zahvalnica: *Zahvaljujemo se Ministarstvu prosvete, nauke i tehnološkog razvoja na finansijskoj pomoći kroz projekat broj III 45006.*

Liquid-solid extraction of the selected pesticides based on ionic liquids for direct analzsis of soil and sedimets samples

Soil contamination of pesticides and their degradation products is a global environmental pollution problem. As an alternative to the currently used extraction methods, aqueous biphasic systems (ABS) composed of ionic liquids (ILs) and K_3PO_4 are here proposed for the simultaneous extraction the mixture of pesticides: imidacloprid (IMI), acetamiprid (ACE), linuron (LIN) and tebufenozide (TBF). The influence of IL on the pesticide extraction was investigated using 1-methyl-3-octylimidazolium chloride [omim][Cl] and 1-butyl-3-methylipyrrolidinium dicyanamide [bmpyr][DCA]. Extraction conditions such as composition of ABS, percentages of K_3PO_4 using ABS, extraction time and centrifugation time was optimized so to reach the maximal removal of the pesticides from the three different soil sample. The extraction efficiency of [bmpyr][DCA]+K_3PO_4 was generally better than that for [omim][Cl] +K_3PO_4 procedure showing good linearity ($R^2 > 0.99$) with recovery higher than 80.68% and limits of detection between 0.2 µg/g and 0.51 µg/g.

Literatura

1. U.S. McKnight, J.J. Rasmussen, B. Kronvang, P.J. Binning, P.L. Bjerg, *Environ. Pollut.* **200** (2015) 64
2. Council Directive (2006/11/EC) on pollution caused by certain dangerous substances discharged into the aquatic environment, *Offic. J. Euro. Union*, **L64** (2006) 52
3. M.H. Naeenia, Y. Yamini, M. Rezaee, *J. Supercrit. Fluid* **57** (2011) 219
4. J. L. Martínez-Vidal, P. Plaza-Bolaňoz, R. Romero-González, A. Frenich-Garrido, *J. Chromatogr. A* **1216** (2009) 6796
5. S. Marchese, D. Perret, A. Gentili, R. Curini, A. Marino, *Rapid Commun. Mass Spectrom.* **15** (2001) 393

6. A. M. Domínguez, M. Funes, X. Fadic, F.Placencia, F. Cereceda, J. P. Muňoz, *Quim. Nova* **38** (2015) 884
7. M. A. Ferreira, J. A. P. Coutinho, A. M. Fernandes, M. G. Freir, *Sep. Purif. Technol.* **128** (2014) 58
8. A. Dimitrijević, Lj. Ignjatović, A. Tot A, M. Vraneš, N. Zec, S. Gadžurić, T. Trtić-Petrović, *J. Mol. Liq.* **243** (2017) 646
9. J.C. Merchuk, B.A. Andrews, J.A. Asenjo, *J. Chromatogr. B Biomed. Sci. Appl.* **711** (1998) 285
10. X. Zhu, J. Yang, Q. Su, J. Cai, Y. Gao, *J. Chromatogr. A* **1092** (2005) 161
11. R. Đurović, T. Đorđević, Lj. Radivojević, Lj. Šantrić, J. Gajić Umiljenić, *Pestic. Phytomed*. **27** (2012) 239

Fizička hemija

Physical Chemistry

Influence of the low frequency 10-1000 Hz magnetic field on *Saccharomyces cerevisiae* respiration activity

Marija Lješević, Branka Lončarević, Itana Nuša Bubanja*, Vladimir Beškoski, Gordana Gojgić-Cvijović, Zoran Velikić**, Dragomir Stanisavljev*
Department of Chemistry, Institute of Chemistry, Technology and Metallurgy, University of Belgrade, Njegoševa 12, Belgrade, Serbia
**Faculty of Physical Chemistry, University of Belgrade, Studentski trg 12-16, Belgrade, Serbia*
***University of Belgrade, Institute of Physics, Laboratory for Atmospheric Physics and Optical Metrology, Zemun, Serbia*

Introduction

Thanks to the fast technological development, a man-made low frequency electromagnetic fields have become a very important part of environmental polution.[1] Therefore, it is not surprising that effects of electric, magnetic or electromagnetic fields on different microbes have become a very popular topic nowadays, mostly because the mentioned physical fields could potentially act as a stress factors and hence affect the survival of the microbial cells as well as their behavior and metabolism.[2] Influence of static and low frequency magnetic field has been investigated on many microorganisms such as *Saccharomyces cerevisiae*[1,3,4,5], *Enterococcus faecalis*[2], *Escherichia coli*[6] and *Spirulina sp.*[7]

Ruiz-Gomez *et al.*[3] studied the influence of long-term exposure to static (0 Hz) and 50 Hz sinusoidal MF induced by a pair of Helmholtz coils (0.35 mT and 2.45 mT) on the growth of *Saccharomyces cerevisiae* by measuring the optical density of the suspension at 600 nm. Authors concluded that neither static nor 50 Hz sinusoidal MF induce alterations in the growth of *S. cerevisiae*.[3] Similarly to the work of Ruiz-Gomez and his coworkers, Novak *et al.*[1] investigated the influence of the 50 Hz MF on the growth of *S. cerevisae,* but the MF was induced in a cylindrical coil (10 mT). Contrary to the first study, they concluded, based on the serial dilution method and measurements of the optical density at wavelengths of 570 and 620 nm, that magnetic field decreases the number of yeast cells, and slows down their growth.[1] Mentioned papers represent only some examples with conflicting results of the bioeffects of the applied magnetic fields. Potential reasons for that could be the use of different cell types, magnetic field exposure protocols, intensities, frequencies *etc*.

Besides magnetic field examinations on the growth of *S. cerevisiae* by the optical density measurements, Motta *et al.*[4] also studied effects of the static MF (220 mT, exposure time 24 h) on ethanolic fermentation by *Saccharomyces cerevisiae* measured by gas chromatography, and concluded that ethanol concentration was 3,4 times higher in magnetized cultures.[4] Nakasono and coworkers[5] performed detailed study of the effect of 50 Hz magnetic-field exposure on genome-wide gene expression, of the yeast *Saccharomyces cerevisiae*. Their results indicate that a 50 Hz magnetic field below 300 mT did not act as a stress factor like heat shock or DNA damage.[5]

In this study the influence of magnetic field on yeast cells is examined by measuring respiration activity. This is the first experimental report of the changes in respiration influenced by magnetic field which was measured by Micro-Oxymax® respirometer, to the best of our knowledge. Also, contrary to the previously performed studies, in this study the

low frequency magnetic field with constant frequency scan regime from 10 to 1000 Hz was used.

Experimental part

Prior to the experiment, *S. cerevisiae* was grown on the malt extract agar. In order to prolong log phase of cell division which will be monitored in experiments, the diluted (1:1) Sabouraud dextrose broth (SBD) was inoculated with overnight culture suspension. All experiments were performed in pair: control (CC) and magnetic field exposed cells (MFEC) and lasted 24 h (Figure 1). As it can be noticed from Figure 1, CC and MFEC bottles were installed in a glass water recirculation jacket and were mutually connected in line with a thermostat in order to minimize possible temperature differences between samples.

Low frequency magnetic field was generated by wrapping one bottle together with recirculation jacket in Cu-coil. Inside of the mentioned Cu-coil 10-1000 Hz magnetic field was induced and generator was used to set up a frequency range and a scan interval to 100 s. An amplifier was used to set up a maximal effective current trough the coil (2 A which corresponds to magnetic induction of 33 mT), and an oscilloscope was used to control changes in effective current during frequency scanning.

Respiration activity of CC and MFEC was continuously measured by a twelve-channel Micro-Oxymax® respirometer (Columbus Instruments, USA). All experiments were performed in two light-proof 5 mL glass bottles with 3 mL of the inoculated SBD medium. Constant temperature at 28 °C was maintained by thermostat (Julabo, F12 Refrigerated/Heating Circulator, Germany). Cell respiration was measured every 20 min during 24 h and experiments were performed in five replicates. Cumulative O_2 consumption and cumulative CO_2 production (in μL) were determined.

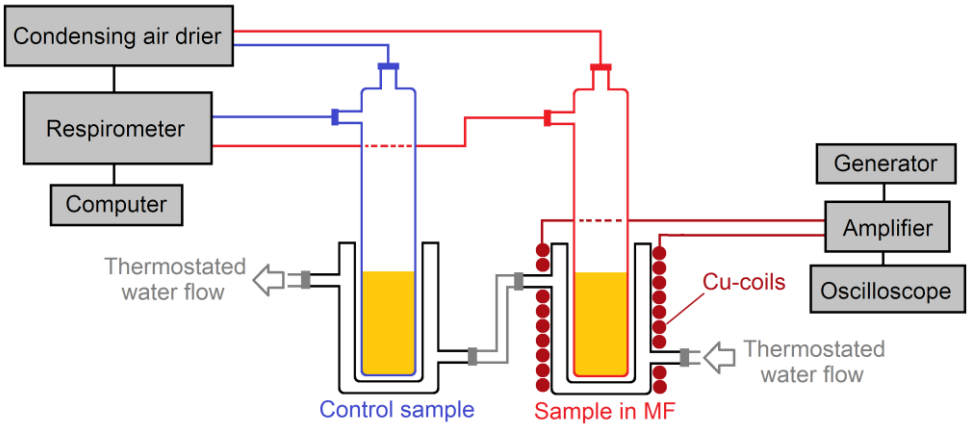

Figure 1. *Schematic view of the experimental setup.*

Results and discussion

In this paper the influence of the magnetic field with constant low frequency scan regime from 10 to 1000 Hz on yeast cells respiration activity was examined. Like it was mentioned in Experimental part, cumulative O_2 consumption and cumulative CO_2 production were monitored in CC and MFEC during 24 h. It should be stressed out that for all frequency ranges experiments were repeated five times.

The Figure 2. shows cumulative O_2 consumption and cumulative CO_2 production in CC and MFEC over 24 h, obtained in all five repeated experiments.

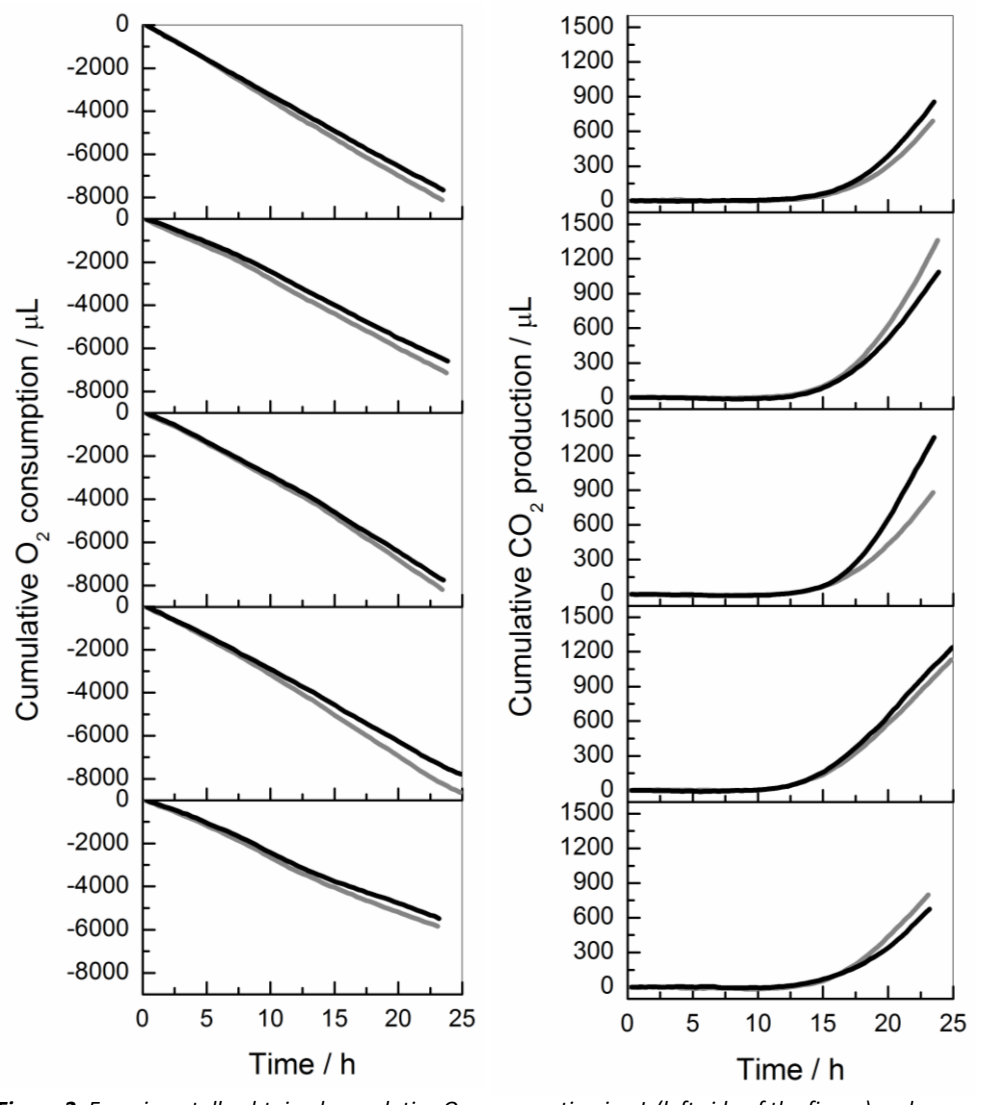

Figure 2. *Experimentally obtained cumulative O_2 consumption in µL (left side of the figure) and cumulative CO_2 production in µL (right side) over 24 h for magnetic field frequency range 10 – 1000 Hz. Gray curve corresponds to changes in CC while the black curve represents changes of the O_2 and CO_2 in MFEC.*

As it can be seen from Figure 2, up to 15th hour, the differences in cumulative O_2 consumption and cumulative CO_2 production between CC and MFEC at investigated frequency range are negligible. After 15th hour those differences begin to grow and are the biggest at the end of the magnetic field exposure. For examined magnetic field frequency

range from 10 to 1000 Hz all five repeated experiments showed that cumulative O_2 consumption in MFEC was lower in comparison to CC. However, for the same frequency range behavior in cumulative CO_2 production differed. Namely, in three experiments it was obtained that cumulative CO_2 production in MFEC was higher in comparison to CC, while in other two repeated experiments for the same experimental conditions cumulative CO_2 production in magnetic field sample was lower.

Obtained results were statistically considered by a paired two sample one tail T-test. Results from the T-test showed that statistically important differences between CC and MFEC exist for cumulative O_2 consumption, but do not exist for cumulative CO_2 production.

Even though evident inconsistency was found in cumulative CO_2 production, we believe that obtained results still represent a good basis for further investigations in this field. Namely, paired two sample one-tail T-test showed statistically important differences for cumulative O_2 consumption which suggests that applied low frequency magnetic field could influence yeast cell respiration activity. The inconsistency in cumulative CO_2 production could be influenced by the lack of sample stirring and differences in the initial cell number between replicates. Therefore, it is important for the future investigations, besides respiration activity, to take into account other important parameters of the system such as cells growth, glucose uptake and ethanol production. On the other hand, if we consider most results available in the literature where a static or 50 Hz magnetic field was examined[1,3,4,5], than the potential reason for the inconsistency in cumulative CO_2 production could indicate that different frequencies could have an opposite effect on respiration. This would lead to the combination of positive and negative effects during the exposure time which could explain the absence of statistically significant differences. So, further investigations should consider shorter frequency intervals up to 1 kHz. By narrowing the frequency range, we could more precisely isolate positive or negative effects on yeast cells.

Conclusion

Obtained results represent a good basis for the following investigations in this area. Examined magnetic field with constant low frequency scan regime from 10 to 1000 Hz in all five repeated experiments showed lower cumulative O_2 consumption of cells exposed to magnetic field. Also applied paired two sample one-tail T-test showed statistically important differences for cumulative O_2 consumption between control cells and magnetic field exposed cells. In order to ascertain the effects of magnetic field on the CO_2 production, further experiments should be conducted.

Acknowledgement: *This research was financially supported by the Ministry of Education, Science and Technological Development of Republic of Serbia, through Projects No. III 43004 and OI 172015.*

Uticaj niskofrekventnog magnetnog polja (10-1000 Hz) na respiracionu aktivnost ćelija kvasca *Saccharomyces cerevisiae*

Veoma popularna tema današnjice je ispitivanje električnog, magnetnog i elektromagnetnog polja na različite mikroorganizme, jer pomenuta fizička polja potencijalno deluju kao faktori stresa i tako utiču na njihovo preživljavanje, ponašanje i metabolizam. U ovom radu ispitivan je uticaj niskofrekventnog magnetnog polja sa

konstantnim intervalom skeniranja od 10 do 1000 Hz na respiraciju ćelija kvasca, Saccharomyces cerevisiae. Eksperimenti su rađeni u pet ponavljanja i kumulativna potrošnja O_2 i produkcija CO_2 praćena je pomoću Micro-Oxymax® respirometra. U svih pet ponavljanja, ćelije koje su bile izložene magnetnom polju pokazale su manju kumulativnu potrošnju kiseonika u poređenju sa uzorcima van magnetnog polja i nekonzistentnu produkciju CO_2. Rezultati su obrađeni uporednim jednosmernim T-testom, koji je pokazao da postoje statistički značajne razlike u kumulativnoj potrošnji O_2 između kontrolnih ćelija i onih izloženih magnetnom polju, što nije slučaj sa kumulativnom produkcijom CO_2. Iako su dodatna ispitivanja neophodna da se objasni nekonzistentnost produkcije CO_2, dobijeni rezultati ovih inicijalnih eksperimenata predstavljaju dobru osnovu za dalja istraživanja u ovoj oblasti.

References

1. J. Novák, L. Stražák, L. Fojt, I. Slaninová, V. Vetterl, *Bioelectrochemistry* **70** (2007) 115
2. W. Fan, Z. Huang, B. Fan, *Microb. Pathog.* **115** (2018) 117
3. M.J. Ruiz-Gomez, M.I. Prieto-Barcia, E. Ristori-Bogajo, M. Martınez-Morillo, *Bioelectrochemistry* **64** (2004) 151
4. M. A. da Motta, J. B. F. Muniz, A. Schuler and M. da Motta, *Biotechnol. Prog*, **20** (2004) 393
5. S. Nakasono, C. Laramee, H. Saiki and K. J. McLeod, *Radiat. Res.* **160** (2003) 25
6. L. Stražák, V. Vetterl, J. Šmarda, *Bioelectrochem. Bioenerg.* **55** (2002) 161
7. K. M. Deamici, L. O. Santos, J. A. V. Costa, *Bioresour. Technol* **249** (2018) 168

Elektrohemija

Electrochemistry

Elektrohemijsko ponašanje bakra u prisustvu macerata hmelja

Vesna J. Grekulović, Mirjana M. Rajčić Vujasinović, Aleksandra M. Mitovski, Zoran M. Stević
Univerzitet u Beogradu, Tehnički fakultet u Boru, VJ 12, Bor, Srbija

Izvod
Primena biljnih ekstrakata za inhibiciju korozije metala i legura je predmet mnogobrojnih naučnih istraživanja. U ovom radu su prikazani rezultati ispitivanja elektrohemijskog ponašanja bakra pri oksidaciji u rastvoru 0,5 mol/dm3 NaCl u odsustvu i prisustvu macerata hmelja različitih koncentracija. Elektrohemijsko ponašanje bakra ispitivano je metodom merenja potencijala otvorenog kola i metodom ciklične voltametrije. Istraživanje primenom ciklične voltametrije pokazuje da se na anodnim polarizacionim krivama pojavljuju tri strujna pika koji odgovaraju adsorpciji anjona i formiranju hlorida bakra i oksida bakra. Vrednost gustine struje strujnih pikova koji su povezani sa reakcijama formiranja jedinjenja bakra opada sa dodatkom macerata hmelja u elektrolit u koncentracijama većim od 10 ml/l, što ukazuje na to da macerat hmelja ima inhibitorsko dejstvo na te reakcije.

Uvod

Bakar je metal koji zbog svojih dobrih osobina ima široku primenu. Koristi se u elektrotehnici, za izradu limova, cevi, žica, kao i za dobijanje legura. Otporan je u velikoj meri na uticaj atmosfere i mnogih hemikalija. Međutim, bakar u rastvorima hlorida podleže koroziji. Elektrohemijsko ponašanje čistog bakra u raznim sredinama predmet je istraživanja u velikom broju radova koji su štampani i citirani u elektrohemijskoj literaturi.[1-4] Takođe, mogućnost prevencije korozije bakra privukla je veliki broj istraživača i do danas je ispitan veliki broj mogućih inhibitora. Organski inhibitori se intenzivno koriste za zaštitu metala i legura od korozije u različitim sredinama. Među njima, široko je ispitivana efikasnost azola za zaštitu bakra i bakarnih legura od korozije.[5-9] U poslednje vreme aktuelna su istraživanja u oblasti primene takozvanih „zelenih“ inhibitora kod kojih se kao ključni kriterijum za primenu postavlja njhova ekološka prihvatljivost.[10-16] Zeleni inhibitori predstavljaju skup jedinjenja koja mogu da budu životinjskog ili biljnog porekla. Oni su biorazgradivi, te ne sadrže teške metale što ih čini ekološki prihvatljivim. Ekstrakte najčešće čini mešavina jedinjenja koja sadrže kiseonik, sumpor i vodonik. Oni su i prirodni antioksidansi, jeftini su i ne štete okolini. Inhibitorski efekat ekstrakta nekih biljaka postiže se zahvaljujući prisutnosti tanina u njihovom sastavu. Kao neke od prihvatljivih supstanci za inhibiciju korozije pokazale su se: tanini, prirodni polimeri, vitamini i ekstrakti bilja, vanilin.[17] U literaturi nije pronađeno da je istraživan ekstrat biljke hmelj u ovu svrhu, a poznajući prirodu ove biljke može se očekivati da bi ekstrat dobijen iz listića šišarke hmelja mogao da ispolji inhibitorsko dejstvo na korozione procese.

Eksperimentalni deo

Eksperimenti su izvedeni na sistemu koji se sastoji od:

- elektrohemijske ćelije sa tri elektrode (radna, referentna i pomoćna),
- hardvera (PC, AD/DA konvertor PCI-20428 W proizveden od strane Burr- Brown-a i analogni interfejs razvijen na Tehičkom fakultetu u Boru),
- softvera za merenje i upravljanje (LabVIEW platforma i specijalno razvijena aplikacija za elektrohemijska merenja).[18]

Ispitivanja elektrohemijskog ponašanja bakra u 0,5 mol/dm^3 NaCl bez i uz dodatak macerata hmelja vršena su merenjem potencijala otvorenog kola u odnosu na zasićenu kalomelsku elektrodu (ZKE) u trajanju od 60 sekundi, i snimanjem anodnih polarizacionih krivih u opsegu potencijala od -0,4 V *vs.* ZKE do 1 V *vs.* ZKE brzinom promene potencijala od 20 mV/s.
Supstance korišćene za pripremu radnih rastvora su NaCl p.a čistoće proizvođača d.d. "Zorka Pharma" Šabac i listići šišarki hmelja proizvođača d.o.o. "Adonis" iz Sokobanje i destilovana voda. Dobijanje biljnog ekstrakta odvija se na sledeći način: na 1000 ml destilovane vode zagrejane do 60 ˚C dodaje se 25 g listića šišarki hmelja. Proces dobijanja ekstrata traje 3 časa uz mešanje na magnetnoj mešalici (broj obrtaja je 600 obrtaja u minuti). Nakon 3 časa, dobijeni rastvor se filtrira vakuumski i dobijeni macerat se čuva u frižideru.

Rezultati i diskusija

Rezultati merenja potencijala otvorenog kola za bakar u 0,5 mol/dm^3 NaCl bez i uz dodatak macerata hmelja prikazani su na slici 1.

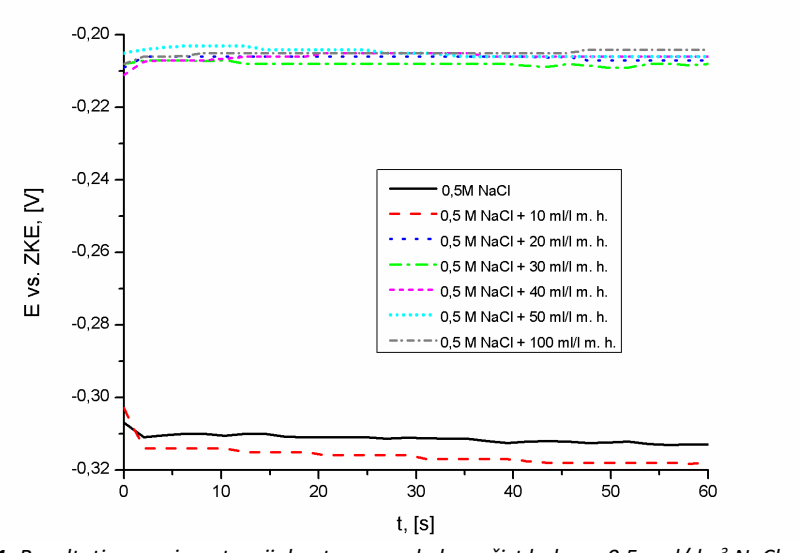

Slika 1. *Rezultati merenja potencijala otvorenog kola za čist bakar u 0,5 mol/dm^3 NaCl sa i bez dodatka macerata hmelja u trajanju od 60 s (m. h. - macerat hmelja)*

Na slici 1 se vidi da potencijal otvorenog kola bakra u 0,5 mol/dm^3 NaCl iznosi -0,313 V *vs.* ZKE. Sa dodatkom 10 mL/L macerata hmelja vrednost potencijala otvorenog kola je približno ista kao i bez dodatka macerata. Pri većim koncentrcijama macerata vrednosti potencijala otvorenog kola su pozitivnije od vrednosti potencijala otvorenog kola koje su dobijene za bakar u 0,5 mol/dm^3 NaCl i iznose oko -0,206 V *vs.* ZKE.
Na slici 2 su prikazane anodne polarizacione krive snimljene za čist bakar pri brzini promene potencijala od 20 mV/s u rastvoru 0,5 mol/dm^3 NaCl bez i u prisustvu macerata hmelja u razlilčitim koncentracijama.

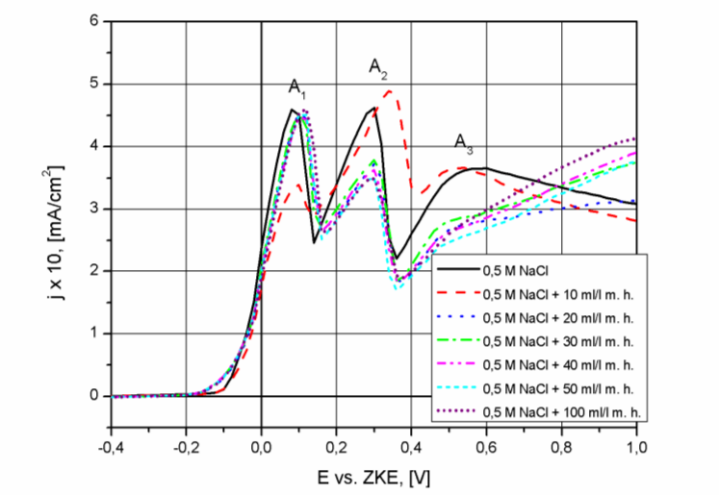

Slika 2. *Anodne polarizacione krive za čist bakar pri brzini promene potencijala od 20 mV/s u 0,5 mol/dm³ NaCl sa i bez dodatka macerata hmelja (m. h. - macerat hmelja)*

Na polarizacionoj krivoj snimljenoj za bakar u 0,5 mol/dm³ NaCl pojavljuju se tri strujna pika A_1, A_2 i A_3. U skladu sa pregledanom literaturom može se zaključiti da strujni pikovi A_1 i A_2 odgovaraju formiranju hlorida bakra po sledećem mehanizmu[3-5]:

$$Cu + Cl^- = CuCl_{ads} + e \quad (1)$$

$$CuCl_{ads} + Cl^- = CuCl_2^- \quad (2)$$

$$Cu + CuCl_2^- = 2CuCl + e^- \quad (3)$$

Strujni pik A_3 odgovara formiranju oksida bakra Cu_2O, što se prema Purbeovom dijagramu može očekivati u rastvoru hlorida[4]:

$$2\,CuCl + 2OH^- = Cu_2O + 2Cl^- + H_2O \quad (4)$$

Upoređujući polarizacione krive u prisustvu macerata hmelja sa polarizacionom krivom bez prisustva macerata može se videti da se strujni pikovi u prisustvu macerata pojavljuju na pozitivnijim potencijalima. Vrednosti gustine struje strujnih pikova A_2 i A_3 na polarizacionim krivama u prisustvu macerata u koncentracijama većim od 10 mL/L su niže u odnosu na strujne pikove na polarizacionoj krivoj bez prisustva macerata. Visina strujnog pika A_1 je pri tome ostala nepromenjena, što bi moglo da znači da je proces adsorpcije ušao u zasićenje već pri najnižoj posmatranoj koncentraciji potencijalnog inhibitora korozije. Gustine struje na toku ovih krivih su niže u odnosu na referentnu samo do određenih potencijala koji zavise od koncentracije dodatog macerata i kreću se od 0,7 do oko 0,9 V vs.ZKE. Ova merenja su pokazala da se prisustvo macerata hmelja u agresivnoj korozionoj sredini kakav je 0,5 molarni rastvor natrijum hlorida, odražava na brzinu reakacije formiranja hlorida bakra tako što je usporava, dok rekaciju formiranja oksida usporava samo do određenih vrednosti anodne polarizacije. Pri tome gustine struje i dalje zadržavaju znatno visoke vrednosti.

Rezultati eksperimenata su pokazali da postoji značajna razlika u obliku krive koja je dobijena pri najnižoj ispitivanoj koncentraciji macerata hmelja. Naime, pri dodatku u količini od 10 ml/l macerat hmelja utiče tako da reakcija koja odgovara strujnom piku A_1 bude usporena, ali istovremeno gustina struje strujnog pika A_2 raste ukazujući na intenziviranje

procesa formiranja jedinjenja CuCl na površini elektrode. Dalji tok krive pokazuje da nije došlo do promene brzine nastajanja oksida bakra kao ni do značajnog pomeranja potencajala na kome se taj proces odigrava (reakcija 4).
Prikazani eksperimenti ukazuju na to da macerat hmelja ima delimično inhibitorsko dejstvo na procese oksidacije bakra u jako koroziono agresivnoj sredini kao što je rastvor natrijum hlorida koncentracije 0,5 mol/dm^3.
Zaključak
Na osnovu izvedenih eksperimenata mogu se izvesti sledeći zaključci:

- Na osnovu merenja potencijala otvorenog kola za čist bakar u 0,5 mol/dm^3 NaCl bez i uz dodatak macerata hmelja može se zaključiti da prisustvo macerata hmelja u koncentraciji većoj od 10 mL/L pomera potencijal otvorenog kola ka pozitivnijim vrednostima.
- Na polarizacionoj krivoj snimljenoj za čist bakar u 0,5 mol/dm^3 NaCl se pojavljuju tri strujna talasa koji se pripisuju formiranju hlorida bakra i oksida bakra Cu_2O.
- U prisustvu macerata hmelja u koncentracijama većim od 10 mL/L na polarizacionim krivama za bakar strujni pikovi se pojavljuju na pozitivnijim potencijalima i pri nižim vrednostima gustine struje (osim za strujni pik koji odgovara procesu adsorpcije) nego na polarizacionoj krivi snimljenoj bez dodatka macerata, na osnovu čega se može zaključiti da macerat hmelja delimično usporava procese koji odgovaraju tim pikovima.

Zahvalnica: *Ovaj rad je finansijski podržan od strane Ministarstva prosvete, nauke i tehnološkog razvoja Republike Srbije (Projekti: TR 34003 i ON 172060).*

Electrochemical behaviour of copper in the presence of hops macerate

The use of plant extracts to inhibit the corrosion of metals and alloys is the subject of numerous scientific researches. In this paper the results of the examination of electrochemical behaviour of copper during its oxidation in a solution of 0.5 mol/dm^3 NaCl in the absence and presence of hops macerate of different concentrations are presented. The electrochemical behaviour of copper was examined by measuring the open circuit potential and by the cyclic voltammetry method. The study using cyclic voltammetry shows that three current peaks corresponding to adsorption and the formation of copper chloride and copper oxide occur on anodic polarization curves. The value of the current density of current peaks corresponding to the formation of copper compounds decreases with the increase in the concentration of hops macerate in the electrolyte over 10 ml/l, which indicates an inhibitory effect.

Literatura:

1. D. Tromans, R. Sun, *J. Electrochem. Soc*., **138** (1991) 3235.
2. G. Kear, B. D. Barker, F. F. Walsh, *Corros. Sci*., **46** (2004) 109.
3. H. Otmačić, E Stupnišek-Lisac, *Electrochem. Acta*, **48** (2003) 985.
4. T. Kosec, I. Milosev, B. Pihlar, *Appl. Surf. Science*, **253** (2007) 8863.
5. Mamas S., Kıyak T., Kabasakaloglu M., Koc A., *Mater. Chem. Phys*., **93** (2005) 41.
6. M. Finšgar, I. Milošev, Corros. Sci., **52** (2010) 2737.
7. A. D. Modestov, G.-D Zhou, Y.-P. Wu, T. Notoya, D. P. Schweinsberg, *Corros. Sci*. **36 (**11) (1994) 1931.

8. V. Grekulović, M. Rajčić Vujasinović, A. Mitovski, *J. Min. Metall. Sect. B-Metall*., **53** (3) (2017) 349.
9. A. M. Abdullah, F. M. Al-Kharafi, B. G. Ateya, *Scripta Mater*., **54** (2006) 1673–1677.
10. M. Rajčić Vujasinović, V. Grekulović, A. Mitovski, Z. Stević, Electrochemical behavior of copper in presence of chestnut macerate, XXV International Scientific and Profesional Meeting Ecological Trith, Proceedings,University of Belgrade-Technical Faculty in Bor, 12.-15. june, hotel "Breza", Vrnjacka Banja, Serbia, (2017) 171-175.
11. M. Rajčić Vujasinović, V. Grekulović, Z. Stević, D. Dragulović, S. Dimitrijević, *Bakar*, **41**, 2 (2016) 35.
12. J. Radošević, *Zaštita materijala*, **53 (**2012) 313.
13. A. M. Shah, A. A. Rahim, S. A. Hamid, S. Yahya*, Int. J. Electrochem. Sci*, **8** (2013) 2140.
14. T. V. Sangeetha, M. Fredimoses, *E-J Chem*., **8** (2011) 51.
15. P. Deepa Rani, S.Selvaraj Emblica, *Appl. Sci. Res*., **2**(6) (2010)140.
16. L. Valek, S. Martinez, *Materials Letters*, **61** (1) (2007) 148.
17. D. A. Todorović, D. D. Milenković, M. M. Milosavljević, D. A. Marković*, Hem. Ind*. **66** (2) (2012) 193.
18. Z. Stević, M. Rajčić-Vujasinović, *Chem. Ind*., 61 (2007) 1-6.

Hemijsko inženjerstvo

Chemical Engineering

Experimental determination and modeling of the sunflower oil ozonization process

Maja Z. Milošević, Mirjana Lj. Kijevčanin, Ivona R. Radović, Jelena M. Vuksanović
Faculty of Technology and Metallurgy, University of Belgrade, Karnegijeva 4, 11120 Belgrade, Serbia

Abstract
Ozonization is a significant reaction in vegetable oil chemistry since the ozonization products are involved in therapeutical application because of its antimicrobial effect. Information on the standard preparation procedures of ozonized sunflower oil is limited. The development of an adequate technology for the effective production of ozonized oil was carried out on the laboratory level. The purpose of this study was to establish an experimental setup using two different types of apparatus in order to optimize the ozonization process. Within the first procedure, the reaction was carried out inside a bubble reactor, while following the second procedure the reaction was performed inside an absorption column. The second procedure gave better results regarding the content of ozonized products in the final sample. It was concluded that the ozonization process should be carried out in a packed-bed absorption column.

Introduction

Ozone is a powerful oxidant, principally applied as a disinfectant of drinking and waste water [1]. Recently, ozone in different forms has also been used in a large number of medical indications [2] due to its ability to damage bacterial nucleic acids [3]. Structural analysis of tRNA has shown that degradation occurs preferentially at guanine residues [4]. The overuse of antibiotics in the treatment of infectious diseases and the appearance of bacterial strains resistant to two or more antibiotics has driven research towards the study of antimicrobial agents from essential oils. Ozone does not contaminate the atmosphere and no bacterial resistance to this substance has been reported so far.

Sunflower oil is obtained from the seed of the sunflower flower. It contains fatty acids and it is rich in linoleic (48–74%) and oleic acids (14–39%) [5]. Sunflower ozonized oil (Oleozon) has remarkable bactericidal properties [6-7], and acts directly on the pathogenic micro-organism without damaging the human epithelium [4]. The Cuban "Centro de estudio the medicamento CECMED" approved the Registration of OLEOZON® in 1999 (no. 1498) after the pre-clinical trial conducted in 1997 which tested the dermal toxicity of Oleozon in rabbits and mice [8]. OLEOZON® is a wide spectrum antimicrobial product with inhibitory and lethal activity on gram-positive and gram-negative bacteria, resistant strains to the antibiotics and mycobacterium species [6].

The reaction of ozone with sunflower oil occurs almost exclusively with the carbon-carbon double bond present in unsaturated fatty acids by the Criegee mechanism [9]. Taking into account the unsaturated fatty acids composition of sunflower oil and the ozone-olefin reaction mechanism, several oxygenated compounds are produced through the ozonization process, such as hydroperoxides, ozonides, aldehydes, peroxides, diperoxides and polyperoxides. The yield of oxygenated compounds from unsaturated oils depends on necessary reaction conditions, such as type of medium where the reaction takes place, presence of additives, reaction temperature, type of the reactor, agitation of the reaction

mixture, applied ozone doses, etc. [9]. The ozonides and peroxides have high germicide effect of great utility in the field of medicine [10].
As for natural preparation ozonized oil is now available in several countries, but information with regards to the chemical data, standard preparations and antimicrobial activity is limited [2]. The purpose of this research is to assembly an experimental setup through which the ozonization process can be conducted in order to form a standard preparation method for the ozonized sunflower oil.

Experimental section

Solvents and reagents

Potassium iodide, sodium thiosulfate, chloroform, glacial acetic acid, phenolphthalein, starch, vegetable sunflower oil. OLEOZON® was produced at the Ozone Research Center.

General ozonization procedure

The ozonization process was carried out in two diverse experimental setups, under the same working conditions.
During the first stage of the studies, a mixture of sunflower oil and water, with volume ratio 10:1, was introduced into a bubble reactor at room temperature of 25 °C. The ozonization process was carried out for 8h in a batch system providing a continuous inlet of ozone. Sample of the final product was taken at the end of the reaction.
During the second stage of the studies, a different apparatus was assembled in order to optimize the amount of ozone contained by the ozonized oil, compared to the product gained in the previous stage. Pure sunflower oil was introduced into a packed-bed absorption column (Figure 1), where the reaction took place in a water bath at room temperature of 25 °C. The ozonization process was carried out in a continuous system for a period of 8 hours after which a sample was taken.

Column:	Height 108cm, Diameter 6cm, Packed-bed height 60 cm
Pump:	Flowrate 2 l/h, Voltage 24 Volt DC
Ozone convertor	Flowrate 35 l/h

Results and discussion

The amount of ozone contained in ozonized oils produced within the processes described in this paper, as well as the amount of ozone found in the commercially available OLEOZON®, was determined. Briefly, 1.5 g of the sample was mixed with glacial acid, chloroform and saturated potassium iodide solution. The mixture was mixed with water and slowly titrated, shaking continuously, with 0.01019 M sodium thiosulfate until the yellow color disappears.
The volumes of the titrant used in order for the discoloration of the prepared solutions to take place for all three samples are shown in Table 1. Based on these values, it is shown that the ozonization process that takes place in an absorption column gives better results than the process conducted within a bubble reactor. Nevertheless, comparison of the results gained for the OLEOZON® sample and the sample of the ozonized oil from the absorption column shows superiority of the previous. Therefore, further optimization of the absorption system and its working conditions hves to be done in order to optimize the procedure and achieve the desired results.

Schematic presentation for the described and assembled absorption system is shown in Figure 2.

Table 1. *Titrant volumes used for the determination of ozone within the samples*

No.	Type of Sample	Mass of the sample, g	Titrant volume, mL
1.	OLEOZON	1.51	5.00
2.	Ozonized oil (glass tube)	1.50	0.1
3.	Ozonized oil (absorption column)	1.50	0.2

For the ozonization process carried out in an absorption column, the model of the process should be created using software Design II in order to virtually determine optimal working conditions of the system.

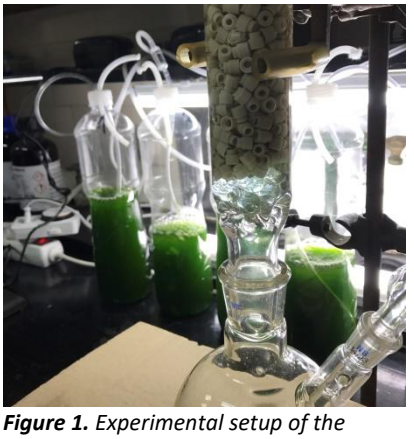

Figure 1. *Experimental setup of the absorption column*

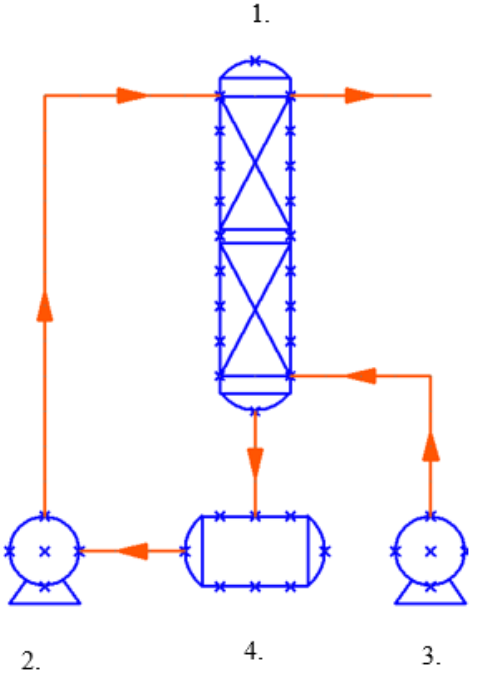

1. Absorption column
2. Peristaltic pump
3. Ozone convertor
4. Round-bottom flask

Figure 2. *Schematics for the ozonization process carried out in an absorption column*

Conclusion

Ozonized sunflower oil, a competitive antimicrobial agent as shown from numerous studies, was produced using two different apparatus, under the same conditions. Taking into consideration the obtained results it can be said that the ozonization process carried out inside an absorption column gives better results regarding the content of the desired products than the ozonization process carried out inside a bubble reactor. A model of the assembled absorption system should be created using software Design II in order to determine optimal working conditions for the ozonization process.

In order to continue with the process optimization, further experimental research should take place, using the information obtained from the software simulations of the process model.

The authors gratefully acknowledge the financial support received from the Research Fund of Ministry of Education, Science and Technological Development (project No 172063), Serbia and the Faculty of Technology and Metallurgy, University of Belgrade.

Eksperimentalno određivanje i modelovanje procesa ozonizacije suncokretovog ulja

Reakcije ozonizacije imaju značajnu ulogu u hemiji jestivih ulja uzimajući u obzir da se ozonizovani proizvodi koriste u medicinske svrhe zbog njihovog antimikrobnog dejstva. Informacije o standardnim postupcima pripreme ozonizovanog suncokretovog ulja u dostupnoj i relevantnoj literaturi je ograničena. Razvijanje adekvatne tehnologije za efektivnu proizvodnju ozonizovanog ulja odrađeno je na laboratorijskom nivou. Cilj ovog istraživanja bio je postavljanje dva različita tipa aparature u cilju optimizacije procesa ozonizacije. U okviru prve procedure, reakcija se odvijala u reaktoru s barbortiranjem, dok se u okviru druge procedure reakcija odvijala u apsorpcionoj koloni. Druga procedura je pokazala bolje rezultate po pitanju sadržaja ozonizovanih proizvoda u finalnom uzorku. Shodno tome, zaključeno je da se proces ozonizacije treba odvijati u kontinualnom sistemu koji uključuje apsorpcionu kolonu s pakovanim slojem.

Literature

1. G. Vanden Bossche, U. Wustmann, S. Krietemeyer, Microbiology Research **149** (1994), 351.
2. S. Menendez, L. Re, L. Falcon, M.B. Argote, I. Mendez, D. Fernandez, B. Elias-Calle, M. Valero, Internation Journal of Ozone Therapy **8** (2008) 25.
3. K. Sawadaishi, K. Miura, E. Ohtsuka, T. Ueda, N. Shinriki, K. Ishizaki, Nucleic Acid Research **3** (1986) 1159
4. N. Shinriki, K. Ishizaki, A. Ikehata, T. Yoshizaki, A. Nomura, K. Miura, Y. Mizuno, Biochimica et Biophysia Acta **655** (1981), 323.
5. F.D. Gunston, J.L. Harwood, F.B. Padley, The Lipid Handbook. Occurrence and Characteristics of Oils and Fats, 2nd ed., Champan & Hall: London (1994).
6. I. Lezcano, N. Nunez, M. Gutierrez, J. Molerio, M.G. Regeieros, W. Diaz, Revista CENIC Ciencias Biologicas **29** (1998), 46.
7. 1. L.A. Sechi, I. Lezcano, N. Nunez, M. Espim, I. Dupre, A. Pinna, P. Molicotti, G. Fadda and S. Zanetti, Journal of Applied Microbiology, **90** (2001) 279.
8. G. Martinez Sanchez, O.S.L. Fernandez, C. Rodriguez Torres, Revista CENIC CIencias Biologicas **28** (1997), 35
9. P. Bailey, Ozonolysis of Olefins: Introduction, Initial Ozone Attack and Adduct; The Peroxides Products. Ozonization in Organic Chemistry, Academy Press: New York (1978).
10. 3. M. F. Díaz, J. A. G. Sazatornil, O. Ledea, F. Hernández, M. Alaiz, R. Garcés, *Ozone-Science & Engineering*, **27** (2005) 247.

Modeling of mixture densities using PC-SAFT equation of state

Mirko Z. Stijepović, Nikola D. Grozdanić, Gorica R. Ivaniš, Mirjana. LJ. Kijevčanin
Faculty of Technology and Metallurgy, University of Belgrade, Karnegijeva 4, 11120 Belgrade, Serbia

Abstract
PC-SAFT equation of state is used for correlation of thermodynamic properties and phase equilibria of both pure components and mixtures. In this work PC-SAFT equation of state was applied to binary mixtures for the correlation of densities in temperature range T=288-15-323.15 K and at atmospheric pressure. Calculations of densities were performed for two binary mixtures, 1-butanol(1)+tetrahydrofurane(2) and 2-butanol(1)+tetrahydrofurane(2). The results show that PC-SAFT model density predictions deviate from experimental value more and more as the fraction of alcohol in mixture increase. This can be explained by increasing impact of hydrogen bonds on density.

Introduction

An efficient development of complex products in chemical industry requires the ability to find the molecular structures with the required funcionality and without undesirable side effects for health or the environment. Therefore, predicting the physical thermodynamic properties of the molecules and the mixtures involved becomes very important. PC-SAFT[1,2,3] equation of state have been widely used for applying to different type of mixtures consisted of small spherical molecules such as gases, non-spherical solvents and polymers. PC-SAFT model require three parameters for non-associating fluids, segment number (m), the interaction energy (ε/k), and the hard-core segment diameter (σ) that are typically estimated from liquid density data over extended temperature ranges.
In our previous study[4], we successfully applied PC-SAFT model determinating the new sets of parameters and calculating densities of pure components. In this work, PC-SAFT model will be applied to solvent mixtures of tetrahydrofurane and two alcohols, 1-butanol and 2-butanol. Experimental densities for these two systems were determined in our previous works[5, 6].

Modeling

PC-SAFT is non-cubic equation of state and unlike cubic equations of state it does not rely on critical properties of molecules such as critical pressure, critical temperature, critical volume, *etc.* PC-SAFT require other parameters that can be determined from density and vapor pressure experimental data that can be easily measured.
The residual Helmholtz free energy is used for characterizing specific molecules and it is represented as a sum of molecular contributions, the hard-chain reference contribution and the dispersion contribution:

$$a^{\text{res}} = a^{\text{hs}} + a^{\text{disp}} \qquad (1)$$

where a represents Helmholtz free energy per mole.
The hard-sphere term can be expressed as:

$$a^{\text{hs}} = \frac{1}{\zeta_0}\left[\frac{3\zeta_1\zeta_2}{(1-\zeta_3)} + \frac{\zeta_2^3}{\zeta_3(1-\zeta_3)^2} + \left(\frac{\zeta_2^3}{\zeta_3^2} - \zeta_0\right) ln(1-\zeta_3)\right] \quad (2)$$

and

$$\varepsilon_n = \frac{\pi}{6}\rho\sum_i x_i m_i d_i^n \quad n \in \{0,1,2,3\} \quad (3)$$

$$d_i = \sigma_i\left[1 - 0.12\exp\left(-3\frac{\epsilon_i}{kT}\right)\right] \quad (4)$$

where x_i represents mole fraction of chains and d_i is temperature dependent segment diameter[3].

The dispersion term attempts to describe dispersion attraction between whole chains. Dispersion contributions in PC-SAFT model can be calculated as:

$$a^{\text{disp}} = -2\pi\rho I_1(\eta,\bar{m})\overline{m^2\epsilon\sigma^3} - \pi\rho\bar{m}C_1 I_2(\eta,\bar{m})\overline{m^2\epsilon^2\sigma^3} \quad (5)$$

$$C_1 = \left(1 + \bar{m}\frac{8\eta - 2\eta^2}{(1-\eta)^4} + (1-\bar{m})\frac{20\eta - 27\eta^2 + 12\eta^3 - 2\eta^4}{\left[(1-\eta)(2-\eta)\right]^2}\right)^{-1} \quad (6)$$

$$\bar{m} = \sum_i x_i m_i \quad (7)$$

$$\overline{m^2\epsilon\sigma^3} = \sum_i\sum_j x_i x_j m_i m_j\left(\frac{\epsilon_{ij}}{kT}\right)\sigma_{ij}^3 \quad (8)$$

$$\overline{m^2\epsilon^2\sigma^3} = \sum_i\sum_j x_i x_j m_i m_j\left(\frac{\epsilon_{ij}}{kT}\right)^2\sigma_{ij}^3 \quad (9)$$

The ε_{ij} parameter, the cross-diameter σ_{ij} and the interaction parameter k_{ij} are given as:

$$\sigma_{ij} = \frac{1}{2}(\sigma_i + \sigma_j) \quad (10)$$

$$\epsilon_{ij} = \sqrt{\epsilon_i\epsilon_j}(1-k_{ij}) \quad (11)$$

$$I_1(\eta,\bar{m}) = \sum_{i=0}^{6} a_i(\bar{m})\eta^i \quad (12)$$

$$I_2(\eta,\bar{m}) = \sum_{i=0}^{6} b_i(\bar{m})\eta^i \quad (13)$$

$$a_i(\bar{m}) = a_{0i} + \frac{\bar{m}-1}{\bar{m}}a_{1i} + \frac{\bar{m}-1}{\bar{m}}\frac{\bar{m}-2}{\bar{m}}a_{2i} \quad (14)$$

$$b_i\left(\bar{m}\right) = b_{0i} + \frac{\bar{m}-1}{\bar{m}} b_{1i} + \frac{\bar{m}-1}{\bar{m}} \frac{\bar{m}-2}{\bar{m}} b_{2i} \tag{15}$$

Equations (12)-(15) were developed using the Lennard-Jones potential and the radial distribution function of O'Lenic *et al.*[7]. Mixing rules are needed in the dispersion term of the PC-SAFT equation eq. (7). PC-SAFT model can describe phase equilibria for a non-associating mixtures varying in complexity and asymmetry using a single system-dependent interaction parameter. The interaction parameter k_{ij} is introduced to correct the dispersion energies of unlike molecules.

$$-\left(\frac{\partial a^{res}}{\partial V}\right)_T = p^{\text{res}} \tag{16}$$

$$p = p^{\text{id}} + p^{\text{res}} \tag{17}$$

$$\rho^2\left(\frac{\partial a^{\text{res}}}{\partial \rho}\right)_T = p^{\text{res}} \tag{18}$$

$$p = kT\rho\left(10^{30}\frac{A}{m}\right)\left(1+\rho\left(\frac{\partial a^{\text{res}}}{\partial \rho}\right)\right) \tag{19}$$

Objective function is defined as:

$$f = \sum_{i=1}^{N} \frac{\left(\rho^{\text{exp}} - \rho^{cal}\right)^2}{\left(\rho^{\text{exp}}\right)^2} \tag{20}$$

The densities using PC-SAFT equation of state were estimated using second order forward differentiation formula and given by the following expression:

$$\frac{\partial a^{\text{res}}}{\partial \rho} = \frac{a^{\text{res}}\left(\rho+2\Delta\rho\right) + 4a^{\text{res}}\left(\rho+\Delta\rho\right) - 3a^{\text{res}}\left(\rho\right)}{2\Delta\rho} \tag{21}$$

Results and disscusion

Densities of two binary systems, 1-butanol+tetrahydrofurane and 2-butanol+tetrahydrofurane, were calculated using PC-SAFT equation of state and compared with previously published values of density measured in our laboratory[5, 6] showing not so good agreement. Table 1 shows average percent deviations and total percent deviations for 1-butanol+tetrahydrofurane and 2-butanol+tetrahydrofurane, at temperature range T=288.15--323.15 K.

The estimated densities for two binary mixtures are presented graphically in Fig. 1. The results show that PC-SAFT model density predictions deviate from experimental value more and more as the fraction of alcohol in mixture increase. This can be explained by increasing impact of hydrogen bonds on density.

Table 1. *Average percent deviation and total percent deviation for two binary systems, 1-butanol+tetrahydrofurane and 2-butanol+tetrahydrofurane at temperature range T=288.15-323.15 K and atmospheric pressure*

T / K	1-butanol+tetrahydrofurane		2-butanol+tetrahydrofurane	
	Average percent deviation, %	Absolute percent deviation, %	Average percent deviation, %	Absolute percent deviation, %
288.15	4.8040		5.4244	
293.15	4.7317		5.3553	
298.15	4.6649		5.2916	
303.15	4.6037		5.2328	
308.15	4.5481		5.1789	
313.15	4.5084		5.1303	
318.15	4.4769		5.0867	
323.15	4.4513	4.5986	5.0488	5.2186

a) b)

Fig. 1. *The comparison of calculated density data (symbols) for a) 1-butanol+tetrahydrofurane and b) 2-butanol+tetrahydrofurane with experimental values (lines) at temperature range T=288.15-323.15 K and atmospheric presure using PC-SAFT model.*

Conclusion

The goal of this work was to demonstrate the applicability of the PC-SAFT equation of state on two binary mixtures of 1-butanol(1)+tetrahydrofurane(2) and 2-butanol(1)+tetra-hydrofurane(2). The average percent deviations and absolute percent deviations obtained by PC-SAFT model for both systems were higher probably because of the assumption that those components are capable to form homoassociates.

Acknowledgement: *The authors gratefully acknowledge the financial support received from the Research Fund of Ministry of Science and Environmental Protection, Serbia and the Faculty of Technology and Metallurgy, University of Belgrade (Project No. 172063).*

Modelovanje gustina binarnih smeša korišćenjem PC-SAFT jednačine stanja

PC-SAFT jednačina stanja koristi se za korelisanje termodinamičkih osobina i fazne ravnoteže kako čistih komponenti tako i njihovih smeša. U ovom radu PC-SAFT jednačina stanja primenjena je na binarnim smešama za korelisanje gustina u temperaturnom opsegu

T=288.15-323.15 K i pri atmosferskom pritisku. Izračunavanje gustina izvedeno je za dve binarne smeše, 1-butanol(1)+tetrahidrofuran(2) i 2-butanol(1)+tetrahidrofuran(2). Rezultati pokazuju da predvidjanje gustina pomoću PC-SAFT modela sve više odstupa od eksperimentalnih vrednosti sa povećanjem udela alkohola u smeši. To se može objasniti povećanim uticajem vodoničnih veza na gustine.

Literature:

1. G. M. Kontogeorgis, G. K. Folas, *Thermodynamic Models for Industrial Applications: From Classical and Advanced Mixing Rules to Association Theories*, John Wiley & Sons, Wiltshire, 2010.
2. J. Gross, G. Sadowski, Ind. Eng. Chem. Res., **40** (2001) 1244.
3. S. H. Huang, M. Radosz, Ind. Eng. Chem. Res., **29** (1990) 2284.
4. J. Ilić Pajić, M. Stijepović, G. Ivaniš, I. Radović, J. Stajić Trošić and M. Kijevčanin, *J. Serb. Chem. Soc.*, **82** (2017) 1.
5. A. Knežević-Stevanović, S. Šerbanović, I. Radović, B. Djordjević and M. Kijevčanin, *J. Chem. Eng. Data*, **58** (2013) 2932.
6. A. Knežević-Stevanović, I. Radović and M. Kijevčanin, to be published.
7. R. O'Lenick, X.J. Li, Y.C. Chiew, *Mol. Phys.,* **86** (1995) 1123.

Viscosity modeling of binary mixtures ethyl butyrate + n-alcohol

Divna M. Majstorović, Emila M. Živković, Jovan D. Jovanović, Mirjana Lj. Kijevčanin
Faculty of Technology and Metallurgy, University of Belgrade, Karnegijeva 4, 11120 Belgrade, Serbia

Abstract
Modeling of viscosity of three binary ethyl butyrate + n-alcohol mixtures was done using predictive UNIFAC-VISCO and ASOG-VISCO models. Group contribution based models are suitable for obtaining quick evaluations of thermophysical properties under different conditions of temperature, pressure and composition. The significance of the predictive approach is that the mixture viscosity could be calculated from the pure component data and the interaction parameters between functional groups present in the system. However, having in mind the fact that correlative models often lead to better results, the viscosity data were also correlated by Teja-Rice, Grunberg-Nissan, McAllister, Eyring-UNIQUAC and Eyring-NRTL models. Correlative models involve interaction parameters (one or more) obtained by some optimization technique. These models require some experimental data in order to establish the value of an interaction parameter specific for each mixture for the defined temperature and pressure. All correlative models for investigated mixtures give very good results with percentage deviations within 2%. Predictive models can be used to calculate viscosity of investigated systems only on higher temperatures.

Introduction
The food industry includes a large part of production that cannot be imagined without food additives. Substances present in wine production are, among other, also used for this purpose. Some of these substances can only be isolated from wine production. Wine is a complex mixture of chemical compounds which consists of more than 800 components that contribute to its aroma[1-5].
Esters as a group are the next largest wine constituent, after water, ethanol and fusel alcohols, and the primary source of fruit aromas. Ethyl butyrate is one of the most commonly used substances as artificial flavor due to its favorable properties and low price. The reported concentrations[6] of this ester in wine are from 0.07 to 0.53 $mg \cdot l^{-1}$. The natural odor of this substance is the most similar to pineapple and is very often used in the industry as an additive to orange juice.
Fusel, or higher alcohols, are alcohols that have more than two carbon atoms[7]. These alcohols are formed in small amounts by yeast metabolism during the fermentation process. They form from either sugar or amino acids, which are transformed into alcohols through a series of reactions. These alcohols also have an effect on wine aroma, positive or negative. Their total concentration in the wine is between 100 - 500 $mg \cdot l^{-1}$.
Binary mixtures of wine congeners have been analyzed before[8-11], but in this work viscosity of three binary mixtures of ethyl butyrate and n-alcohol is calculated using predictive and correlative models.
Based on experimental data for viscosity[12], it is possible to test its prediction and correlation capabilities using different models. In modeling thermodynamic properties, it is important to have insight into limitations associated with different approaches[13]. The advantage of predictive approach is that viscosity of the mixture can be calculated using only viscosity

data of pure components and interaction parameters between functional groups present in component molecules. On the other hand, correlative models usually obtain better results, but experimental data for mixture viscosity are necessary in order to determine the parameter(s), which then can be applied only to certain temperature and pressure conditions.

In this study, predictive UNIFAC-VISCO[14,15] and ASOG-VISCO[16] models, as well as correlative Teja-Rice[17,18], Grunberg-Nissan[19], Eyring-UNIQUAC[20], Eyring-NRTL[21] and McAllister[22] models have been selected to calculate viscosity of three binary mixtures, ethyl butyrate + + 1-propanol / 1-butanol or 1-hexanol.

Results and discussion

The quality of models used in this paper for predicting and correlating measured data for the viscosity of binary systems ethyl butyrate + *n*-alcohol is estimated by calculating the percentage deviation (PD_{max}) using the equation:

$$PD_{\max} = \frac{100}{N}\sum_{i=1}^{N}\left(\frac{\eta_{\exp}-\eta_{\text{calc}}}{\eta_{\exp,\max}}\right)_i \quad (1)$$

where $\eta_{\exp}$ and η_{cal} are experimental and calculated viscosity values, and $\eta_{\exp,\max}$ is the maximum value of the experimental η.

The percentage deviations values for all models at each of the temperatures are given in Table 1.

In order to obtain correlative model parameters, Marquardt optimization technique[23] was used to minimize the target function, given by the equation:

$$OF = \frac{1}{m}\sum_{i=1}^{m}\left(\frac{\eta_{i,\exp}-\eta_{i,\text{calc}}}{\eta_{i,\exp}}\right)^2 \rightarrow \min \quad (2)$$

For these systems, UNIFAC-VISCO and ASOG-VISCO models were used as purely predictive models because all interaction parameters of the groups present in the investigated compounds are known, and can be found in original works[14-16].

For the correlative Eyring-NRTL model two values of PD_{max} were calculated. The first value is observed for the Eyring-NRTL model as a two-parameter, where α has a value of 0.3, and the other where parameter α as optimized, so the model is considered as a three-parameter.

For systems with ethyl butyrate, the McAllister-4 model yields the best results, but other correlative models, except Teja-Rice and Grunberg-Nissan, also give percentage deviations below 1 %. In Figure 1 the results of viscosity modeling of the ethyl butyrate + 1-propanol system at 298.15 K are shown for some of models.

The general conclusion is that correlative models with a higher number of parameters give better results. For one-parameter models, the smaller values of the percentage deviations are mainly with the Teja-Rice model, except for the system with 1-hexanol. Between two-parameter McAllister-3 and Eyring-UNIQUAC models, Eyring model gives better results. As far as three-parameter models are concerned, McAllister-4 model gives slightly lower deviations than the Eyring-NRTL model with the optimized α parameter.

Table 1. *The results of predicting the viscosity of binary mixtures ethyl butyrate (1) + n-alcohol (2) with UNIFAC-VISCO and ASOG-VISCO models, and correlation with Teja-Rice, Grunberg-Nissan, McAlister, Eyring-UNIQUAC and Eyring-NRTL models.*

T / K	PD_{max} / %								
	Predictive approach		Correlative *approach*						
	UNIFAC-VISCO	ASOG-VISCO	Teja-Rice	Grunberg-Nissan	McAllister-3	McAllister-4	Eyring-UNIQUAC	Eyring-NRTL	
ethylbutyrate (1) + 1-propanol (2)									
288.15	7.43	16.18	1.82	3.08	0.64	0.09	0.25	0.66[a]	0.15[b]
293.15	6.51	9.13	1.66	2.96	0.60	0.06	0.22	0.67	0.13
298.15	5.67	5.69	1.53	2.82	0.58	0.04	0.19	0.67	0.13
303.15	4.69	5.02	1.35	2.61	0.50	0.06	0.25	0.61	0.14
308.15	3.88	5.33	1.25	2.51	0.47	0.10	0.22	0.65	0.17
313.15	3.14	5.81	1.13	2.38	0.42	0.15	0.27	0.63	0.21
318.15	2.54	6.68	0.99	2.22	0.37	0.20	0.30	0.58	0.24
323.15	2.18	8.35	0.92	2.15	0.40	0.28	0.35	0.64	0.30
ethyl butyrate (1) + 1-butanol (2)									
288.15	6.43	16.23	2.01	2.31	0.46	0.11	0.14	0.18[a]	0.10[b]
293.15	5.85	10.16	2.03	2.34	0.64	0.26	0.32	0.37	0.36
298.15	5.04	6.65	1.83	2.15	0.50	0.10	0.20	0.25	0.19
303.15	4.29	5.55	1.73	2.12	0.48	0.09	0.21	0.28	0.19
308.15	3.50	5.62	1.65	2.06	0.51	0.11	0.23	0.31	0.24
313.15	2.67	6.03	1.48	1.84	0.50	0.09	0.28	0.29	0.26
318.15	2.16	7.33	1.42	1.86	0.48	0.09	0.25	0.26	0.24
323.15	1.74	9.04	1.20	1.69	0.34	0.13	0.17	0.26	0.17
ethyl butyrate (1) + 1-hexanol (2)									
288.15	4.95	15.15	2.26	1.34	0.30	0.04	0.22	0.17[a]	0.09[b]
293.15	4.38	10.03	2.16	1.35	0.30	0.04	0.25	0.18	0.10
298.15	3.77	7.26	2.04	1.32	0.32	0.05	0.32	0.20	0.12
303.15	3.13	6.02	1.93	1.30	0.31	0.07	0.31	0.20	0.13
308.15	2.40	5.79	1.79	1.23	0.29	0.05	0.29	0.19	0.13
313.15	1.75	6.22	1.65	1.15	0.29	0.04	0.31	0.18	0.15
318.15	1.31	7.23	1.51	1.08	0.27	0.04	0.27	0.18	0.14
323.15	1.08	8.53	1.34	1.00	0.24	0.11	0.26	0.17	0.16

[a]Eyring-NRTL as two-parameter model (α = 0.30)

[b]Eyring-NRTL as three-parameter model (optimized α)

In Figure 2(b)-(d) differences between models with same number of parameters are presented for system ethyl butyrate + 1-butanol at 298.15 K. It can be noticed that, although differences between PD_{max} values in Table 1 exist, even models with one parameter follow the trend of experimental points and can be used to calculate viscosity. Differences between models with two and three parameters are actually negligible.

Predictive models give generally higher values of percentage deviations, from 1% to 16%. PD_{max} values depend on the system, but even more on the temperature for the same system. It can be noticed that of these two models UNIFAC-VISCO is better for investigated systems with ethyl butyrate (Figure 2(a)).

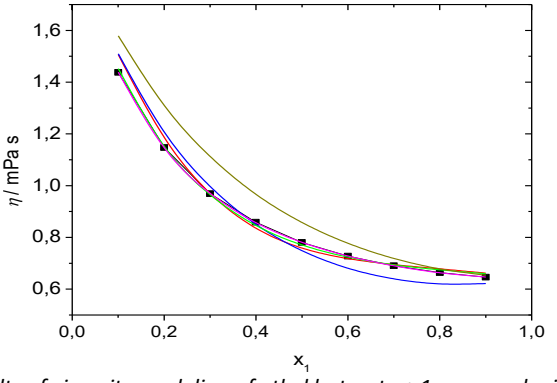

Figure 1. Results of viscosity modeling of ethyl butyrate + 1-propanol mixture at 298.15 K: (■) experimental data, (—) UNIFAC-VISCO, (—) Teja-Rice, (—) Grunberg-Nissan,(—) McAllister-3, (—) McAllister-4 models.

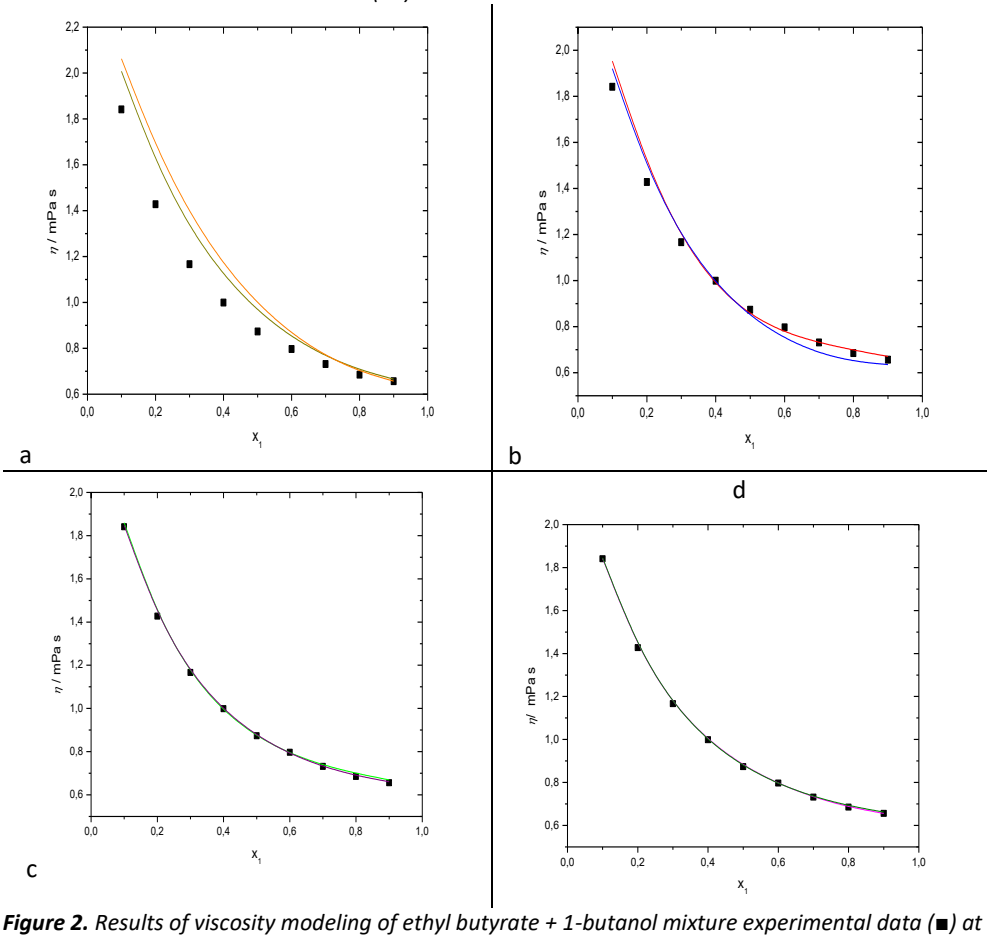

Figure 2. *Results of viscosity modeling of ethyl butyrate + 1-butanol mixture experimental data (■) at 298.15 K with: (a) predictive (—) UNIFAC-VISCO and (—) ASOG-VISCO models, (b) one-parameter*

(—) Teja-Rice and (—) Grunberg-Nissan models, (c) two-parameter (—) McAllister-3 and (—) Eyring-UNIQUAC models, and (d) three-parameter (—) McAllister-4 and (—) Eyring-NRTL models.

On Figure 3 results of viscosity modeling for system ethyl butyrate + 1-hexanol at 298.15 K for some models are presented. From the graph the above mentioned statements can be confirmed; both two- and three-parameter models follow experimental points very well.

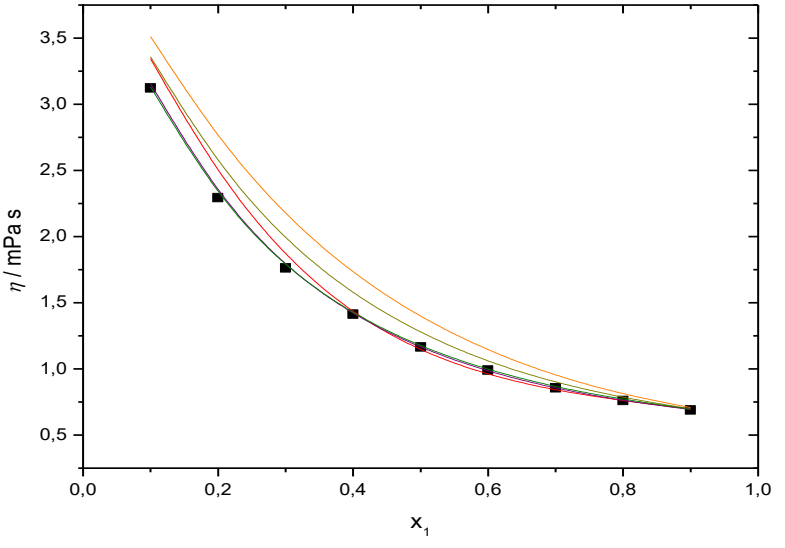

Figure 3. *Results of viscosity modeling of ethyl butyrate + 1-hexanol mixture at 298.15 K: (■) experimental data, (—) UNIFAC-VISCO, (—) ASOG-VISCO, (—) Teja-Rice, (—) Eyring-UNIQUAC and (—) Eyring-NRTL models.*

Conclusion

The viscosity, as one of the most important property used in numerous chemical-engineering correlations for fluid flow analysis and mass and heat transfer calculations, were calculated using predictive (UNIFAC-VISCO, ASOG-VISCO) and correlative (Teja-Rice, Grunberg-Nissan, Eyring-UNIQUAC, Eyring-NRTL, McAllister-3 and McAllister-4) models. The quality of the results obtained for each of the mentioned models was determined by comparison with the experimentally measured values. The predictive UNIFAC-VISCO model for all systems gives better results than the ASOG-VISCO model. The Teja-Rice one-parameter model is generally better than the Grunberg-Nissan model. Eyring-UNIQUAC model better correlates viscosity data of systems with ethyl butyrate than McAllister-3. The McAllister-4 model gives excellent results, however not as good as the three-parameter Eyring-NRTL model. Two-parameter Eyring-NRTL is better for some systems than the other two tested models with two parameters, but for system with 1-propanol higher PD_{max} values are obtained. It cannot be concluded that the length of a chain of alcohol effects on the results of the viscosity modeling.

The authors gratefully acknowledge the financial support received from the Research Fund of Ministry of Education, Science and Technological Development, Serbia and the Faculty of Technology and Metallurgy, University of Belgrade (project No 172063).

Modelovanje viskoznosti binarnih smeša etilbutirat + n-alkohol

Modelovanje viskoznosti tri binarne etil butirat + n-alkohol smeše urađeno je koristeći prediktivne UNIFAC-VISCO i ASOG-VISCO modele. Modeli doprinosa grupa su pogodni za brzo izračunavanje termofizičkih veličina pri različitim uslovima temperature, pritiska i udela. Njihov značaj je u tome što se viskoznost smeše može izračunati samo iz podataka za čiste komponente i interakcione parametre između funkcionalnih grupa prisutnih u sistemu. Međutim, imajući u vidu da korelativni modeli uglavnom daju bolje rezultate, podaci za viskoznost su takođe korelisani Teja-Rice, Grunberg-Nissan, McAlister, Eyring-UNIQUAC i Eyring-NRTL modelima. Korelativni modeli koriste interakcione parametre (jedan ili više), dobijene nekom od optimizacionih tehnika. Ovi modeli zahtevaju eksperimentalne podatke da bi se odredile vrednosti interakcionih parametara posebne za svaku smešu za definisane uslove temperature i pritiska. Svi korelativni modeli za ispitivane smeše daju veoma dobre rezultate sa vrednostima procentualnih odstupanja do 2 %. Prediktivni modeli mogu da se koriste za računanje viskoznosti ispitivanih sistema uglavnom na višim temperaturama.

Literature

1. M. Ortega-Heras, M. L. González-SanJosé, S. Beltrán, *Anal. Chim. Acta* **458** (2002) 85.
2. M. Aznar, T. Arroyo, *J. Chromatogr. A* **1165** (2007) 151.
3. V. Ferreira, R. Lopez, J. F. Cacho, *J. Sci. Food Agric.* **80** (2000) 1659−1667.
4. M. J. Gómez-Míguez, J. F. Cacho, V. Ferreira, I. M. Vicario, F. J. Heredia, *Food Chem.* **100** (2007) 1464.
5. H. Guth, *J. Agric. Food Chem.* **45** (1997) 3027.
6. K. M. Sumby, P. R. Grbin, V. Jiranek, *Food Chem.* **121** (2010) 1.
7. Waterhouse Lab, http://waterhouse.ucdavis.edu/whats-in-wine/higher-alcohols, (15.5.2018.)
8. C. A. Faúndez, J. O. Valderrama, *J. Food Eng.* **65** (2004) 577.
9. J. M. Resa, C. Gonzalez, J. M. Goenaga, *J. Chem.Eng. Data* **50** (2005) 1570.
10. J. M. Resa, E. A. Cepeda, J. M. Goenaga, A. Ramos, S. Aguirre, C. Urbano, *J. Chem. Eng. Data* **55** (2010) 1017.
11. J. M. Resa, J. M. Goenaga, A. I. Sanchez, *J. Chem. Eng. Data* **51** (2006) 1294.
12. D. M. Bajić, E. M. Živković, S. S. Šerbanović, M. Lj. Kijevčanin, *J. Chem. Eng. Data* **59** (2014) 3677.
13. D. M. Bajić, S. P. Šerbanović, E. M. Živković, J. Jovanović, M. Lj. Kijevčanin, *J. Mol. Liq.* **197** (2014) 1.
14. J. L. Chevalier, P. Petrino, Y. Gaston-Bonhomme, *Chem. Eng. Sci.* **43** (1988) 1303.
15. Y. Gaston-Bonhomme, P. Petrino, J. L. Chevalier, *Chem. Eng. Sci.* **49** (1994) 1799.
16. K. Tochigi, K. Yoshino, V. K. Rattan, *Int. J. Thermophys.* **26** (2005) 413.
17. A. S. Teja, P. Rice, *Ind. Eng. Chem. Fundam.* **20** (1981) 77.
18. A. S. Teja, P. Rice, *Chem. Eng. Sci.* **36** (1981) 7.
19. L. Grunberg, A. H. Nissan, *Nature* **164** (1949) 799.
20. R. J. Martins, M. J. E. D. Cardoso, O. E. Barcia, *Ind. Eng. Chem. Res.* **39** (2000) 849.
21. L. T. Novak, *Ind. Eng. Chem. Res.* **43** (2004) 2602.
22. R. A. McAllister, *AIChE J.* **6** (1960) 427.
23. D. W. Marquardt, *J. Soc. Ind. Appl. Math.* **11** (1963) 431.

Tekstilno inženjerstvo
Textile Engineering

The influence of the content of hemicelluloses on moisture sorption and effective relative dielectric permeability of alkali modified jute woven fabrics

Aleksandra Ivanovska, Mirjana Kostic, Dragana Cerovic*, Koviljka Asanovic
Department of Textile Engineering, Faculty of Technology and Metallurgy, Karnegijeva 4, 11000 Belgrade, Serbia
**The College of Textile Design, Technology and Management, Starine Novaka 24, 11000 Belgrade, Serbia*

In this investigation, the influence of alkali modification conditions on the chemical composition, *i.e.* content of hemicelluloses, moisture sorption and effective relative dielectric permeability of jute woven fabric were studied. In that purpose, jute woven fabric has been alkali modified with NaOH solution (1 %, 5 % and 17.5 %) at room temperature for different periods of time (5 and 30 min). Compared to the unmodified, the alkali modified fabrics have lower hemicelluloses content and higher moisture sorption. With decreasing the content of hemicelluloses, and increasing the moisture sorption, values of effective relative dielectric permeability of investigated jute woven fabrics increased.

Key words: *jute woven fabric, alkali modification, hemicelluloses, moisture sorption, effective relative dielectric permeability*

Introduction

Jute (*Corchorus capsularis* and *Corchorus olitorius*) is one of the best known and most extensively used textile fiber, with the exception of cotton. According to the International Jute Study Group, traditionally jute has been used to manufacture packaging materials such as hessian, sacking, ropes, twines, carpet backing cloth, *etc*. The major breakthrough in the uses of jute came when the industries of automobile, pulp, paper as well as the furniture and bedding started to use jute fibers in order to manufacture 'non-wovens' and other technical textiles and composites[1,2].

Jute fibers have three principal chemical constituents, namely: α-cellulose, hemicelluloses, and lignin. α-cellulose forms the bulk of the ultimate cell walls with the molecular chains lying broadly parallel to the direction of the fiber axis. The hemicelluloses consist of polysaccharides of comparatively low molecular weight built up from hexoses, pentoses and uronic acid residues. The third major constituent, lignin, is a high molecular weight polyphenolic polymer with a three-dimensional network, which, like hemicelluloses varies in composition from one type of plant material to another [3,4].

Jute fibers have been subjected to various types of chemical modifications to improve their suitability as textile materials and reinforcing materials in composites. The available literature[5,6] reveals that alkali modification removes one of jute fiber's cementing materials, hemicelluloses, depending on the concentration of used alkali, time and temperature of treatment, liquor ratio, and so on. Many researchers investigated the influence of alkali modification on structural and mechanical properties[7-11] of jute fibers. According to the literature survey, most of the previous works on dielectric properties have been conducted on jute based composites[12-14]. The results of our investigation should provide useful

additional information on the influence of alkali treatment conditions on effective relative dielectric permeability and relationship between content of hemicelluloses, moisture sorption and effective relative dielectric permeability of jute fabrics. The importance of determining the effective relative dielectric permeability of jute fabrics lies in the fact that this dielectric parameter, which describes the polarization in the material, is an indirect indicator of the tendency of fibrous materials to generate static electricity[15].

Materials and methods

Materials

A commercially produced raw jute plain woven fabric with the chemical composition: 1.88 % water soluble components, 1.92 % fats and waxes, 0.84 % pectin, 13.48 % lignin, 21.76 % hemicelluloses and 60.09 % α-cellulose was used in this investigation as experimental material. All used chemical agents obtained from commercial sources were of analytical grade and used without further purification.

According to the procedure described in literature[16], raw jute fabric was subjected to alkali modifications in order to partially remove hemicelluloses and keep the lignin content unchanged. Jute woven fabric was treated with 1 % and 17.5 % NaOH solution, 1:50 liquid ratio, at room temperature for 30 min and with 5 % and 17.5 % NaOH solution, 1:50 liquid ratio, at room temperature for 5 min. Alkali treatments were followed by neutralization with 1 % acetic acid, than, jute fabrics were rinsed with 0.5% $NaHCO_3$, washed and dried at room temperature for 72 h. In all, four alkali modified samples (H30/1, H5/5, H5/17.5, and H30/17.5) and unmodified sample (C) were prepared for investigation, Table 1.

Methods

Jute woven fabrics were characterised regarding their chemical composition and subjected to alkali modifications in order to form a knowledge-base for how different content of hemicelluloses and different moisture sorption affects the effectrive relaive dielectric permeability.

The weight loss, as a consequence of partial removal of hemicelluloses after different chemical modifications of jute woven fabrics, was determined by direct gravimetric method. The chemical composition of jute fabrics was determined according to the scheme of Soutar and Bryden[16] by successive removal of non-cellulosic components. After that, α-cellulose remains as a solid residue.

Moisture sorption was calculated as a weight percentage of absolutely dry material, according to thermo gravimetric method using – Infrared Moisture Analyzer MA35.

Effective relative dielectric permeability was determined at room temperature, 22 °C and 30 % relative humidity. Investigation of effective relative dielectric permeability was carried out by using the Precise LCR Hameg 8118 at three different frequency of 30 Hz, 300Hz and 30 kHz. The instrument was coupled to a LD-3 Rigid Dielectric Cell 3-terminal (guarded) in which the samples in form of thin disks (63.5 mm in diameter) was placed. The spacing of the electrodes was equal to the thickness of the sample. The susceptance B (S) and susceptance of an empty cell, B_0 (S), were obtained directly from the bridge from which the effective relative dielectric permeability (ε'_m) was calculated according to the following equation:

$$\varepsilon'_m = \frac{B}{B_0} \quad (1)$$

ε'_m refers to the fiber-air-moisture system.

Results and discussion

The influence of different alkali modifications on the weight loss and chemical composition of jute woven fabrics

The sample codes and explanations of unmodified and alkali modified jute woven fabrics together with the weight loss and chemical composition after different alkali modifications are given in Table 1.

The effects of alkali modification conditions on the chemical composition of jute woven fabrics are generally characterized by the weight loss. In all cases of jute fabric modifications, it is evident that loss in weight increased proportionally to the increase of the modification time and concentration of NaOH, Table 1. The highest weight loss (12.07%) occurred when jute woven fabric was treated with 17.5% NaOH for 30 min (sample H30/17.5). This is in agreement with the literature data[5,6,11,17].

Table 1. *Weight loss and chemical composition of unmodified and alkali modified jute woven fabrics*

Sample code	Explanation	Weight loss, %	Content of Hemi-celluloses, %	Content of lignin, %	Moisture sorption, %
C	Control, unmodified	/	21.76	13.48	8.26
H30/1	1% NaOH, 30 min	5.87	17.87	13.68	8.65
H5/5	5% NaOH, 5 min	7.67	16.28	12.64	8.69
H5/17.5	17.5% NaOH, 5 min	9.98	13.85	13.11	9.01
H30/17.5	17.5% NaOH, 30 min	12.07	11.97	13.27	9.38

The obtained results clearly showed that partial removal of hemicelluloses can be achieved by modification of jute woven fabric with NaOH. Many researchers came to the same results for different bast fibers: jute[5,6], hemp[18-20] and flax[21,22]. There was an evident tendency that the content of hemicelluloses decreased with increasing the concentration of NaOH, Table 1. During 30 min modification of jute fabric with 1 % NaOH (sample H30/1), the content of hemicelluloses decreased for 17.9%, while in the case of treatment with 17.5 % NaOH during the same time (sample H30/17.5), content of hemicelluloses decreased for 45.0%, compared to the unmodified fabric. During 5 min modification of jute woven fabric with 5% NaOH (sample H5/5), the content of hemicelluloses decreased for 25.2 %, while in the case of treatment with 17.5 % NaOH during the same time (sample H5/17.5), content of hemicelluloses decreased for 36.4%, compared to the unmodified fabric. These results are comparable with the results obtained for jute and other bast fibers reported in the literature[6,20,22]. On the basis of the presented results, it is evident that both concentrations of NaOH, as well as the duration of modification, have influence on the content of hemicelluloses. In the case of chemical modification with 17.5 % NaOH, with increasing the modification time from 5 min (sample H5/17.5) to 30 min (H30/17.5), content of hemicelluloses decreased for 13.6 %, Table 1. Certain content of residues of hemicelluloses after alkali modifications could be explained by existing the strong hydrogen bonds between hemicelluloses and cellulose fibrils[20,22]. Also, it is clear that after chemical modifications with

NaOH, lignin content remains almost unchanged. This occurs as a result of presence of strong carbon-carbon linkages and other chemical groups (aromatic) in the lignin which contributed to its limited degradation or fragmentation[20,23,24].

The influence of different chemical modifications on the moisture sorption of jute woven fabrics

Due to the presence of free hydroxyl groups in jute amorphous regions and at the crystallite's surfaces, the moisture sorption of jute fibers is high (8.26 % for unmodified jute fabric). Moisture sorption values provide information on the extent of areas accessible to water vapor within the fiber[2]. The obtained data (Table 1) showed that hemicelluloses removal increased the moisture sorption of jute woven fabrics compared to the unmodified fabric.

With decreasing the hemicelluloses content for about 18, 25, 36 and 45 % for H30/1, H5/5, H5/17.5 and H30/17.5, moisture sorption values increased for 4.7, 5.2, 9.1 and 13.6 %, respectively. Due to the penetration of NaOH and fiber swelling, many hydrogen bonds are broken and it is expected that the number of available hydroxyl groups is increased[25]. Also, chemical modification with NaOH causes some disorientation of fibrils and changed the amorphous and crystallinity region ratio, in favor to amorphous one[18,20]. This increase in the portion of amorphous part is directly related to the moisture sorption. There is small difference (about 4 %) between moisture sorption values of jute fabrics modified with 17,5% NaOH (sample H5/17.5 and H30/17.5). High coefficient of negative linear correlation (r = -0.98) between content of hemicelluloses and moisture sorption prove that content of hemicelluloses has significant influence on the moisture sorption.

The influence of different alkali modifications on effective relative dielectric permeability of jute woven fabrics

Jute woven fabric is a non-homogenous material with a very complex structure. Because of that, dielectric behavior of jute fabrics in real conditions of use depends on various factors such as chemical composition, moisture content and external influences (frequency, temperature, air humidity, etc.)[19].

Figure 1. shows influence of frequency and content of hemicelluloses on the effective relative dielectric permeability (ε'_m) of alkali modified jute woven fabrics. It may be noted that increasing of frequency caused decreasing value of ε'_m. When frequency increased, polarizability decreases as dipoles cannot follow the changes of the applied electric field[15]. Control sample has lower values of ε'_m than alkali modified samples. Further, from results shown in Figure 1 it is evident that with decreasing the content of hemicelluloses, values of ε'_m increased significantly at lower frequency. It may be noted that increasing of frequency caused decreasing of ε'_m for all samples and that reduction is more intense for the samples with the lowest content of hemicelluloses. When content of hemicelluloses decreased for about 18, 25, 36 and 45 % for H30/1, H5/5, H5/17.5 and H30/17.5, the ε'_m increased for about 60, 66.5, 110.5 and 153% (at 30 Hz), 20, 24, 53.5 and 7 2 % (at 300 Hz) and 2, 3, 23 and 28 % (at 30000 Hz) in comparison with unmodified, respecively. High coefficients of negative linear correlation (r = -(0.89-0.99)) between content of hemicelluloses and ε'_m at different frequences prove that content of hemicelluloses has significant effect on the effective relative dielectric permeability of alkali modified jute woven fabrics. As we mentioned earlier, the duration of alkali modification and concentration of NaOH have influence on the content of hemicelluloses and consequently on the values of ε'_m.

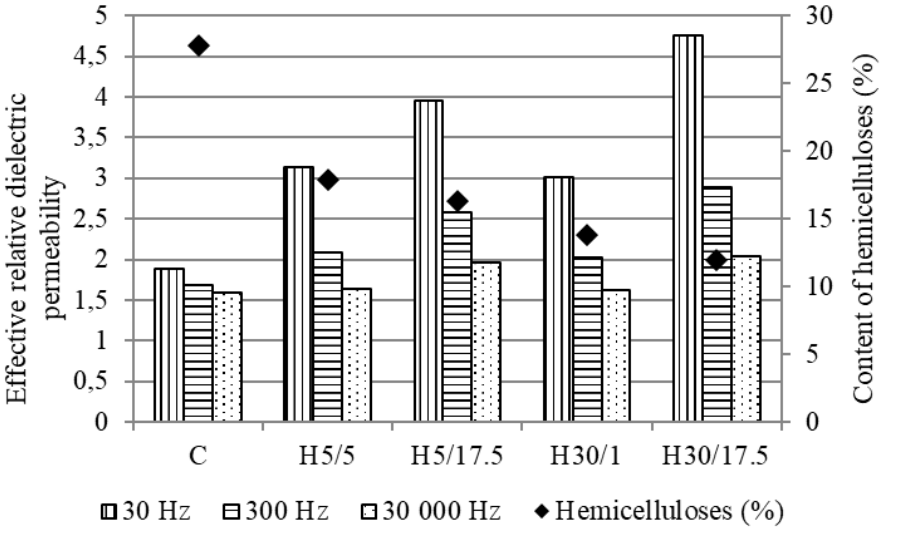

Figure 1. *Influence of content of hemicelluloses on the effective relative dielectric permeability of alkali modified jute woven fabrics*

Alkali modifications with NaOH increased the moisture sorption of the fibers due to the increase in the probability for the interaction between polar –OH groups of jute fibers and water molecules. In untreated fabric, the cellulosic hydroxyl –OH groups were relatively unreactive, since they formed strong hydrogen bonds. Alkali modifications of jute fibers destroyed the hydrogen bonds and it is expected that the number of available hydroxyl groups is increased. Thus, alkali modified fabrics showed a considerable increase in effective relative dielectric permeability compared to unmodified fabric, Figure 2.

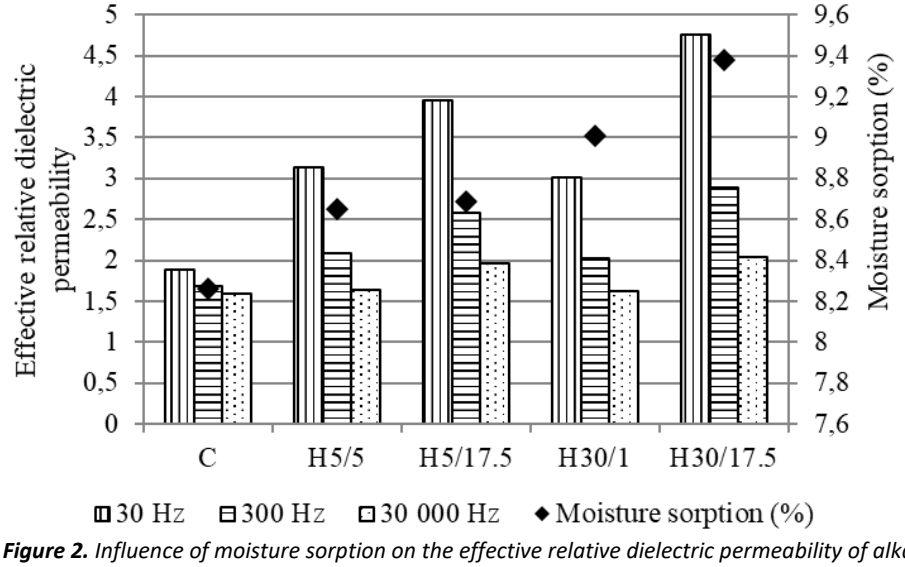

Figure 2. *Influence of moisture sorption on the effective relative dielectric permeability of alkali modified jute woven fabrics*

With increasing the moisture sorption, ε'_m increased. There is a high coefficients of linear correlation (r = 0.92-0.99) between content of moisture sorption and ε'_m at different frequences. The same connection between the frequency and moisture content was obtained for cellulose-based fabric[15]. By comparing the results showed in figures 1 and 2, it can be noticed that when frequency increase the highest reduction in the value of ε'_m has sample with the lowest content of hemicelluloses and the highest value of moisture.

Conclusion

In order to partially remove hemicelluloses, jute woven fabric was alkali modified with NaOH solutions of different concentrations during the different period of time. The obtained results showed that with increasing the concentration of NaOH and duration of modification, content of hemicelluloses decreased. With decreasing the content of hemicelluloses, the moisture sorption increased. The values of effective relative dielectric permeability are directly related to the content of hemicelluloses and moisture sorption, i.e. with decreasing the content of hemicelluloses and increasing the moisture sorption, values of effective relative dielectric permeability increased. Also, when frequency increased, the value of effective relative dielectric permeability decreased.

Acknowledgement: *Auhors are grateful to the Ministry of Education, Science and Technological Development of the Government of the Republic of Serbia for funding the study under the Projects (OI 172029 and 171029).*

Uticaj sadržaja hemiceluloza na sorpciju vlage i efektivnu relativnu dielektričnu propustljivost alkalno modifikovane tkanine od jute

U ovom radu je proučavan uticaj alkalnog modifikovanja na hemijski sastav, tj. sadržaj hemiceluloza, sorpciju vlage i na efektivnu relativnu dielektričnu propustljivost tkanina od jute. U tom cilju, tkanina od jute je modifikovana sa NaOH (1%, 5% i 17,5%) na sobnoj temperaturi u toku različitog vremena (5 i 30 min). U odnosu na nemodifikovanu, alkalno modifikovane tkanine imaju niži sadržaj hemiceluloza i povećanu sorpciju vlage. Sa sniženjem sadržaja hemiceluloza, i povećanjem sorpcije vlage, rastu vrednosti efektivne relativne dielektrične propustljivosti ispitivanih tkanina.

Ključne reči: *tkanina od jute, alkalna modifikacija, hemiceluloze, sorpcija vlage, efektivna relativna dielektrična propustljivost*

References:

1. R. Kozlowski, P. Baraniecki, J. Barriga-Bedoya, Biodegradable and sustainable fibres,Woodhead Publishing Limited, Blackburn, 2005, p. 36.
2. Md. S Rahman, Industrial Applications of Natural Fibers, A. John Wiley and Sons, Ltd., Publication, 2010, p 135.
3. P. J. Wakelyn, N. R. Bertoniere, A. D. French, D. P. Thibodeaux, B. A. Triplett, M.-A. Rousselle, W. R. Goynes, J. V. Edwards, L. Hunter, D. D. McAlister, G. R. Gamble, Handbook of fiber chemistry, Third edition, Taylor & Francis Group, London, 2007, p 521-66.
4. K. B. Krishnan, I. Doraiswamy, K. P. Chellamani, Bast and other plant fibers, Woodhead Publishing Limited, 2005, p. 24.
5. D. Ray, B. K. Sarkar, *J. Appl. Polym. Sci.* **80** (2001) 1013.
6. P. K. Ganguly, S. Chanda, *Indian J. Fibre Text. Res.* **19** (1994), 38.

7. D. Ray, M. Das, D. Mitra, *J. Appl. Polym. Sci.* **123** (2012) 1348.
8. J. Gassan, A. K. Bledzki, *J*. Appl. Polym. Sci. **71** (1999) 623.
9. R. K. Varshney, Indian *J. Fiber. Text. Res.* **31** (2006) 274.
10. L. Y. Mwaikambo, *Bioresources* **4** (2009) 566.
11. P. Ghosh, A. K. Samanta, G. Basu, *Indian J. Fiber. Text. Res.* **29** (2004) 85.
12. G. George, K. Joseph, E. R. Nagarajan, E. T. Jose, K. C. George, *Composites Part A.* **47** (2013) 12.
13. M. K. Mihai, F. Ahmed, A. Hossain, K&M Khan, *Polymer-plastics technology and engineering* **44** (2005) 1443.
14. E. Jayamania, S. Hamdan, M. R. Rahman, M. Khusairy, B. Bakr, Comparative Study of Dielectric Properties of Hybrid Natural Fiber Composites, in Proceedings of 12th Glob congress on manufacturing and management (2014), Vellore, India, Elsevier Ltd., 2014, p. 534-544.
15. D. D. Cerovic, K. A. Asanovic, S. B. Maletic, J. R. Dojcilovic, *Composites: Part B* **49** (2013) 65.
16. W. Garner, Textile Laboratory Manual, Heywood Books, London, 1967, pp. 52–113.
17. R. K. Varshney, Indian J. Fiber. Text. Res, **31** (2006) 274.
18. M. M. Kostic, B. M. Pejic, K. A. Asanovic, V. M. Aleksic, P. D. Skundric, *Ind. Crop. Prod*. **32** (2010) 169.
19. W. E. Morton, J.W.S. Physical Properties of Textile Fibers, Wood head Publishing Limited in association with The Textile Institute, Cambridge, England, 2008, p. 635.
20. B. M. Pejic, M. M. Kostic, P. D. Skundric, J. Z. Praskalo, *Bioresour. Technol.* **99** (2008) 7152.
21. B. D. Lazic, B. M. Pejic, A. D. Kramar, M. M. Vukcevic, K. R. Mihajlovski, J. D. Rusmirovic, M. M. Kostic, *Cellulose* **25** (2018) 697.
22. B. D. Lazic, S. D. Janjic, T. Rijavec, M. M. Kostic, *J. Serb. Chem. Soc.* **82** (2017) 83.
23. M. Kostić, B. Pejić, P. Škundrić, *Bioresour. Technol.* **99** (2008) 94.
24. H. M. Wang, R. Postle, R. W. Kessler, *Text. Res. J.* **73** (2003) 664.
25. S. R. Karmakar, Chemical technology in the pre-treatment processes of textiles, Elsevier, 1999, p. 279.

Protein-repellent and antioxidative properties of bioactive coatings based on TEMPO oxidized cellulose nanofibrils and chitosan

Matea Korica, Lidija Fras Zemljič*, Matej Bračič*, Rupert Kargl*, **, Mirjana Kostić***
University of Belgrade, Innovation Center of Faculty of Technology and Metallurgy, Karnegijeva 4, 11000 Belgrade, Serbia
**Institute of Engineering Materials and Design, Faculty of Mechanical Engineering, University of Maribor, Smetanova ul. 17, 2000 Maribor, Slovenia*
***Institute for Chemistry and Technology of Materials, Graz University of Technology, Stremayrgasse 9, 8010 Graz, Austria*
****University of Belgrade, Faculty of Technology and Metallurgy, Karnegijeva 4, 11000 Belgrade, Serbia*

In this work, regenerated cellulose (RC) films was coated with TEMPO oxidized cellulose nanofibrils (TOCN) and chitosan (CS) by means of subsequent spin-coated deposition. The bioactivity of coatings was achieved by addition of chitosan. The chitosan was either mixed with the TOCN (TOCN+CS) and deposited on the RC film by spin-coating or deposited on the RC/TOCN bilayer film by pumping its aqueous solution at pH 5.5 over the surface of the film. The pH dependant charging behaviour of the TOCN, TOCN+CS, and CS were evaluated by pH-potentiometric titrations. The protein-repellent properties of investigated coatings were evaluated *in situ* using a continuous flow of bovine serum albumin (BSA) by means of quartz crystal microbalance with dissipation (QCM-D). Antioxidative activity of TOCN, CS and their amphoteric mixture was determined using the 2,2'-azino-bis(3-ethyl-benzothiazoline-6-sulfonic acid) radical scavenging assay. Coating with improved protein-repellent properties was obtained using TOCN+CS amphoteric mixture, but on the other hand TOCN+CS amphoteric mixture showed weaker antioxidative properties in comparison to TOCN and CS.

Introduction

Coatings based on cellulose for biomedical application and more specifically medical devices serve numerous purposes and can be found applied to a wide range of surfaces of medical materials [1]. With the emergence and development of nanotechnology a new form of so called nanocellulose, which is described as the products or extracts from native cellulose composed of nanoscale structured material [2], attracted attention as substrate for coating different surfaces. It is a highly reproducible and environmentally friendly nanomaterial suitable for modification of various materials in order to improve existing or to give completely new properties and has been used as thin coating layers for many generic and cutting-edge products [3, 4, 5, 6]. Among various methods, TEMPO oxidation of cellulose and successive mechanical and/or ultrasound treatments is one of the most promising method for obtainig of nanocellulose so called TEMPO oxidized cellulose nanofibrils (TOCN) [4].

In order to achieve bioactivity, many researches focused on the nanocellulose functionalization performed by the use of non-toxic, biodegradable, and environmentally-friendly reagents such as chitosan [7]. Chitosan is a natural amino polysaccharide having multifunctional properties, and wide ranging applications in biomedical and other industrial areas. The positive attributes of excellent biocompatibility, biodegradability, ecological

safety and low toxicity [8] with versatile biological activities such as anti-microbial[9], antiviral[10], antitumor[11], haemostatic[12] and low immunogenicity[8] have provided ample opportunities for further application development. From the standpoint of wound-dressing products, chitosan possesses many interesting properties such as promotion of fibroblast proliferation, collagen synthesis, integrin engagement and expression of cytokines and growth factors that promote wound healing and angiogenesis[13].

In many medical application, understanding and controling protein adsorption on surfaces is a great challenge. Wherever proteins come into contact with a solid interface they will most likely adsorb to it, *i.e.* it is complicated to avoid protein adsorption[14]. Protein adsorption can trigger adhesion of particles, bacteria or cells possibly promoting inflammation cascades, or fouling processes[15]. In fact there is a huge community seeking for biocompatible and protein-repellent materials applicable to biomedical purpose and a number of recent studies are devoted to understanding and controlling protein adsorption on planar surfaces[16]. Even more, for the new generation of medical products antioxidative properties are very important, since the antioxidative agents can reduce the amount of free radicals that could otherwise damage deoxyribonucleic acid (DNA). Moreover, antioxidative properties may also contribute to anti-inflammatory effects[17]. Oxidative stress, induced by oxygen radicals, is believed to be a primary factor in various degenerative diseases as well as in the normal process of aging. Reactive oxygen species (superoxide anion, hydroxyl radical and hydrogen peroxide) are generated by normal metabolic process or from exogenous factors and agents and they can easily initiate the peroxidation of membrane lipids, leading to the accumulation of lipid peroxides. These reactive oxygen species (ROS) are capable of damaging a wide range of essential biomolecules[18]. There has been increasing interest for natural antioxidants, since they can protect the human body from free radicals, and retard the progress of many chronic diseases[19].

For the fundamental study of the interaction of polymer solutions with solid matrices, model films with a thickness below 100 nm turned out to be promising since these films have the advantage of a homogeneous surface and morphology. In this study, in order to obtain bioactive coatings based on polysaccharide with improved protein-repellent properties, RC thin film was coated with TOCN and CS, as well as TOCN+CS amphoteric mixture. TOCN was obtained from cotton fibers through 2,2,6,6-tetramethylpiperidine-1-oxyl TEMPO oxidation and successive defibrillation, and RC was obtained through regeneration of trimethysilyl cellulose (TMSC). Protein adsorption on the surface thin films of RC coated with TOCN, CS and TOCN+CS amphoteric mixture, was investigated by QCM-D using bovine serum albumin (BSA) as model solute. Finally, considering targeted biomedical application of RC materials coated with TOCN and CS, antioxidative properties of TOCN, CS and amphoteric TOCN+CS mixture were assessed by inhibition of 2,2′-azino-bis(3-ethylbenzothiazoline-6-sulfonic acid) (ABTS) radicals.

Materials

Cotton fibers: Russian, I class, 32/33 mm, were used in this study. Chitosan from crab shells with low molecular weight (Aldrich, 448869), 75-85 % deacetylated, was used. Trimethylsilyl cellulose (TMSC) with a degree of substitution (DS) of 2.55 was purchased from Thueringisches Institut fuer Textil- und Kunststoff-Forschung e.V., Germany. Quartz crystal microbalance (QCM-D) sensors coated with a gold layer (QSX303) were purchased from LOT-Oriel, Germany. 2,2,6,6-tetramethylpiperidine-1-oxyl radical (TEMPO), sodium

bromide, 13 % sodium hypochlorite solution, bovine serum albumin (BSA-lyophilized powder, ≥96 %), 2,2'-azino-bis(3-ethyl-benzothiazoline-6-sulfonic acid) (ABTS), and other chemicals obtained from commercial sources (Sigma-Aldrich, Fluka) were analytical grade and used without further purification.

Working solutions preparation
Chitosan (0.1%, w/v) was dissolved in MQ water set to pH 2.5 using 37% HCl. The solution was stirred overnight at room temperature and filtered through a 5 µm PTFE syringe filter. For the phosphate buffered saline (PBS) solution 8.0 g NaCl, 0.2 g KCl, 1.44 g $Na_2HPO_4 \cdot H_2O$ and 0.24 g KH_2PO_4 were dissolved in 900 mL of Milli-Q water, the pH was adjusted to 7.4 with 0.1 M NaOH and the solution was filled up to a volume of 1000 mL.
The protein solutions were prepared by dissolving 5 g BSA in 100 mL of PBS-buffer. All solutions were prepared at least 24 h before measurements, using Milli-Q water.

TEMPO-mediated oxidation of cotton fibers and cellulose nanofibrils preparation
In order to decrease energy needed for fibrillation and to prepare cellulose nanofibrils without significant aggregation, cotton fibers were oxidized with NaClO, catalytic amounts of TEMPO and sodium bromide according to a method described previously [20, 21]. In a typical experiment, 10 g of cotton fibers were suspended in water (750 mL) containing TEMPO (0.0250 g) and sodium bromide (0.250 g). A designated amount of the 13 wt% NaClO solution, corresponding to 15 mmol/g cellulose, was added slowly to the cellulose slurry under continuous stirring. The pH of the slurry at room temperature was maintained at 10.5 by addition of 0.5 M NaOH during 3 h. After stirring for a designated time, the oxidation was quenched by adding ethanol (ca. 5 mL). The oxidized cellulose was washed thoroughly with water, subsequently with ethanol and lastly with water on a filter paper set in a Büchner funnel. A slurry of TEMPO-oxidized cotton fibers (0.1, 1 and 2% solid consistency) in water (100 mL) was then passed through a double cylinder-type homogenizer (T 25 digital ULTRA-TURRAX, IKA, Germany) 5 min at 1000 rpm. The obtained gel-like dispersion was further sonicated for 15 min using an ultrasonic homogenizer (WCX 750, SONICS, USA) with a 19 mm diameter probe tip at 20 kHz and 750 W output power. The dispersion was centrifuged at 12,000×g for 15 min to remove a small amount of non-fibrillated and partly fibrillated fraction (<5%) to obtain TEMPO-oxidized cellulose nanofibrils with sodium carboxylate groups (TOCN-COONa) dispersed in water.

1 % (w/v) amphoteric TOCN+CS mixture (TOCN+CS) preparation
50 mL of 2 % (w/v) TOCN dispersion (pH 8.0), 22 mL of 0.5 % (w/v) CS solution (pH 2.5) and 39 mL of Milli-Q water (pH 5.5) were homogenized for 1 min using an ultrasonic homogenizer (WCX 500, SONICS, USA) with a 9 mm diameter probe tip at 20 kHz and 500 W output power. Obtained 1 % (w/v) TOCN and CS mixture had pH 5.5 without additional adjustment.

RC thin film preparation
Prior to spin-coating of the RC thin film, the QCM-D sensors were soaked into a mixture of H_2O/H_2O_2 (30 wt%)/NH_4OH (25 wt%; 5:1:1; v/v/v) for 10 min at 70°C, then immersed in a "piranha" solution containing H_2O_2 (30 wt%)/H_2SO_4 (98 wt%; 1:3; v/v) for 60 s, and then rinsed with MQ-water and finally blow dried with N_2 gas.

RC film was prepared by spin-coating of TMSC, 100 µL of TMSC solution (1 % (w/v)), dissolved in hexamethyldisiloxane (HMDSO), filtered using 5 µm PTFE syringe filter, deposited onto the QCM-D sensors, and rotated for 60 s at a spinning speed of 4000 rpm and an acceleration of 2500 rpm s^{-1}. For converting TMSC into regenerated cellulose (RC), the TMSC–coated sensors were placed into a polystyrene Petri dish (5 cm in diameter) containing 3 mL of 10 wt% hydrochloric acid (HCl). The dish was covered with its cap and the TMSC films were exposed to the vapors of HCl for 15 min.

Coating of RC films by TOCN, CS, and TOCN+CS amphoteric mixture

Three different methods were chosen for RC film coating.

Method I: RC film was coated with TOCN by spin-coating of TOCN. 50 µL of the TOCN dispersion (1 % (w/v)) was deposited onto the RC film, rotated for 60 s at a spinning speed of 4000 rpm and an acceleration of 2500 rpm s^{-1}.

Method II: RC film was coated with amphoteric TOCN+CS mixture by spin-coating of the amphoteric mixture based on CS and TOCN: 50 µL of 1 % (w/v) amphoteric TOCN+CS mixture was deposited onto the RC film, rotated for 60 s at a spinning speed of 4000 rpm and an acceleration of 2500 rpm s^{-1}.

Method III: RC film was coated with TOCN by spin coating of TOCN, as it is described in Method I, followed by deposition of CS using QCM-D technique. Au sensors coated with cellulose film prepared according to the method I were mounted into the QCM-D flow cell and equilibrated with MQ-water until a constant frequency signal was obtained. Five minutes after purging with MQ-water, CS solution (0.1 %, w/v) was allowed to adsorb onto the cellulose surfaces for 240 min. To remove reversible bound and free chitosan, the film was rinsed with MQ water for 60 min. The measurement was terminated at this stage. The flow rate was kept at 0.1 mL min^{-1} throughout all experiments performed at 21±0.1°C. Chitosan adsorption has been performed at pH value 5.5. The pH of the MQ-water and CS solution was adjusted to 5.5 with 0.1 M NaOH.

List of the samples with description is given in Table 1.

Table 1. Sample denotations and descriptions

Sample denotation	Sample preparation
RC/TOCN	RC ultra-thin film coated with 1 % TOCN dispersion (method I)
RC/TOCN+CS	RC ultra-thin film coated with 1 % amphoteric TOCN+CS mixture (method II)
RC/TOCN/CS	RC ultra-thin film coated with 1 % TOCN dispersion after adsorption/desorption CS (method III)

Methods

pH-potentiometric titrations

The pH dependent potentiometric titration was performed on 0.1% (w/v) TOCN dispersion, 0.1 % (w/v) CS solution and 1 % (w/v) amphoteric TOCN+CS mixture. Samples were prepared by dilution using Milli-Q water (a very low carbonate ion content, $c<10^{-6}$ mol L^{-1}). Samples were titrated in a forward (from acidic to alkaline) and backward (alkaline to acidic) manner from pH 2 to pH 11 using 0.1 M HCl and 0.1 M NaOH. The KCl concentration of samples was set to 0.1 M using potassium chloride. The titrants were added to the system in a dynamic

mode using a double burette Mettler Toledo T70 automatic titration unit, and the pH value was measured using a Mettler Toledo DG-111-SC combined glass electrode. Details on the measurements as well as the calculation of the charge and content of functional groups are described in literature [22].

Protein-repellent characterization

The quartz crystal microbalance with dissipation (QCM-D) as a nanogram-sensitive balance is powerful tool for studying polymer adsorption on thin films. In this study, a QCM-D device (model E4, Q-Sense, Gothenburg, Sweden) was used to investigate the protein adsorption on polysaccharide films, samples listed in Table 1. The QCM-D instrument determines changes in frequency (f) of an oscillating quartz crystal caused by deposition of mass whereas negative frequency shifts (Δf) indicate a deposition of mass.

The change in frequency can be directly related to the adsorbed mass using the Sauerbrey equation [23]:

$$\Delta f = -C\frac{\Delta m}{n}$$

where Δf represents the frequency shift, Δm is the mass change, C is the Sauerbrey constant (C=17.7 ng Hz^{-1} at the frequency of 5 MHz), and n is the number of the overtone (n= 1, 3, 5, *etc*.) of oscillation.

Sauerbrey equation is only applicable for thin and rigid films, which fully couple to the oscillation of the quartz sensor. The model investigated films in this study were treated as a rigid extension of the quartz crystal when estimations were done using the Sauerbrey equation.

For the data analysis in this study, the change in the third overtone's frequency (f_3) was used. For all QCM-D experiments, sensors coated with films were mounted into the QCM-D flow cell and the initial resonance frequency of the sensor was measured. Afterwards, the films were equilibrated with Milli-Q water followed by rinsing with the background solution (PBS buffer was used for protein adsorption experiments) until a constant frequency was established.

In each QCM-D experiment, before protein injection tested films were equilibrated with MQ-water until a constant frequency signal was obtained. All frequencies were set to zero and the measurement was started. Five minutes after purging with MQ-water, PBS-buffer was purged through the cells for 10 min and subsequently the BSA solution with a concentration of 50 mg mL^{-1} for 15 min. The films were rinsed with PBS-buffer in the cells for 10 min to desorb reversibly bound protein. The measurement was terminated at this stage. The flow rate was kept at 0.1 mL min^{-1} throughout all experiments. All measurements were performed at 21±0.1°C and physiological pH 7.4. The amount of adsorbed protein was determined as the overall change in frequency of the third overtone of the oscillation frequency (f_3) after the desorption step with PBS-buffer. Mean values and standard deviations were calculated from three individual measurements.

ABTS radical scavenging assay

The antioxidative activity of CS solution (1 % w/v), TOCN dispersion (1 % w/v) and TOCN+CS amphoteric dispersion (1 % w/v) was measured in order to get the antioxidative profile of all used components of investigated coatings. The antioxidative activity was assessed as

described below. Experiments were performed on the Cary 60 spectrophotometer (Agilent technologies, UK) fitted with peltier temperature control.
Preformed radicals of ABTS were generated by the oxidation of ABTS (7.0 mM) with potassium persulfate (2.75 mM $K_2S_2O_8$) for 12 h in the dark at room temperature. After generation, ABTS was diluted with PBS buffer to an appropriate concentration (absorbance of 0.70 ± 0.02 at 734 nm), affording the working solution. The absorbance of a mixture of a 0.1 g of sample and a 3.9 mL of working solution was measured 15 and 60 min after beginning of reaction, at 734 nm.
The antioxidative activity of CS solution (1 % w/v), TOCN dispersion (1 % w/v) and TOCN+CS amphoteric dispersion (1 % w/v) was measured as the decrease in absorbance of the ABTS and was expressed as percent inhibition of ABTS radicals calculated according to the following equation:

$$\text{Inhibition},\% = \frac{\text{Abs}_0 - \text{Abs}_1}{\text{Abs}_0} 100$$

where Abs_0 is the absorbance measured at the initial concentration of ABTS, Abs_1 is the absorbance measured at the residual concentration of ABTS.

Result and discussion

Preparation TOCN from cotton fibers

TOCN dispersions of different concentrations were prepared by fibrillation of the TEMPO-oxidized cotton fibers. During the disintegration treatment, significant amounts of sodium carboxylate groups (0.83 mmol/g cell) and aldehyde groups (0.09 mmol/g cell) in the cotton fibers formed by oxidation allowed the nanofibrils within the fibers to separate more easily due to the repulsive forces between the ionized carboxylates, which overwhelmed the hydrogen bonds holding them together [6].

Charging behaviour of the TOCN, TOCN+CS, and CS

For polyelectrolytes such as TOCN, CS and their mixture used in this work, the charging behaviour is an important surface property with respect to adsorption and swelling. Results of the pH dependent potentiometric titrations performed on 0.1 % (w/v) TOCN dispersion, 0.1 % (w/v) CS solution and 1 % (w/v) amphoteric TOCN+CS mixture are shown in Figure 1a c. Increasing negative surface charges of TOCN with increasing pH values can be seen since all carboxyl moieties are uncharged at pH below 2 and exhibit the highest surface charge at pH≥7 (full deprotonation of carboxylic groups). Potentiometric charge titration of CS shows an increasing positive surface charge with reducing pH values due to the fact that all amino moieties are uncharged at pH≥ 8 and exhibit the highest surface charge at pH ≤ 4 (Figure 1b). Potentiometric charge titration of TOCN+CS amphoteric mixture shows typical amphoteric curve with zero charge at pH 7 (Figure 1c) *i.e.* when the pH equals 7 the numbers of negative and positive charges are in balance resulting in a net neutral mixture. At lower pH conditions the mixture is positively charged whereas at higher pH conditions the mixture is negatively charged due to pH dependent protonation/deprotonation of weak acids/base. The content of anionic functional groups present in TOCN (COO^-) and cationic functional groups present in CS (NH_3^+) is 0.83 mmol g^{-1} and 4.28 mmol g^{-1}, respectively. For TOCN+CS amphoteric mixture the content of anionic (COO^-) and cationic (NH_3^+) functional groups is equal (0.45 mmol g^{-1}*) i.e.* total quantity of negative surface charge from TOCN is

completely neutralized with same quantity of positively charged ammonium groups from CS. From the results, it can also be seen that by preparation of TOCN+CS mixture electrostatic interaction between anionic charged TOCN and cationic charged CS are established.

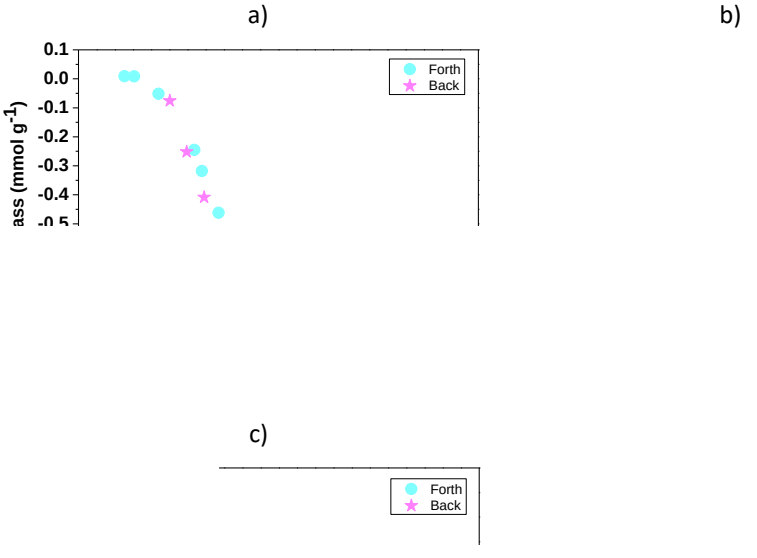

Figure 1. *Potentiometric charge titration values of TOCN dispersion (a), CS solution (b) and TOCN+CS amphoteric mixture (c) as a function of pH*

Protein adsorption

In this study, using QCM-D technique, protein-repellent properties, *i.e.* adsorption and desorption of BSA from surface of RC/TOCN and RC/TOCN/CS films, were compared. Additionally, considering fact that proteins tend to adhere more strongly to charged then to uncharged substrates[24], 1 % amphoteric dispersion based on TOCN and CS with low charge density at pH 7.4 (Figure 1c) was also used for coating RC surfaces (method II for preparing RC/CS+TOCN film). Figure 2 shows representative plots of Δf_3 versus time for RC/TOCN, RC/TOCN/CS and RC/TOCN+CS films switched from H_2O, PBS buffer, BSA solution and back to PBS buffer. The amount of adsorbed BSA on the surface of investigated films is shown in Figure 3.

Change in the frequency of -33 Hz between BSA adsorptive and PBS buffer rinse step (Figure 2) clearly shows that adsorption of BSA on the surface of RC/TOCN film occurs. Isoelectric point of BSA is around 4.7-4.9[25], so at higher pH conditions BSA is negatively

charged. Actually, at pH 7.4 the net surface charges of both BSA and TOCN are negative, so it is possible that there is an electrostatic repulsion between them. Therefore it is suggested that the interaction of BSA with TOCN may be very specific, in accordance with the anionic groups of polysaccharides [25].

Figure 2. *QCM-D change in frequency for the adsorption of BSA on a) RC/TOCN, b) RC/TOCN/CS and c) RC/TOCN+CS films*

In the case of RC/TOCN/CS film, amino groups of chitosan are minorly protonated at pH 7.4 (Figure 1b) so it is possible that there is an electrostatic attraction between them and BSA. Figure 2 shows that frequency shift of -39 Hz between BSA adsorptive and PBS buffer rinse step for RC/TOCN/CS film is bigger than frequency shift of -33 Hz for RC/TOCN film *i.e.* deposited chitosan has contributed to the deterioration of protein-repellent properties. If we analyze these results together with the TOCN and CS surface charge at pH 7.4 (Figure 1a-b), which amounts -0.8 mmol g^{-1} and +0.23 mmol g^{-1}, respectively, it is logical that the amount of adsorbed BSA increases as a consequence of the surface negative charge decrease and decreased electrostatic repulsion. Namely, a significant portion of the carboxyl groups is covered with the bound CS molecules and unavailable for electrostatic repulsion with BSA molecules. Additionally, bounded positively charged CS molecules can electrostatically attract negatively charged BSA molecules.

In the case of both films (RC/TOCN and RC/TOCN/CS), considerable adsorption of BSA was recorded (Figure 3). Due to the high surface charge of TOCN as well as CS, we get the idea to make film with amphoteric character of its surface and with low surface charge at pH 7.4. For that purpose amphoteric dispersion based on TOCN and CS i.e. polyanion/polycation complex was prepared. For this complex, at pH 7.4 anionic charge is -0.04 mmol g^{-1} (Figure 1c). As expected, frequency change of 7 Hz observed for BSA adsorption on RC/TOCN+CS film was significantly smaller than in the case of both RC/TOCN and RC/TOCN/CS films (Figure 2) confirming on such way a weak adsorption of BSA on the RC/TOCN+CS film (Figure 3).

Upon rinsing with PBS buffer an increase in frequency is detected due to the reversible protein adsorption. We may assume that the weak adsorption of proteins to a surface only

occurs on the top of the swollen film and the weakly bound protein rapidly dissociates from the surface when the solution of protein is replaced with buffer. With respect to the fact that TOCN, CS and their amphoteric mixture are different substrates, as well as their possibility to interact by various and still incompletely researched mechanisms with BSA[24], it is very hard to give detailed explanation for obtained results.

Figure 3. *The amount of adsorbed BSA on surface of the RC/TOCN, RC/TOCN/CS and RC/TOCN+CS films*

ABTS radical scavenging assay

Antioxidative activity is one of the well-known functions of CS, but according to our best knowledge this function still is not studied for TOCN and TOCN/CS mixture. Figure 4 shows the antioxidative inhibition percentages of ABTS radical by CS solution (1 % w/v), TOCN dispersion (1 % w/v) and TOCN+CS amphoteric mixture (1 % w/v). In this test, an anti-oxidative molecule reduces the ABTS radical to 2,2'-azino-bis-3-ethylbenzothiazoline-6-sul-fonic acid.

Figure 4. *Scavenging ability of 1% CS solution, 1% TOCN dispersion, and 1% TOCN+CS amphoteric mixture*

The extent of discoloration will depend on the hydrogen-donating ability. For all investigated samples, inhibition increases with the progress of time. According to the

results, after 60 min CS shows 18.34 %, and TOCN 13.38% of inhibition of ABTS radicals. Many studies have shown that CS inhibits the ROS and several mechanisms about the antioxidative action of CS have been proposed[26]. CS can scavenge free radicals or chelate metal ions from the donation of a hydrogen or the lone pairs of electrons[27]. The hydroxyl groups and amino groups in CS are the key functional groups for its antioxidative activity, but can be difficult to be dissociated due to the semi-crystalline structure of chitosan with strong hydrogen bonds[27]. At the same time, amphoteric TOCN+CS mixture shows significantly lower inhibition (2.23%) in comparison with CS and TOCN which could be due to the interactions between CS and TOCN i.e. their H-atom donating groups.

Conclusion

In this work, a new approach to obtain protein-repellent and antioxidative coatings based on TEMPO oxidized cellulose nanofibrils and chitosan was proposed. Coating with improved protein-repellent properties was obtained using TOCN+CS amphoteric mixture with almost zero charge (-0.04 mmol g^{-1} at pH 7.4) considering the fact that proteins tend to adhere more strongly to charged than to uncharged surfaces. The amount of adsorbed BSA on surface RC/TOCN+CS is significantly lower than on surfaces RC/TOCN and RC/TOCN/CS (TOCN and CS are highly surface charged at pH 7.4 (-0.8 mmol g^{-1} and +0.23 mmol g^{-1}, respectively)). On the other hand, TOCN+CS amphoteric mixture shows significantly weaker antioxidative properties in comparison to TOCN and CS, which could be due to the interactions between CS and TOCN i.e. their H-atom donating groups. Obtained results are good starting point to create upgraded coatings of TOCN and CS that will show both properties simultaneously.

Acknowledgments: *The authors wish to thank the Ministry of Education, Science and Technological Development of the Republic of Serbia for financial support through the project OI 172029.*

Protein-odbijajuća i antioksidativna svojstva bioaktivnih prevlaka na bazi TEMPO oksidisanih celuloznih nanofibrila i hitozana

U ovom radu, filmovi od regenerisane celuloze (RC) su naslojeni sa TEMPO oksidisanim celuloznim nanofibrilima (TOCN) i hitozanom (CS) metodom rotirajućeg diska. Bioaktivnost prevlaka postignuta je dodavanjem hitozana. Hitozan je ili pomešan sa TOCN (TOCN+CS) i naslojen na RC film tehnikom rotirajućeg diska ili nanesen na RC/TOCN dvoslojni film propumpavanjem njegovog vodenog rastvora, pH vrednosti 5,5, preko površine filma. Naelektrisanje TOCN, TOCN+CS i CS u zavisnosti od pH je okarakterisano pH-potenciometrijskim titracijama. Protein-odbijajuća svojstva ispitivanih prevlaka određena su in situ, u kontinualnom toku goveđeg serumskog albumina (BSA) primenom kvarc-kristal mikrovage sa praćenjem disipacije (QCM-D). Antioksidativna svojstva TOCN, CS i TOCN+CS amfoterne mešavine su određena metodom inhibicije radikala 2,2'-azino-bis(3-etil-benzotiazolin-6-sulfonske kiseline). Prevlaka sa poboljšanim protein-odbijajućim svojstvima je dobijena upotrebom TOCN+CS amfoterne mešavine, ali sa druge strane TOCN+CS amfoterna mešavina je pokazala slabija antioksidativna svojstva u poređenju sa TOCN i CS.

References:

1. R. LaPorte (1997) Hydrophilic polymer coatings for medical devices: structure/properties, development, manufacture and applications, CRC Press LLC, Boca Raton, Florida USA

2. N. Lin, A. Dufresne, *Eur. Polym. J.,* **59** (2014) 302.
3. N. Lavoine, I. Desloges, A. Dufresne, J. Bras, *Carbohydr. Polym*., **90** (2012) 735.
4. A. Isogai, T. Saito, H. Fukuzumi, *Nanoscale,* **3** (2011) 71.
5. D. Klemm, F. Kramer, S. Moritz, D. Gray, A. Dorris, T. Lindstrom, M. Aknerfors, *Angew. Chem. Int. Ed.,* **50** (2012) 5438.
6. A. Khalil, A. Bhat, I. Yusra, *Carbohydr. Polym.*, **87** (2012) 963.
7. L. Windler, M. Height, B. Nowack, *Environ. Int.,* **53** (2013) 62.
8. C. Pillai, W. Paul, C. Sharma, *Prog. Polym. Sci.,* **34** (2009) 641.
9. S. Tokura, K. Ueno, S. Miyazaki, N. Nishi, *Macromol. Symp*., **120** (1997) 1.
10. B. Alarcón, J. C. Lacal, J. M. Fernández-Sousa, L. Carrasco, *Antiviral Res.,* **4** (1984) 234.
11. S. Suzuki, Y. Ogawa, Y. Ohura, K. Hashimoto, M. Suzuki (1982) *Proceedings of the 2nd International Conference on Chitin/Chitosan*, Tottori, Japan, Eds. Hirano, S., Tokura, S. Japan Soc. Chitin/Chitosan. p. 210.
12. T. Phaechamud, K. Yodkhum, J. Charoenteeraboon, Y. Tabata, *Mater. Sci. Eng.,* **50** (2015) 210.
13. S. Zeronian, M. Inglesby, *Cellulose,* **2** (1995) 265.
14. T. A. Horbett, J. L. Brash (1995) *Proteins at Interfaces II: Fundamentals and Applications.* American Chemical Society, Washington DC.
15. S. Kalasin, M. Santore, *Colloids Surf. B: Biointerfaces,* **73** (2009) 229.
16. V. Vogel, G. Baneyx, *Annu. Rev. Biomed. Eng*. **5** (2003) 441.
17. N. S. Mashhadi, R. Ghiasvand, G. Askari, M. Hariri, L. Darvishi, M. R. Mofid, *Int. J. Prev. Med.,* **4** (2013) 36.
18. A. Rajalakshmi, N. Krithiga, A. Jayachitra, *Antioxidant Activity of the Chitosan Extracted from Shrimp Exoskeleton*, Middle East J. Sci. Res., **16** (2013) 1446.
19. J. Kinsella, E. Frankel, E. German, B. Kanner, *Food technol.,* **47** (1993) 85.
20. T. Saito, A. Isogai, *Biomacromolecules,* **5** (2004) 1983.
21. V. Kumar, T. Yang, *Carbohydr. Polym*., **48** (2002) 403.
22. L. Zemljič, D. Čakara, N. Michaelis, T. Heinze, K. Stana Kleinschek, *Cellulose*, **18** (2011) 33.
23. Sauerbrey, G. Mikrowägung. Z. Phys., **155** (1959) 206.
24. M. Rabe, D. Verdes, S. Seeger, *Adv. Colloid Interface Sci.,* **162** (2011) 87.
    A. Teramoto, Y. Takagi, *Polym. Adv. Technol*., **10** (1999) 681.
25. W. Kim, R. Thomas, *Food chem.,* **101** (2007) 308.
26. W. Xie, P. Xu, Q. Liu, *Bioorg. Med. Chem. Lett.,* **11** (2001) 1699.

Antibacterial activity of Cu-based nanoparticles synthesized on the cotton fabrics previously modified with succinic and citric acids

Darka Marković, Tim Nunney*, Christopher Deeks*, Željko Radovanović, Marija Radoičić**, Maja Radetić***
Innovation Center of the Faculty of Technology and Metallurgy, University of Belgrade, Karnegijeva 4, Belgrade
**Thermo Fisher Scientific,The Birches Industrial Estate, Imberhorne Lane, East Grinstead, West Sussex, RH19 1UB, UK*
***Institut of Nuclear Sciences "Vinča", University of Belgrade, P.O. Box 522, Belgrade*
****Technology and Metallurgy, University of Belgrade, Karnegijeva 4, Belgrade*

Introduction

Cu-based nanoparticles (NPs) are increasingly gaining scientific attention due to the abundance of this metal, its relative inexpensiveness compared to Ag and excellent antimicrobial activity against various bacteria strains. Gram-negative bacteria *E. coli* and Gram-positive bacteria *S. aureus* are especially sensitive to the action of Cu-based NPs which can be utilized for treatment of burns, surgical wounds and diabetic foot ulcer infections[1]. Recently, the potential application of copper in different forms (metallic, ionic, copper oxides, copper complexes) for fabrication of medical textiles with antimicrobial activity became the focus of several research groups[2-4]. The exploitation of Cu, Cu_2O and CuO NPs or their mixtures for imparting antibacterial activity to cotton fabrics is of particular interest. The dominant method for synthesis of Cu-based NPs relies on the introduction of carboxyl groups to cotton fibers by coating them with adequate polymer or chemical modification of cellulose, adsorption of Cu^{2+}-ions and their reduction.

Our approach for fabrication of Cu-based NPs on cotton fabrics was oriented towards modification of fabrics with polycarboxylic acids. It was assumed that ester bonds between the hydroxyl groups of cotton and the carboxyl groups of acids are formed while the rest of the free carboxyl groups can be utilized for adsorption of Cu^{2+}-ions from aqueous solution of $CuSO_4$. To get better insight into the influence of carboxyl group number in the acid structure and further, on the cotton fabric, the study was carried out using a dicarboxylilic succinic acid and tricarboxylic citric acid.

Experimental

Desized and bleached cotton (Co) woven fabric (117.5 g/m^2, 52 picks/cm, 27 ends/cm, thickness of 0.26 mm) was used as a substrate. Co fabrics were cleaned in the bath containing 0.1% nonionic washing agent Felosan RG-N (Bezema) at liquor-to-fabric ratio of 50:1. After 15 min of washing at 50 ^oC, the fabrics were rinsed first with warm water (50 ^oC) and then thoroughly with cold water. The samples were dried at room temperature.

Modification of Co fabrics with succinic and citric acids was carried out by immersion of 0.50 g of the sample in 20 mL of the acid aqueous solution (10 w/v) in the presence of 2.06 g of the catalyst sodium hypophosphite (SHP) for one hour. After drying at 80 ^oC for 10 min the samples were cured at 170 ^oC for 3 min. The samples were then rinsed in distilled water and dried at room temperature. Co fabrics modified with succinic and citric acids are marked as Co+SUC and Co+CA, respectively.

Subsequently, 0.50 g of Co+SUC and Co+CA fabrics were soaked in 25 mL of 10 mM solution of $CuSO_4$ for 2 h. In order to eliminate the excessive Cu^{2+}-ions, the samples were rinsed three times with deionized water. 0.050 g of sodium borohydride ($NaBH_4$) was dissolved in 25 mL of 0.1 mM NaOH solution and the samples were immediately dipped into the solution where the reduction process took place in the following 30 min at room temperature. The samples were thoroughly rinsed with deionized water and left to dry at room temperature. These samples are marked as Co+SUC+Cu and Co+CA+Cu.

Determination of carboxyl content in oxidized Co fabric was based on the calcium acetate method described by Kumar and Yang and modified by Praskalo *et al.*[5,6].

Fourier transform infrared (FTIR) spectra of the control Co fabric, Co fabrics modified with polycarboxylic acids and Co fabrics modified with polycarboxylic acids after rinsing in 0.1 M NaOH solution were recorded in the ATR mode using a Nicolet 6700 FTIR Spectrometer (Thermo Scientific) at 2 cm^{-1} resolution, in the wavenumber range 500–4000 cm^{-1}.

The morphology of the control and Co fibers impregnated with Cu-based NPs was assessed by field emission scanning electron microscopy (FESEM, Tescan Mira3 FEG). The samples were coated with a thin layer of Au prior to analysis.

The amounts of adsorbed Cu^{2+}-ions on the Co+SUC and Co+CA fabrics from $CuSO_4$ solution were calculated on the basis of the concentration of residual Cu^{2+}-ions in the solution which was measured using a Spectra AA 55 B (Varian) atomic absorption spectrometer (AAS). AAS was also used for the measurement of the total Cu content in the Co fabrics after reduction process. Dry impregnated Co fabrics were dissolved in the 1:1 HNO_3 solution.

X-ray photoelectron spectroscopy (XPS) measurements were performed in order to evaluate the chemistry of the control Co, Co+SUC+Cu and Co+CA+Cu fabrics. The XPS analysis was carried out using a K-Alpha spectrometer (Thermo Scientific, UK) utilizing a monochromated Al *Kα* (*hv* = 1486.6 eV) X-ray source.

The antibacterial activity of Co fabrics was tested against Gram-negative bacteria *E. coli* ATCC 25922 and Gram-positive bacteria *S. aureus* ATCC 25923 using a standard test method for the determining the antimicrobial activity of immobilized antimicrobial agents under dynamic contact conditions ASTM E 2149-01 (2001). The percentage of bacterial reduction (*R*, %) was calculated by the following equation:

$$R = \frac{C_0 - C}{C_0} \cdot 100$$

where C_0 (CFU – colony forming units) is the number of bacteria colonies on the control fabric and C (CFU) is the number of bacteria colonies on the fabric with NPs.

Results and discussion

Chemical changes induced by modification of Co fabrics with polycarboxylic acids were assessed by FTIR spectroscopy. FTIR spectra of the Co+SUC and the Co+CA fabrics are shown in Fig. 1a and 1b, respectively. The bands characteristic for cellulose are clearly identified in all spectra. The appearance of the band with a peak centered at 1720 cm^{-1} in the spectra of the Co+SUC and Co+CA fabrics proved the formation of ester bonds between hydroxyl groups of cellulose and carboxyl groups of polycarboxylic acids[7,8]. An immersion of the samples in 0.1 M solution of NaOH caused the deprotonation of free carboxyl groups i.e. a formation of carboxylates. The presence of carboxylates was confirmed by appearance of the band at 1565/1575 cm^{-1}. The existence of both bands at 1720 cm^{-1} and 1565/1575 cm^{-1}

in these spectra showed that applied polycarboxylic acids were bound to cellulose by ester bonds, but a certain number of carboxyl groups of the SUC and CA remained free.

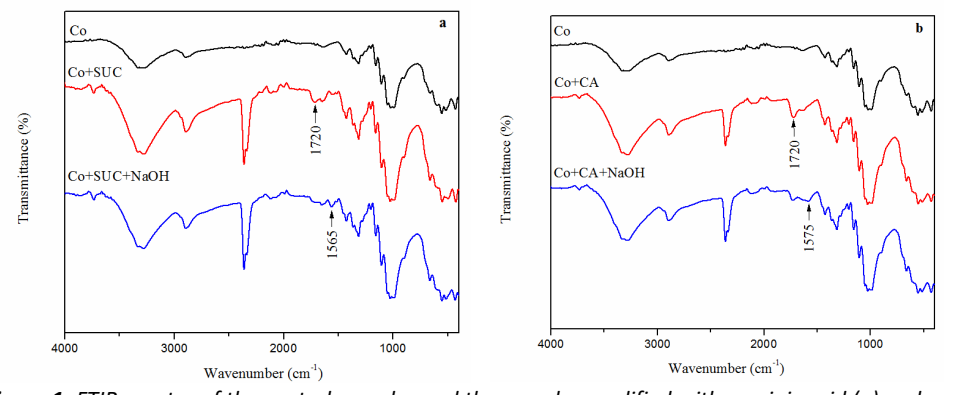

Figure 1. *FTIR spectra of the control samples and the samples modified with succinic acid (a) and citric acid (b)*

The content of free carboxyl groups in the Co+SUC and Co+CA fabrics was determined titrimetrically. The results in Table 1 show that the content of free carboxyl groups was higher in the Co+CA than in the Co+SUC fabric. This indicates that the higher the content of carboxyl groups in precursor acid the higher content of free carboxyl groups in the sample. Free carboxyl groups introduced to Co fabrics are considered as potential sites for binding of Cu^{2+}-ions and they were exploited for their adsorption. The Cu^{2+}-ions uptakes of Co fabrics modified with polycarboxylic acids after 2 hours long adsorption in aqueous solution of $CuSO_4$ are also summarized in Table 1. As expected, the larger the number of free carboxyl groups, the larger the uptake of Cu^{2+}-ions. The total Cu content in Co fabrics impregnated with Cu-based NPs after reduction of adsorbed Cu^{2+}-ions was determined by AAS (Table 1). A trend of increase in total Cu content with an increase of free carboxyl groups in Co fabrics was maintained.

Table 1 *Carboxyl groups content, Cu^{2+}-ions uptake and total content of Cu after Cu^{2+}-ions reduction in Co fabrics modified with polycarboxylic acids*

Sample	COOH content, μmol/g	Cu^{2+}-ions uptake, μmol/g	Total content of Cu after reduction, μmol/g)
Co+SUC	304±59	81±13	58±3.7
Co+CA	436±62	102±4.5	91±1.8

The presence of Cu-based NPs was confirmed by FESEM analysis. The FESEM images of the control, Co+SUC+Cu and Co+SUC+Cu samples are shown in Fig. 2a, 2b and 2c, respectively. As can be seen, Cu-based NPs are unevenly distributed over the surface of the fibers.

In order to get insight into the oxidation state of the copper in fabricated NPs a single points on the surface of the Co+SUC+Cu and Co+CA+Cu samples were analyzed by XPS. A high resolution scans of the Co+SUC+Cu and Co+CA+Cu samples were accomplished in the Cu2p region and they are shown in Fig. 3a and 3b, respectively. Fig. 3 shows two main peaks corresponding to $Cu2p_{3/2}$ and $Cu2p_{1/2}$ followed by shakeup satellites in the Cu2p spectra of all investigated samples.

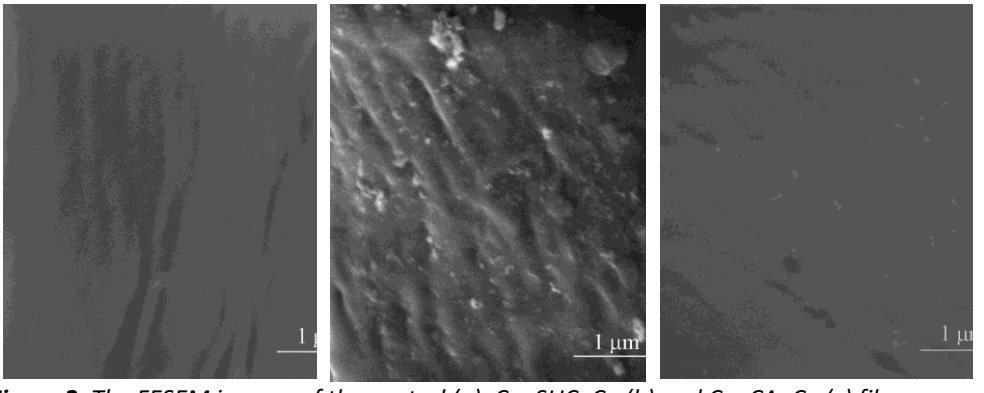

Figure 2. *The FESEM images of the control (a), Co+SUC+Cu (b) and Co+CA+Cu (c) fibers*

Asymmetric $Cu2p_{3/2}$ peak can be deconvoluted into two components: the peak related to metallic Cu or Cu_2O and the peak assigned to CuO. There is no doubt that copper appeared in the form of CuO in studied NPs since the shakeup satellites are evident in both Cu2p spectra. The shakeup satellites are characteristic of materials possessing a d^9 configuration like in a Cu^{2+9}. On the basis of XPS results it was not possible to distinguish metallic Cu from the Cu_2O form due to their spectral overlap[9]. The difference in binding energies of the $Cu2p_{3/2}$ signal for these two forms is only 0.1 eV (932.6 and 932.7 eV for Cu and Cu_2O, respectively). Therefore, it is suggested that synthetized Cu-based NPs consist of the mixture of Cu/Cu_2O and CuO.

The antibacterial activity of the Co fabrics was tested against Gram-negative bacterium *E. coli* and Gram-positive *S. aureus*. The Co+SUC and Co+CA samples alone did not show any antibacterial activity. The results summerized in Table 2 show that the presence of the Cu-based NPs in the Co+SUC+Cu and Co+CA+Cu fabrics ensured 99.9 % bacterial reduction of both bacteria colonies. It is generally accepted that the larger the amount of loaded Cu-based NPs on the textile substrates, the stronger the antibacterial activity. However, we cannot discuss the results from this point of view as obtained Cu contents were sufficiently high for imparting desired level of antibacterial activity to both studied Co fabrics.

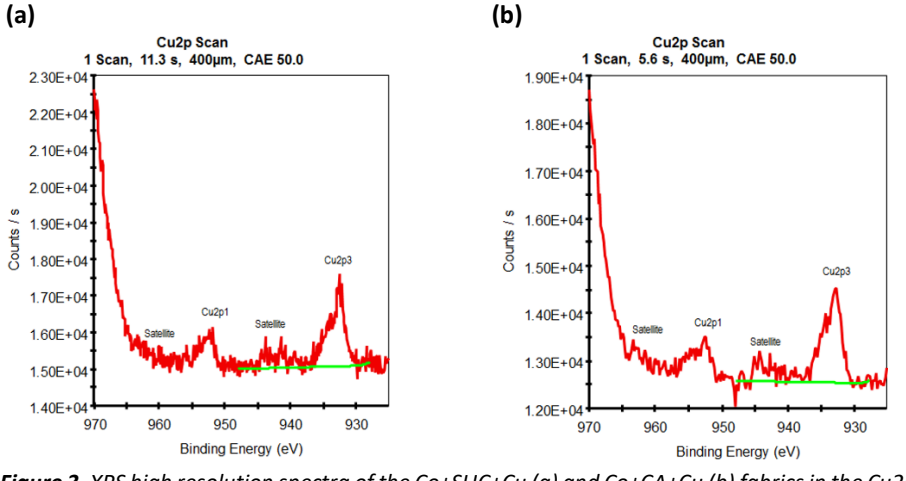

Figure 3. *XPS high resolution spectra of the Co+SUC+Cu (a) and Co+CA+Cu (b) fabrics in the Cu2p region*

Table 2 *Antibacterial activity of the Co fabrics impregnated with Cu-based NPs*

Sample	Number of bacterial colonies (CFU)	R, %	Number of bacterial colonies (CFU)	R, %
	E. coli		*S. aureus*	
Control Co	3.5×10^5		2.6×10^4	
Co+SUC+Cu	<10	99.9	<10	99.9
Co+CA+Cu	<10	99.9	<10	99.9

Conclusions

Modification of cotton fabrics with succinic and citric acids ensured carboxyl groups required for adsorption of Cu^{2+}-ions. Dicarboxylic citric provided higher content of free carboxyl groups on the fabric which led to a larger uptake of Cu^{2+}-ions and generation of larger amounts of Cu-based nanoparticles which were detected by FESEM analysis. XPS analysis suggested that nanoparticles existed in the form of mixture of CuO and Cu/Cu_2O. The presence of Cu-based nanoparticles on both cotton fabrics modified with polycarboxylic acids provided 99.9 % reduction of Gram-negative bacteria *E. coli* and Gram-positive bacteria *S. aureus*, indicating that fabricated textile nanocomposite exhibit excellent antibacterial activity.

Acknowledgement: *The financial support for this study was provided by the Ministry of Education, Science and Technological Development of Republic of Serbia (projects no. 172056 and 45020).*

Antibakterijska aktivnost nanočestica na bazi Cu sintetisanih na pamučnim tkaninama prethodno modifikovanim ćilibarnom i limunskom kiselinom

U ovom radu je diskutovana mogućnost in situ sinteze nanočestica na bazi Cu na pamučnim tkaninama prethodno modifikovanim ćilibarnom i limunskom kiselinom u cilju dobijanja tekstilnih nanokompozita sa antibakterijskom aktivnošću. Utvrđeno je da veći broj karboksilnih grupa u prekursoru obezbeđuje veći broj slobodnih karboksilnih grupa na tkanini, a time veću sorpciju Cu^{2+}-jona iz rastvora $CuSO_4$ i veći sadržaj nanočestica nakon redukcije. Prisustvo nanočestica na pamučnoj tkanini potvrđeno je SEM analizom, a XPS analizom je ustanovljeno da se sintetisane nanočestice sastoje iz metalnog Cu/Cu_2O i CuO. Ispitivani nanokompoziti ostvarili su maksimum redukcije bakterija Gram-negativne E. coli i Gram-pozitivne S. aureus.

References

1. F. Oyarzun-Ampuero, A. Vidal, M. Concha, J. Morales, S. Orellana, I. Moreno-Villoslada, *Current Pharmaceutical Design*, **21** (2015) 4329.
2. N.C. Cady, J.L. Behnke, A.D. Strickland AD, *Advanced Functinal Materials*, **21** (2011) 2506.
3. A. Errokh, A.M. Ferraria, D.S. Conceição, L.F. Vieira Ferreira, A.M. Botelho de Rego, M. Rei Vilar, S. Boufi, *Carbohydrate Polymers*, **141**(2016) 229.
4. D. Marković, M. Korica, M. Kostić, Ž. Radovanović, Z. Šaponjić, M. Mitrić, M. Radetić, *Cellulose*, **25** (2018) 829.
5. V. Kumar, T. Yang, *Carbohydrate Polymers*, **48** (2002) 403.
6. J. Praskalo, M. Kostic, A. Potthast, G. Popov, B. Pejic, P. Skundric, *Carbohydrate Polymers*, **77** (2009) 791.
7. O. Šauperl, K. Stana-Kleinschek, V. Ribitsch, *Textile Research Journal*, **79** (2009) 780.
8. R. Khajavi, A. Berendjchi, *ACS Applied Materials & Interfaces*, **6** (2014) 18795.
9. C.K. Wu, M. Yin, S. O' Brien, T. Koberstein, *Chemistry of Materials*, **18** (2006) 6054.

The influence of 1,2,3,4-butantetracarboxylic acid on in situ synthesis of Cu_2O/CuO nanoparticles on the cotton fabric and its antibacterial activty

Darka Marković, Natalija Jocić*, Tim Nunney**, Christopher Deeks**, Željko Radovanović, Zoran Šaponjić***, Maja Radetić*

Innovation Center of the Faculty of Technology and Metallurgy, University of Belgrade, Karnegijeva 4, Belgrade

**Faculty of Technology and Metallurgy, University of Belgrade, Karnegijeva 4, Belgrade*

***Thermo Fisher Scientific, The Birches Industrial Estate, Imberhorne Lane, East Grinstead, West Sussex, RH19 1UB, UK*

****Institute of Nuclear Sciences "Vinča", University of Belgrade, P.O. Box 522, Belgrade*

Introduction

Ag nanoparticles (NPs) are widely applied as an efficient antimicrobial agent active against numerous microorganisms[1]. These NPs can be exploited for manufacturing of medical, protective and hygiene textiles. However, recently, Cu, Cu_2O and CuO NPs or their mixtures became the focus of many research groups[2-4] because of cheaper precursor salts compared to Ag salts and excellent antimicrobial activity against various bacteria strains. Although dip-coating method from the Cu-based NPs colloid/dispersion can be an option, the most dominant method for cotton fabric impregnation with Cu-based NPs relies on *in situ* synthesis which comprises of three steps: the introduction of carboxyl groups to cotton fibers, the adsorption of Cu^{2+}-ions from salt solution and the reduction with appropriate reducing agent. In this study, cotton fabric was modified with 1,2,3,4-butantetracarboxylic acid (BTCA). The intention was to explore the influence of BTCA initial concentration on the fabrication of Cu-based NPs and antibacterial activity of textile nanocomposite against Gram-negative bacterium *E. coli* and Gram-positive bacterium *S. aureus*.

Experimental

Desized and bleached cotton (Co) woven fabric (117.5 g/m^2, 52 picks/cm, 27 ends/cm, thickness of 0.26 mm) has been studied. Co fabrics were cleaned in the bath containing 0.1 % nonionic washing agent Felosan RG-N (Bezema) at liquor-to-fabric ratio of 50:1. After 15 min of washing at 50 ^oC, the fabric was rinsed first with warm water (50 ^oC) and then thoroughly with cold water. The samples were dried at room temperature.

One hour long treatment of Co fabrics with 1,2,3,4-butantetracarboxylic acid (BTCA) was conducted by immersion of 0.50 g of the sample in 20 mL of the acid aqueous solutions of 4, 6 and 10 w/v% in the presence of 0.82, 1.24 and 2.06 g of the catalyst sodium hypophosphite (SHP), respectively. After drying at 80 ^oC for 3 min the samples were cured at 170 ^oC for 3 min. The samples were then rinsed in distilled water and dried at room temperature. Modified samples are marked as Co+BTCA4, Co+BTCA6 and Co+BTCA10.

Afterwards, 0.50 g of Co+BTCA4, Co+BTCA6 and Co+BTCA10 fabrics were soaked in 25 mL of 10 mM solution of $CuSO_4$ for 2 h. In order to eliminate the excessive Cu^{2+}-ions, the samples were rinsed three times (1 min) with deionized water. 0.050 g of sodium borohydride ($NaBH_4$) was dissolved in 25 mL of 0.1 mM NaOH solution and the samples were immediately dipped into the solution where the reduction process took place in the following 30 min at room temperature. The samples were thoroughly rinsed with deionized

water and left to dry at room temperature. These samples are marked as Co+BTCA4+Cu, Co+BTCA6+Cu and Co+BTCA10+Cu.

Fourier transform infrared (FTIR) spectra of the control Co fabric, Co fabric treated with BTCA and Co fabric treated with BTCA after immersion in 0.1 M NaOH solution were recorded in the ATR mode using a Nicolet 6700 FTIR Spectrometer (Thermo Scientific) at 2 cm^{-1} resolution, in the wavenumber range 500–4000 cm^{-1}.

The morphology of Co fibers impregnated with NPs was studied by field emission scanning electron microscopy (FESEM, Tescan Mira3 FEG). The samples were coated with a thin layer of Au prior to analysis.

The amounts of adsorbed Cu^{2+}-ions on the Co+BTCA4, Co+BTCA6 and Co+BTCA10 fabrics from $CuSO_4$ solution were calculated on the basis of the concentration of residual Cu^{2+}-ions in the solution which was measured using a Spectra AA 55 B (Varian) atomic absorption spectrometer (AAS). AAS was also used for the measurement of the total Cu content in the Co fabrics after reduction process. Dry impregnated Co fabrics were dissolved in the 1:1 HNO_3 solution.

X-ray photoelectron spectroscopy (XPS) measurements were performed in order to evaluate the chemistry of the control Co and the Co+BTCA10+Cu fabric. The XPS analysis was carried out using a K-Alpha spectrometer (Thermo Scientific, UK) utilizing a monochromated Al Kα ($h\nu$ = 1486.6 eV) X-ray source.

The XRD powder patterns were acquired using a Philips PW 1050 powder diffractometer with Ni-filtered Cu-Kλ radiation (λ=1.5418 Å). The diffraction intensity was measured by the scanning technique (a step size of 0.05° and a counting time of 50 s per step).

The antibacterial activity of Co fabrics was tested against Gram-negative bacteria *E. coli* ATCC 25922 and Gram-positive bacteria *S. aureus* ATCC 25923 using a standard test method for the determining the antimicrobial activity of immobilized antimicrobial agents under dynamic contact conditions ASTM E 2149-01 (2001). The percentage of bacterial reduction (R, %) was calculated by the following equation:

$$R = \frac{C_0 - C}{C_0} \cdot 100$$

where C_0 (CFU – colony forming units) is the number of bacteria colonies on the control fabric and C (CFU) is the number of bacteria colonies on the fabric with NPs.

Results and discussion

Chemical changes induced by modification of Co fabric with BTCA were evaluated by FTIR spectroscopy. FTIR spectra of the control Co fabric, the Co+BTCA10 sample and the Co+BTCA10 sample which was immersed in 0.1 M NaOH solution are shown in Fig. 1. The bands specific for cellulose can be clearly seen in all spectra. The band with a peak centered at 1720 cm^{-1} in the spectrum of the Co+BTCA10 fabric indicated the establishing of ester bonds between hydroxyl groups of cellulose and carboxyl groups of BTCA[5,6]. An immersion of the Co+BTCA10 sample into NaOH solution brought about the deprotonation of free carboxyl groups. The carboxylate groups were proved by appearance of the band at 1565 cm^{-1}. The presence of both bands at 1720 cm^{-1} and 1565 cm^{-1} in shown spectra pointed out that BTCA was efficiently bound to cellulose by ester bonds, while a certain number of carboxyl groups retained free.

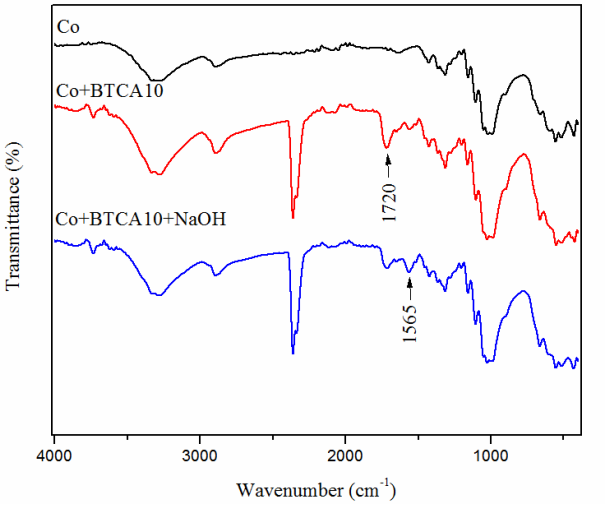

Figure 1. *FTIR spectra of the control sample, the Co+BTCA10+Cu sample and the Co+BTCA10+Cu sample which was immersed in 0.1 M NaOH solution*

Free carboxyl groups were exploited for adsorption of Cu^{2+}-ions from $CuSO_4$ aqueous solution. The values of Cu^{2+}-ions uptakes after 2 h long adsorption are given in Table 1. Obviously, the higher the concentration of applied BTCA solution, the larger the Cu^{2+}-ions uptake and consequently, the higher the content of Cu after reduction (Table 1). Cu content in the Co+BTCA6+Cu and the Co+BTCA10+Cu samples increased by 75 % and 174 % compared to the Co+BTCA4+Cu sample, respectively. In other words, the largest amounts of NPs were generated on the Co+BTCA10+Cu fiber surface. This can be attributed to an increase in the content of free carboxyl groups.

The form and distribution of NPs over the fiber surfaces are illustrated by FESEM images (Fig. 2). It can be noticed that larger amounts of single and agglomerated NPs were present on the surface of the Co+BTCA10+Cu sample. The size of the single NP was approximately 40 nm. The application of BTCA of lower concentrations (4 w/v%) resulted in synthesis of smaller amounts of NPs. Additionally, agglomeration was less prominent in this sample. Uneven distribution of NPs over the fiber surface is common for all studied Co fibers.

Table 1. *Cu^{2+}-ions uptake and total content of Cu after Cu^{2+}-ions reduction in Co fabrics modified with BTCA*

Sample	Cu^{2+}-ions uptake (μmol/g)	Total content of Cu after reduction, μmol/g
Co+BTCA4	55.8±6.4	50.8±1.4
Co+BTCA6	101.1±6.1	89.0±3.4
Co+BTCA10	145.0±7.0	139.0±4.1

XPS analysis was utilized for detection of the copper oxidation state in fabricated NPs. A high resolution scans of the Co+BTCA10+Cu sample were accomplished in the C1s, O1s and Cu2p regions and they are shown in Fig. 3a, 3b and 3c, respectively. Deconvolution of the C1s spectrum (Fig. 3a) revealed the presence of three components corresponding to C-O-, O-C-O and C-O-C groups of cellulose. Additional peak assigned to C-C/C-H groups is likely the contribution of residual waxes[7].

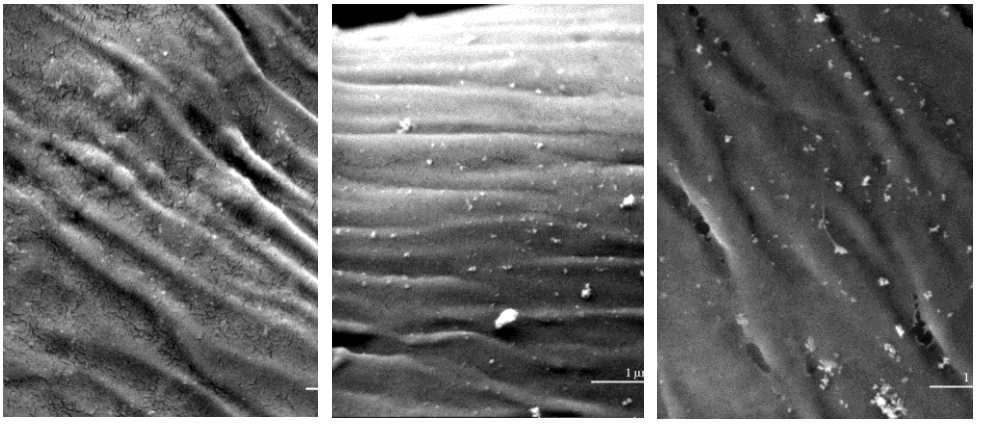

Figure 2. *The FESEM images of the Co+BTCA4+Cu (a), Co+BTCA6+Cu (b) and Co+BTCA10+Cu (c) fibers*

The O1s spectrum (Fig. 3b) was deconvoluted into two components attributed to organic O1s from cellulose and copper oxides. Two main peaks corresponding to $Cu2p_{3/2}$ and $Cu2p_{1/2}$ followed by shakeup satellites can be seen in the Cu2p spectrum (Fig. 3c). Asymmetric $Cu2p_{3/2}$ peak can be deconvoluted into two components: the peak associated to metallic Cu or Cu_2O and the peak ascribed to CuO. The presence of shakeup satellites proves the appearance of copper in the form of CuO. The shakeup satellites are specific for the materials which have a d^9 configuration like in a Cu^{2+}[8]. However, XPS measurements were not helpful for differentiation between metallic Cu and Cu_2O since the binding energies of the $Cu2p_{3/2}$ signal for these two forms differs by only 0.1 eV (932.6 and 932.7 eV for Cu and Cu_2O, respectively). Broader $Cu2p_{3/2}$ main peak and corresponding satellite in the Co+BTCA10+Cu sample may indicate larger amounts of CuO.

The Co+BTCA10+Cu fabric was also mapped and fitted to determine the atomic concentrations across its surface and to detect the uniformity of the surface. The results of the mapping of C1s, O1s and Cu2p signals are demonstrated in Fig. 4. It is obvious that the intensity of Cu2p signal varies over the sample. However, the mapping revealed relatively uniform distribution of Cu-based structures across the surface of the fabric.

Stronger evidence of NPs composition came from the XRD measurements. The XRD patterns of the control Co and Co+BTCA10+Cu samples are shown in Fig. 5. The cotton fabric has the characteristic cellulose I_β diffraction pattern. Shoulders (marked with rectangles) at 2θ~35.5° and 38.7° in difractogram of the Co+BTCA10+Cu composite indicated the formation of (-111) and (111) crystal planes of base centered monoclinic crystal phase of CuO (ICDD 01-089-5899). On the other hand, low intensity peak at 2θ~37.2° could be attributed to shifted peak characteristic for (111) crystal plane of cubic Cu_2O (ICDD 01-077-0199). Therefore, according to XPS and XRD measurements, it can be suggested that NPs are present on the Co fiber surface as a Cu_2O/CuO mixture.

The antibacterial activity of the Co fabrics was tested against Gram-negative bacterium *E. coli* and Gram-positive *S. aureus*. The samples modified with BTCA alone did not show any antibacterial activity. The results summarized in Table 2 reveal that the antibacterial activity depends on the Cu content in the samples. The Co+BTCA6+Cu and the Co+BTCA10+Cu samples provided 99.9 % bacterial reduction of both bacteria strains. However, the

Co+BTCA4+Cu sample ensured 99.9% reduction of *E. coli* colonies while the reduction of *S. aureus* was slightly lower (99.4%). Apparently, the amount of fabricated Cu_2O/CuO NPs was not sufficient for obtaining the maximum reduction of bacteria *S. aureus.*

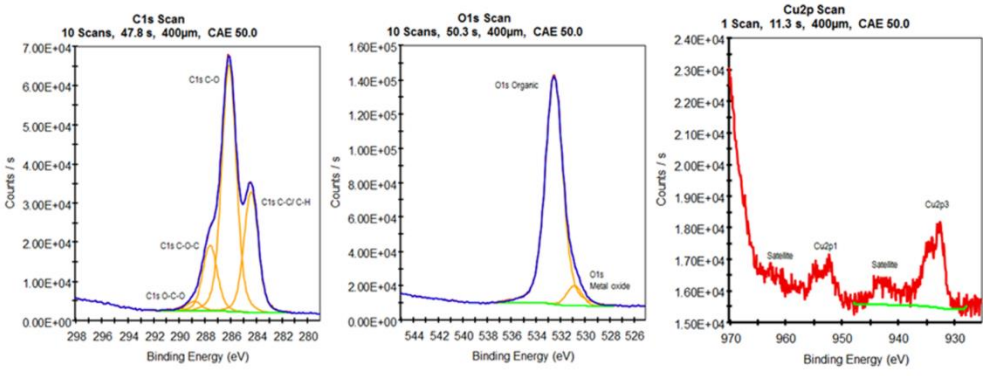

Figure 3. *XPS high resolution spectra of the Co+BTCA10+Cu in the* C1s, O1s, and *Cu2p regions*

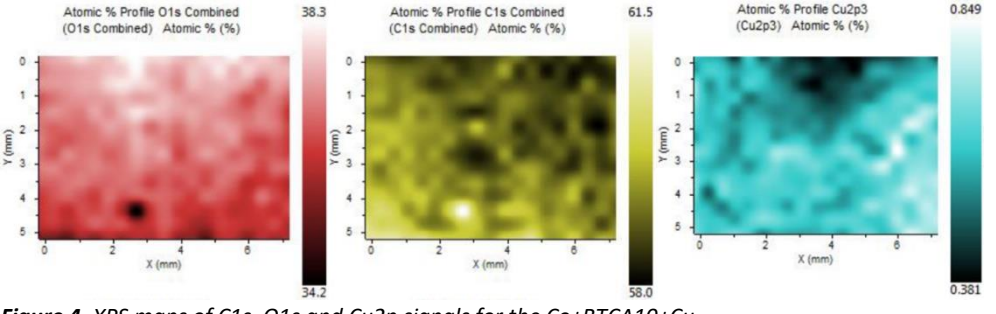

Figure 4. *XPS maps of C1s, O1s and Cu2p signals for the Co+BTCA10+Cu*

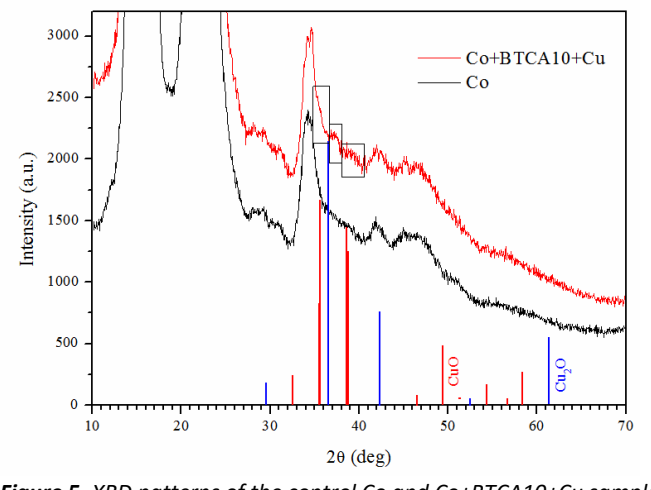

Figure 5. *XRD patterns of the control Co and Co+BTCA10+Cu samples*

Table 2 *Antibacterial activity of the Co fabrics impregnated with Cu_2O/CuO NPs*

Sample	Number of bacterial colonies, CFU	R, %	Number of bacterial colonies, CFU	R, %
	E. coli		*S. aureus*	
Control Co	1.5×10^5		6.6×10^4	
Co+BTCA4+Cu	65	99.9	730	99.4
Co+BTCA6+Cu	<10	99.9	<10	99.9
Co+BTCA10+Cu	<10	99.9	<10	99.9

Conclusions

Treatment of cotton fabrics with BTCA imparted the free carboxyl groups necessary for uptake of Cu^{2+}-ions. The application of higher concentration BTCA brought about larger uptake of Cu^{2+}-ions and fabrication of larger amounts of nanoparticles which were detected by FESEM analysis. XPS and XRD analyses revealed that nanoparticles existed as a mixture of Cu_2O and CuO. The amounts of Cu_2O/CuO nanoparticles on all studied cotton fabrics was sufficient to secure 99.9% reduction of Gram-negative bacteria *E. coli* and Gram-positive bacteria *S. aureus*, except in the case of the fabric modified with 4 w/v% of BTCA which exhibited slightly lower activity against *S. aureus*.

Acknowledgement: *The financial support for this study was provided by the Ministry of Education, Science and Technological Development of Republic of Serbia (projects no. 172056 and 45020).*

Uticaj koncentracije 1,2,3,4-butantetrakarboksilne kiseline na *in situ* sintezu nanočestica Cu_2O/CuO na pamučnoj tkanini i njenu antibakterijsku aktivnost

U ovom radu je ispitana mogućnost in situ sinteze nanočestica Cu_2O/CuO na pamučnoj tkanini prethodno modifikovanoj 1,2,3,4-butantetrakarboksilnom kiselinom (BTCA) različitih koncentracija sa ciljem postizanja antibakterijske zaštite. Utvrđeno je da se većom koncentracijom BTCA postiže bolja sorpcija Cu^{2+}-jona iz rastvora $CuSO_4$ i veći sadržaj nanočestica nakon redukcije. Prisustvo nanočestica na pamučnoj tkanini dokazano je FESEM analizom. XPS i XRD analizama je ustanovljeno da sintetisane nanočestice predstavljaju smešu Cu_2O i CuO. Dobijeni tekstilni nanokompoziti obezbeđuju odličnu antibakterijsku zaštitu prema Gram-negativnoj bakteriji E. coli i Gram-pozitivnoj bakteriji S. aureus koja zavisi od količine sintetisanih nanočestica Cu_2O/CuO.

References

1. M. Radetić, *Journal of Materials Science*, **48** (2013) 95.
2. N.C. Cady, J.L. Behnke, A.D. Strickland AD, *Advanced Functinal Materials*, **21** (2011) 2506.
3. A. Errokh, A.M. Ferraria, D.S. Conceição, L.F. Vieira Ferreira, A.M. Botelho de Rego, M. Rei Vilar, S. Boufi, *Carbohydrate Polymers*, **141**(2016) 229.
4. D. Marković, M. Korica, M. Kostić, Ž. Radovanović, Z. Šaponjić, M. Mitrić, M. Radetić, *Cellulose*, **25** (2018) 829.
5. O. Šauperl, K. Stana-Kleinschek, V. Ribitsch, *Textile Research Journal*, **79** (2009) 780.
6. R. Khajavi, A. Berendjchi, *ACS Applied Materials & Interfaces*, **6** (2014) 18795.
7. D. Mihailović, Z. Šaponjić, M. Radoičić, S. Lazović, C. Baily, P. Jovančić, J. Nedeljković, M. Radetić,*Cellulose*, **18** (2011) 811.
8. C.K. Wu, M. Yin, S. O' Brien, T. Koberstein, *Chemistry of Materials*, **18** (2006) 6054.

Nauka o materijalima

Material Science

Homogenization effect on microstructure Al-Mg-Si alloy containing low-melting point elements

Tamara Radetić, Bojan Gligorijević, Mirjana Filipović, Miljana Popović, Endre Romhanji
Faculty of Technology and Metallurgy, University of Belgrade, Karnegijeva 4, Belgrade

Introduction

Extrdability of 6xxx series aluminium alloys (Al-Mg-Si-X) depends to the great extent on the microstructure of the homogenized billets [1]. In addition to the typical inhomogeneities such as elemental micro- and macro- segregations, the microstructure of as-cast state of Al-Mg-Si-X is characterized by the presence of iron-based intermetallic that can be detrimental for the deformability of these alloys. There are two types of Fe bearing intermetallics; the metastable, β-AlFeSi phase with monoclinic crystal structure and plate or needle-like morphology is impairing extrudability of the as-cast bullet by acting like stress concentrator and inducing local cracking and surface defects in the extrusions (2-4). One of the goals of the homogenization treatment is transformation of metastable β-AlFeSi into stable α-AlFe(Mn)Si, with a cubic crystal structure and benevolent, globular morphology. The temperature range for β-AlFeSi -> α-AlFe(Mn)Si transformation is quite broad, temperature should be above 450 °C in order to achieve appreciable transformation kinetic caused by the low diffusivity of Fe and Mn, so the selection of the homogenization processing parameters depends very much on the Mg and Si content in the alloy [2,4]. The general rule is that the homogenization temperature should be above β-Mg_2Si solvus in order to acheieve an alloy's aging potential and desired mechanical properties, and below the solidus temperature of the pseudobinary Al-Mg_2Si system for the given alloy composition. In the alloys with high Mg and Si content, like AA 6082 and its derivative AW6026, that is subject of this study, the homogenization temperature should be in a range 540°-580 °C [1]. However, the composition of AW6026 alloy is specific as it contains heavy metals Pb and Bi that are added in order to improve machinability of the alloy. These low melting point elements (T_m(Pb)=327 °C, T_m(Bi)=271.4 °C) are essentially insoluble in Al and have a tendency to segregate towards grain boundaries and free surfaces. There are reports [5] that at temperatures above 500 °C excessive migration of Pb and Bi toward surfaces takes place resulting in depletion of the low melting point phases required for good machinability. That would set homogenization temperature in significantly lower range than required for dissolution of Mg_2Si. In addition, there are reports that wetting transition of grain boundaries by Pb occurs at temperatures 520-560 °C, depending on grain boundary type, increasing the propensity toward liquid metal embrittlement.

This study is aimed at evaluating the effect of homogenization parameters on completeness of β-AlFeSi->α-AlFe(Mn)Si transition, Mg_2Si dissolution and extent of loss of Pb and Bi in order to determine optimal homogenization parameters.

Experimental procedure

The chemical composition of the studied AW6026 alloy, industrially cast in NISAL-Niš/Serbia, is presented in Table 1.

Table 1 *Chemical composition of AW6026 alloy*

Si	Fe	Cu	Mn	Mg	Cr	Ni	Zn
1.125	0.097	0.294	0.487	1.033	0.123	0.004	<0.002
Ti	Pb	Sn	Bi	V	Zr	Co	
0.009	0.252	0.006	0.697	0.010	<0.001	<0.002	

The specimens from the section of the as-cast bullet underwent homogenization treatments at a range of temperatures: 12h/480 °C, 12h/530 °C, 12h/550 °C and 6h/550 °C. The microstructural characterization of as-cast state and thermally treated specimens, previously mechanically polished by a standard procedure, was conducted in FEG SEM Tacan Mira and JEOL SEM equipped with EDS detector at 20 kV. For quantitative microstructural analysis, ImageJ software package was used. For evaluation of the effect of homogenization treatment on the grain size, specimens were electrolytically etched in Barkers reagent and characterized by optical microscopy in polarized light. In order to obtain representative statistics, the microstructural characterization and quantification were conducted on the area over 3x3 mm^2.

Results and discussion

Microstructure characterization showed that homogenization 12 h/480 °C has not resulted in β-AlFeSi -> α-AlFe(Mn)Si transformation to the significant degree. The slow diffusion of Fe at 480 °C is responsible for preserval of needle-like morphology (Figure 1a), since it controls the transformation kinetics. However, homogenization at 480 °C not only that it did not dissolve existing β-Mg_2Si (Figure 1a), but resulted in additional β-Mg_2Si precipitation since for the Mg and Si content in the studied alloy, β-Mg_2Si solvus is around 540 °C. Although preferential sites for β-Mg_2Si precipitation are interfaces of intermetallic phases and Al matrix, a fine plate β-Mg_2Si precipitation that has crystallographic orientation relationship with Al matrix was observed to form (Figure 1b).

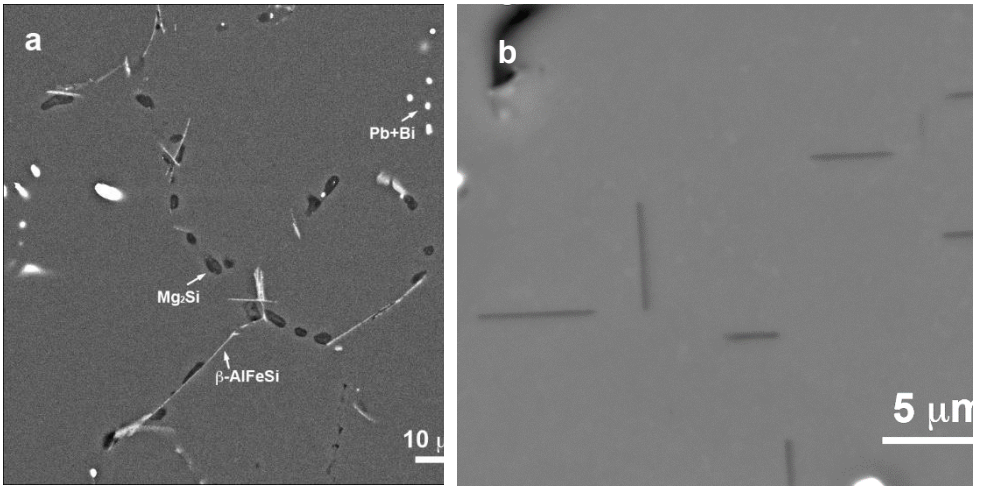

Figure 1. *BE SEM micrographs of the microstructure after homogenization 12 h/480 °C:(a) Light, long needle-like particles are β-AlFeSi phase. Coarse particles in dark contrast are β-Mg_2Si, that coagulate during homogenization; (b) Additional β-Mg_2Si precipitated during the homogenization.*

Homogenization at 530 °C resulted in partial β-AlFeSi -> α-AlFe(Mn)Si transformation (Figure 2). After 12 h of annealing, about 50-70 % of β-AlFeSi has been transformed, indicating that a longer thermal treatment is required to achieve desired transformation over 80 %.

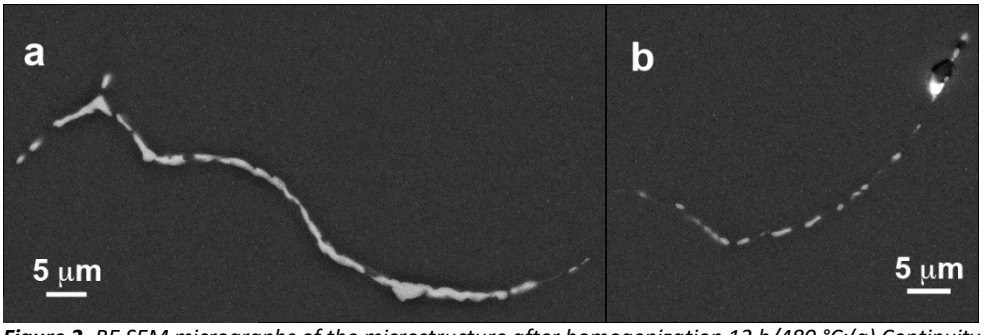

Figure 2. *BE SEM micrographs of the microstructure after homogenization 12 h/480 °C:(a) Continuity of β-AlFeSi is becoming interrupted indicating the initiation of β - > α transformation; (b) Particles of pearl-like morphology along the contour of original β–phase signalize complete transformation.*

The increase in the homogenization temperature for 20 °C, to 550 °C, resulted in the much faster kinetics of the transformation. After 6 h of annealing, the transformation is almost complete (≥90%) (Figure 3a). Extending homogenization time to 12 h does not significantly change the microstructure with respect to the β-AlFeSi -> α-AlFe(Mn)Si transformation. One of the products of high temperature homogenization ($T_{homog.}$>500 °C) is precipitation of fine Al-Mn-Fe-Si dispersoids (Figure 3b).

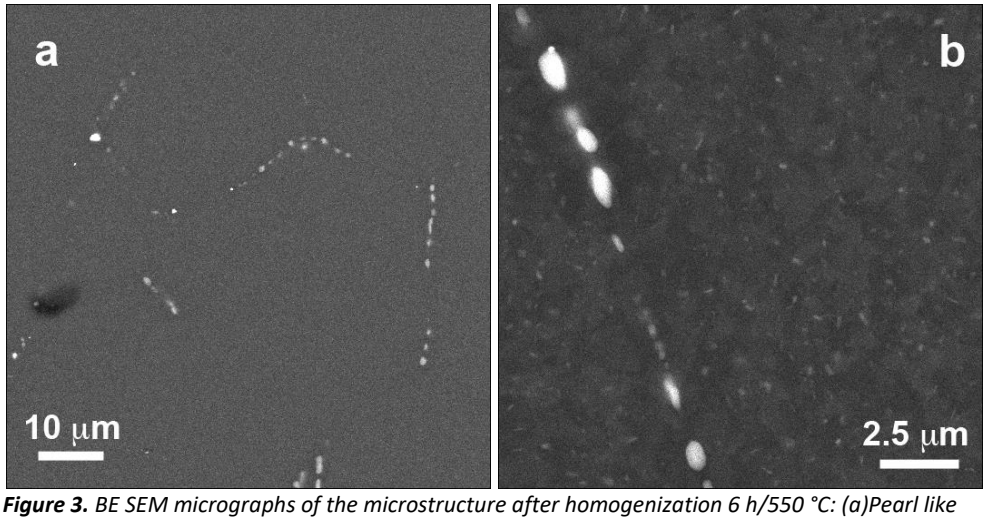

Figure 3. *BE SEM micrographs of the microstructure after homogenization 6 h/550 °C: (a)Pearl like morphology dominates the microstructure indicating complete β - > α transformation; (b) Fine dispersoids precipitate.*

Coagulation of β-Mg_2Si was already observed during homogenization at 480 °C (Figure 1a). However, the process of dissolution of β-Mg_2Si only starts at higher temperatures. As it has

been expected degree of dissolution is higher at 550 °C than at 530 °C, since solvus lies between two temperatures. Longer homogenization time (12 h/550 °C) or even higher temperature (560 °C) might result in more Mg_2Si dissolution, but the effect is not significant, particularly because an increase in exposure of the alloy to very high temperatures might give rise to a higher loss of heavy elements, Pb and Bi.

Table 2. *Stereological parameters of heavy element particles (Pb and Bi)*

State	Area fraction, %	<particle size>, μm	roundness
12 h/480 °C	0.53	1.37	0.47
12 h/530 °C	0.48	1.21	0.57
6 h/550 °C	0.45	1.55	0.59

One of the critical issues with the homogenization at high temperatures is coarsening and escape to the surface of Pb and Bi particles. However, measurements of the area fraction of heavy element particles in as-cast state and after homogenization show a small drop (Table II). Similarily, the mean particle size is almost unchanged, but the increase in the roundness of the particles indicate some degree of shape change and coagulation. The absence of the significant change in fraction and distribution of heavy metal particles is evident in Figure 4.

Characterization of regions close to the edges of the specimens did not reveal depleted regions, while chemical analysis of homogenized specimens showed that Pb and Bi content is in the domain of statistical variation in the as-cast state. Lack of lost of the heavy elements is surprising since even Pb and Bi particles in Al matrix are expected to have high mobility at temperatures above 510-520 °C. This temperature range corresponds to the roughening transition of Al/Pb {111} interfaces. Namely, motion Bi and Pb particles in Al matrix, due to their lack of solubility in Al, does not occur by conventional vacancy mechanism but is controlled by Al self-diffusion and edge nucleation at the interface [6,7]. At roughening transition energetic barrier for edge nucleation becomes zero and particle migration becomes controlled by Al self-diffusion. Likely cause of small Pb and Bi loss is reaction with Mg. Bi has a strong affinity toward Mg to forming high-melting point compound and its function in the alloy is to act as a «gether» for Mg to keep Pb as low-melting elementary particles. EDS analysis showed that Bi particles contain Mg in the great amount. However, in the case of Pb, Mg content is a low indicating the formation of elementary core/shell structure elementary Pb/PbMg. So the formation of such shell can limit the mobility of Mg particles.

From a grain size measurements appears that the different homogenization treatments do not have a significant effect on grain size. Grain growth is limited during the homogenization due to the Zener pinning by dispersoids and intermetallic particles. Interestingly, it appears that Pb and Bi particles take part in Zener pining as the regions with a lower content of Pb and Bi are characterized by the larger grains.

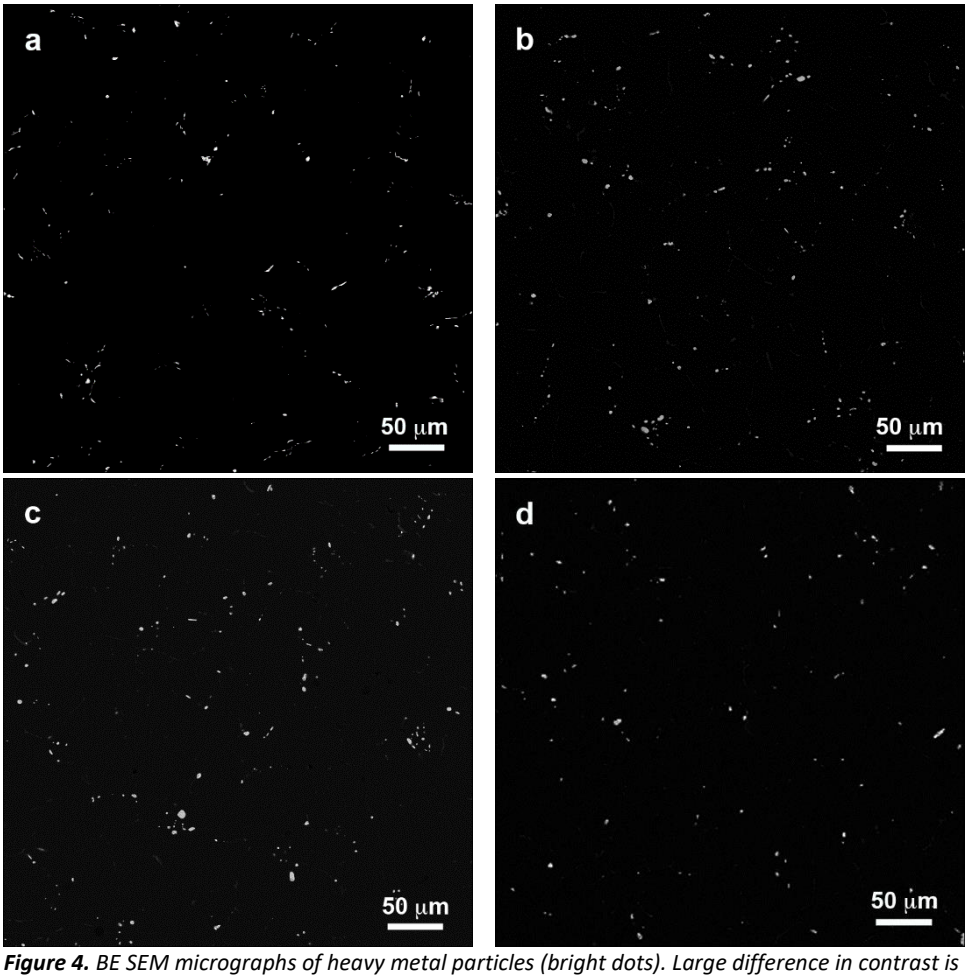

Figure 4. *BE SEM micrographs of heavy metal particles (bright dots). Large difference in contrast is due to the difference in atomic number and scattering power. (a) as-cast state; (b) 12 h/480 °C; (c) 12 h/530 °C; (d) 6 h/550 °C.*

Summary

Low-temperature homogenization ($T_{homog.}$≤500 °C) requires very long annealing times for β-AlFeSi -> α-AlFe(Mn)Si transformation to take place. However, due to the high Mg and Si content in AW 6026 alloys, homogenization at 480 °C results in undesired precipitation of β-Mg_2Si particles.

Increase in homogenization temperature results in faster β-AlFeSi > α-AlFe(Mn)Si transformation kinetics, with annealing at 550 °C cutting homigenization time in half. Dissolution and coagulation of the existing β-Mg_2Si take place increasing the alloy aging potential in further processing. Importantly, high-temperature homogenization did not result in Pb and Bi loss, most likely due to the formation of compounds and core/shell structure around the particles of low-melting point compounds.

Acknowledgement: *This work has been supported by Ministry of Education, Science and Technological Development of the Republic of Serbia, contract No. E!9992.*

Effekat homogenizacije na mikrostrukturu Al-Mg-Si legure koja sadrži nisko-topive elemente

Predmet ovog rada je bilo ispitivanje i karakterizacija uslova homogenizacionog žarenja na mikrostruktu Al-Mg-Si legure legirane nisko-topivim metalima Pb i Bi. Rezultati pokazuju da homogenizacija na temperaturama nižim od 500 °C zahteva izuzetno duga vremena žarenja da bi došlo do β-AlFeSi -> α-AlFe(Mn)Si *transformacije, neophodne za sposobnost legure za presovanje. Dodatno, dolazi do izdvajanja β-Mg_2Si faze, čime se smanjuje sposobnost legure za starenje u daljoj preradi. Visoko-temperaturna homogenizacija ne samo da rezultuje u potpunoj β-AlFeSi -> α-AlFe(Mn)Si transformaciji i rastvarnju β-Mg_2Si faze, već i ne dolazi do očekivanog gubitka Pb i Bi usled izdvajanja na površini uzoraka.*

References

1. T. Sheppard, *Extrusion of Aluminium Alloys*, Kluwer Academic Publishers, Dordrecht, The Netherlands 1999, p. 253. IBSN-13: 978-0412590702
2. N.C.W. Kuijpers, F.J. Vermolen, C. Vuik, P.T.G. Koenis, K.E. Nilsen, S.V.D. Zwaag, *Materials Science and Engineering* A394 (2005) 9 (https//dx.doi.org/10.1016/j.msea.2004.09.073).
3. N.C.W. Kuijpers, F.J. Vermolen, C. Vuik, S. Van Der Zwaag, *Materials Transacations* 44A (2003) 1448 (https//dx.doi.org/10.2320/matertrans.44.1448).
4. S.R. Claves, D.L. Elias, W.Z. Misiolek, *Materials Science Forum* 396-402 (2002) 667 (https//dx.doi.org/10.4028/www.scientific.net/MSF.396-402.667.)
5. M.Bauser, G. Sauer, K. Siegert , *EXTRUSION*, ASM International, Materials Park , Ohio, USA 2006, p.141 (ISBN: 978-0-87170-837-3).
6. H. Gabrich, L. Kieldgaar, d, E. Johnson, U. Dahmen, *Acta Mater.* 49 (2001) 4259 (https://dx.doi.org/10.1016/S1359-6454(01)00307-X).
7. T Radetic, E Johnson, DL Olmsted, Y Yang, BB Laird, M Asta, U Dahmen, Acta Mater. 141 (2017) 427 (https://dx.doi.org/10.1016/j.actamat.2017.09.040)

Hemija životne sredine

Environmental Chemistry

Uticaj pH na vezivanje jona teških metala na površinu lignoceluloznih biosorbenata

Dragana Kukić, Marina Šćiban, Vesna Vasić, Jelena Prodanović
Univerzitet u Novom Sadu, Tehnološki fakultet Novi Sad, Bul. Cara Lazara 1, Novi Sad

Uvod

Razvoj industrije i porast potrošnje sveže vode doveli su do poremećaja u ekosistemu, usled ispuštanja neprečišćenih otpadnih voda u okolinu. Industrijska aktivnost je uticala na tok materija u prirodi tako da su se u akvatičnim sredinama, pored prirodno prisutnih, pojavile i neke druge suspstance, kao što su tekstilne boje, fenoli, pesticidi, deterdženti, teški metali i dr. Neki metali su važni za sve aerobne i većinu anaerobnih organizama, ali je dokazano da isti ti metali u velikim količinama, a neki, kao što su na primer olovo, kadmijum i živa i u vrlo malim količinama mogu ozbiljno negativno uticati na životnu sredinu i zdravlje ljudi. Teški metali su toksični polutanti koji nisu podložni biorazgradnji, pa zbog toga jednom ispušteni u životnu sredinu tu trajno i ostaju, te se sa vremenom nakupljaju u različitim sistemima u koncentracijama višim od dozvoljenih. Još jedna negativna strana ovih polutanata je i činjenica da imaju tendenciju bioakumulacije, usled čega dospevaju u lanac ishrane dovodeći do biomagnifikacije.[1,2]

Mnoge razvijene zemlje imaju strogu zakonsku regulativu u vezi sa ispuštanjem otpadnih voda u okolinu, koje podrazumevaju obradu otpadne vode u cilju smanjenja količina zagađujućih materija pre njenog ispuštanja. Za uklanjanje jona teških metala iz vode mogu se primeniti tradicionalne metode poput adsorpcije na aktivnom uglju, precipitacije, koagulacije, jonske izmene, membranske filtracije i dr. Međutim, ove metode su vrlo često skupe, nedovoljno efikasne ili tehnički komplikovane kada je koncentracija jona metala manja od 100 mg/l, a kod nekih nastaje toksični mulj. Jedna od najčešće primenjivanih metoda je adsorpcija aktivnim ugljem, ali je njena primena ograničena zbog visoke cene proizvodnje i regeneracije aktivnog uglja kao adsorbenta. Poslednjih decenija je iskazan značajan trud u ispitivanju novih, jeftinijih i efikasnijih materijala za ovu primenu.[1,2] Najviše pažnje se poklanja prirodnim materijalima, i to najčešće agro-industrijskom otpadu koji je lako dostupan u velikim količinama. Prednost ove metode u odnosu na tradicionalne postupke je niska cena, visoka efikasnost, minimizacija hemijskog ili biološkog mulja, mogućnost regeneracije biosorbenta i izdvajanja metala.[2]

Najveći izazov za istraživače je izbor odgovarajuće biomase iz tako velikog broja jeftinih biomaterijala, s obzirom da gotovo svi biološki materijali imaju određen afinitet prema jonima metala, ali i drugim polutantima. Zbog toga je neophodno svaki potencijalni biosorbent ispitati detaljno, utvrditi adsorpcioni kapacitet i optimalne uslove adsorpcije, kako bi se ovi materijali mogli uspešno primenjivati u praksi. U ovom radu ispitana je mogućnost vezivanja jona bakra, nikla, kadmijuma i hroma na izlužene rezance šećerne repe, koji zaostaju u velikim količinama nakon proizvodnje šećera, i uticaj pH vode na proces adsorpcije.

Izvedeni su ogledi šaržne adsorpcije iz model vodenih rastvora soli teških metala. Za pripremu model vode početne koncentracije oko 50 mg/l jona metala korišćeni su osnovni rastvori soli teških metala: $CuSO_4 \cdot 5H_2O$, $Cd(NO_3)_2 \cdot 4H_2O$, $NiCl_2 \cdot 6H_2O$ i $K_2Cr_2O_7$,

koncentracije 0,25 mol/l, a za podešavanje pH model vode korišćeni su rastvori sirćetne i azotne kiseline i amonijum-hidroksida.

Ispitivanja adsorpcionih sposobnosti izluženih repinih rezanaca za jone teških metala su izvođena na sobnoj temperaturi po sledećoj proceduri: u Erlenmajer tikvice sa šlifovanim zatvaračem unese se 200 ml model vode poznate početne koncentracije jona metala i željene pH vrednosti i doda adsorbent u količini od 5 g/l. Sadržaj Erlenmajer tikvice se zatim meša na mehaničkoj tresilici (MLW THYS 2) 90 min, a zatim se adsorbent odvaja filtracijom kroz filter papir (Macherey-Nagel 651/120) i u filtratu određuje preostala koncentracija jona metala.

Količina jona metala adsorbovanih po jedinici mase adsorbenta izračunata je na osnovu vrednosti koncentracije jona metala u model vodi pre i posle adsorpcije:

$$Q = (C_0 - C)/m$$

gde je:

q – masa adsorbovanih jona metala po jedinici mase adsorbenta (mg/g)
C_0 – početna koncentracija jona metala u model vodi (mg/l)
C – rezidualna koncentracija jona metala u model vodi (mg/l)
m – masa adsorbenta (g/l).

Svi eksperimenti su rađeni u dva ponovljanja, a rezultati izraženi kao srednja vrednost.

Rezultati i diskusija

pH vrednost je jedan od najznačajnijih parametara koji utiču na proces biosorpcije. Pre svega, utiče na osobine samih jona metala, kompeticiju sa koegzistirajućim jonima u rastvoru i na aktivnost funkcionalnih grupa, jer naelektrisanje funkcionalnih grupa zavisi od pH rastvora. Za pH vrednosti veće od p*K*a funkcionalnih grupa, većina grupa je disocirana i mogu vezati jone metala iz rastvora. Na pH vrednostima nižim od p*K*a može doći do kompleksiranja, posebno kod kiselih karboksilnih grupa.[3] Reakacija jona metala i adsorbenta u rastvoru se može prikazati kao:

$$M^{+n} + BH_n \leftrightarrow BM + nH^+$$

gde je M jon metala, n njegovo naelektrisanje, a B aktivno mesto na adsorbentu.[4]

Uticaj pH vrednosti je ispitan za proces adsorpcije jona Cd(II), Cu(II), Ni(II) i Cr(VI) izluženim repinim rezancima u različitim opsezima pH izabranim na osnovu literaturnih podataka. Za jone kadmijuma ispitan je opseg pH vrednosti od 5 do 9, za jone bakra od 3 do 8, za jone nikla od 3 do 9, a za jone šestovalentnog hroma od 1 do 6. Dobijeni rezultati su prikazani na slici 1.

Može se primetiti da izluženi rezanci šećerne repe imaju mnogo bolje adsorpcione sposobnosti za jone bakra u ispitanim opsezima pH u odnosu na jone drugih metala. Efikasnost adsorpcije jona Cu(II) je najniža na pH 3, dok je na pH 4 nešto viša i zadržava približno istu vrednost na svim ostalim ispitivanim pH vrednostima. Maksimalni ostvareni kapacitet iznosi 6,50 mg/g, što odgovara efikasnosti uklanjanja ovih jona iz vode od 64,8 %. Ovakav uticaj pH vrednosti na efikasnost adsorpcije se može objasniti činjenicom da joni bakra u zavisnosti od pH vrednosti rastvora mogu postojati u različitim oblicima (slika 2). Na pH nižim od 5 pretežno su prisutni kao Cu^{2+}, dok na višim pH precipitiraju u obliku $Cu(OH)_2$,[5] pa njihovo uklanjanje u tim uslovima nije posledica samo adsorpcije.

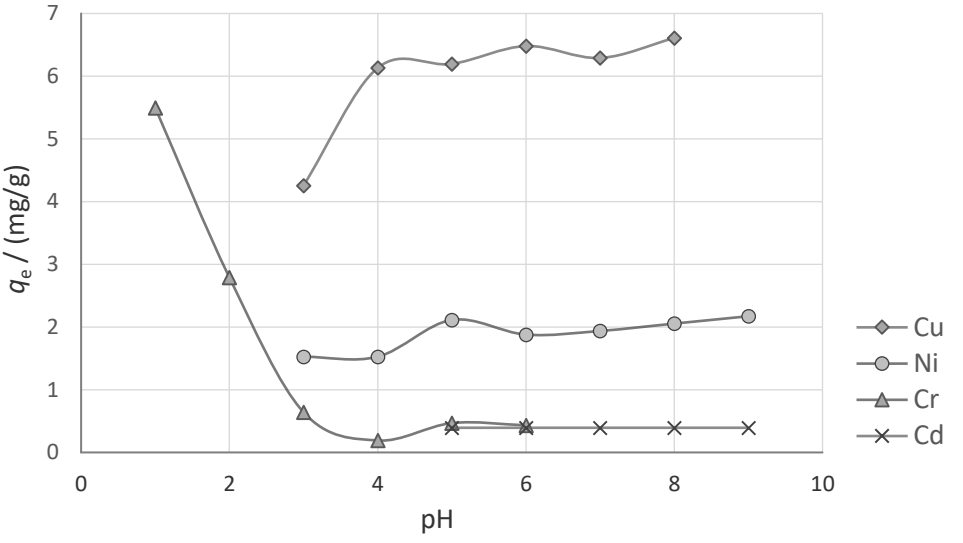

Slika 1. *Uticaj pH vrednosti na adsorpciju jona Cu(II), Ni(II), Cd(II) i Cr(VI)*

Wan Nagh i Hanafiah[5] su ispitivanjem uticaja pH na adsorpciju jona bakra prahom lišća *Hevea brasilien*sis odsustvo adsorpcije na pH 2 objasnili odbojnim silama između Cu^{2+} i H_3O^+ jona koji okružuju adsorbent, dok se povećanjem pH vrednosti smanjuje broj hidronijum jona, pa se omogućava pristup jona bakra aktivnim mestima. Pored toga, povećanje pH može uzrokovati da neke funkcionalne grupe poput amino, hidroksilnih i karboksilnih dobiju negativno naelektrisanje i tako privuku jone bakra. Isto objašnjenje o smanjenju pozitivnog naelektrisanja površine i kompeticiji protona i jona metala dali su i Reddad i dr.[6] za adsorpciju jona bakra izluženim rezancima šećerne repe koji su takođe pokazali najveći afinitet prema jonima bakra u odnosu na ostale ispitane jone, pa bi se dalo pretpostaviti da se ovo objašnjenje može primeniti i na ovde prikazane rezultate.

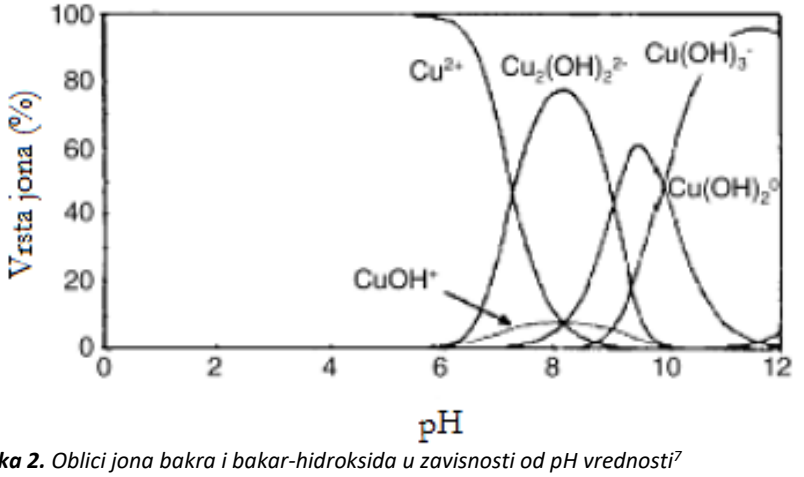

Slika 2. *Oblici jona bakra i bakar-hidroksida u zavisnosti od pH vrednosti*[7]

Efikasnost adsorpcije jona Ni(II) je viša od efikasnosti adsorpcije jona Cd(II), ali niža od efikasnosti adsorpcije jona Cu(II) i blago se povećava sa povećanjem pH do vrednosti 5. U toj tački se postiže maksimum adsorpcije koji neznatno varira sa daljim povećanjem pH. Maksimalni adsorpcioni kapacitet jona Ni(II) pri početnoj koncentraciji od oko 50 mg/l koji je postignut na pH 5, iznosi 2,12 mg/l.

Adsorpcija jona Cd(II) je vrlo slaba u celom opsegu ispitanih pH vrednosti. Količina vezanih jona je svega 0,40 mg/g u celom opsegu ispitivanih pH vrednosti. Kao što se može videti na slici 3, u ovom opsegu pH vrednosti se kadmijum većinom nalazi u obliku dvovalentnih jona i tek se na pH 9 u rastvoru pojavljuje izvesna količina $CdOH^+$, ali je i dalje u obliku pozitivno naelektrisanih jona. Reddad i dr.[6] su takođe došli do saznanja da izluženi rezanci šećerne repe imaju slabiji afinitet prema ovim jonima u odnosu na druge ispitane jonske vrste.

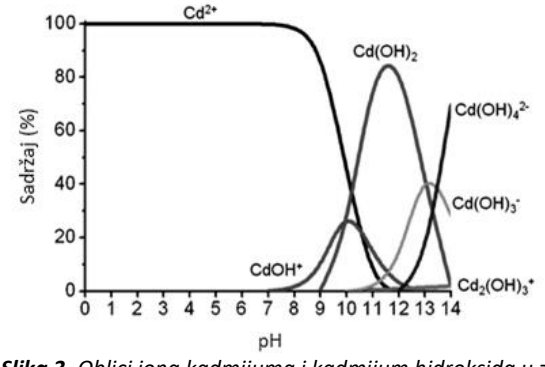

Slika 3. *Oblici jona kadmijuma i kadmijum hidroksida u zavisnosti od pH vrednosti*[8]

Joni Cr(VI) se u vodenim rastvorima mogu naći u više oblika u zavisnosti od njihove koncentracije i pH vrednosti rastvora (slika 4). U ispitivanom opsegu pH od 2 do 6, hrom je u obliku $HCrO_4^-$ ili $Cr_2O_7^{2-}$, a adsorpcija slabih anjona se zasniva na formiranju kompleksa sa protonizovanom aktivnim grupama na površini adsorbenta pri čemu se javlja veliki afinitet prema negativno naelektrisanim jonima u vodi, pa je efikasnost adsorpcije ovih jona veća na nižim pH vrednostima.[9] Kako se pH vrednost povećava, koncentracija H^+ jona se smanjuje, a površina adsorbenta bi u tom slučaju trebala biti negativno naelektrisana što može sprečiti vezivanje jona hroma. Zbog toga može doći do smanjenja adsorpcije jona hroma pri višim pH vrednostima.[10]

U ovde predstavljenim ogledima, joni hroma se najefikasnije uklanjaju na najnižem pH (pH 1), 59,8 %. Na ovom pH kapacitet adsorpcije Cr(VI) iznosi 5,47 mg/g. Sa smanjenjem kiselosti rastvora smanjuje se efikasnost adsorpcije i već na pH 2 iznosi 32,2 %. Sa daljim povećanjem pH vrednosti smanjuje se i efikasnost, a svoj minimum dostiže na pH 4, dok na pH 5 i 6 ima izvesnu malu vrednost. Kobya[12] smanjenu adsorpciju na višim pH objašnjava negativnim naelektrisanjem površine usled povišene koncentracije OH^- jona što onemogućava vezivanje jona hroma, koji na tim pH vrednostima postoji kao CrO_4^{2-} i $Cr_2O_7^{2-}$. Reddad i dr.[13] su u svojim istraživanjima objavili sledeći redosled efikasnosti vezivanja jona izluženim repinim reznacima na pH 5: Pb(II) > Cd(II) > Cu(II) ~ Zn(II) > Ni(II), dok su rezultati ovde prikazanih ispitivanja na pH 5 dali sledeći redosled: Cu(II)> Ni(II) > Cd(II) ~ Cr(VI). Iako se radi o istoj vrsti adsorbenta mora se uzeti u obzir da je to biološki materijal čija se

struktura i sastav mogu razlikovati u zavisnosti od uslova uzgoja ili tehnološkog procesa proizvodnje šećera, koji mogu uzrokovati različite adsorpcione karakteristike.

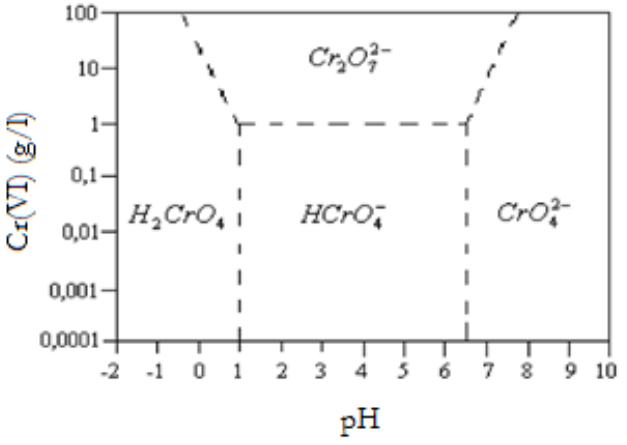

Slika 4. *Oblici jona hroma u zavisnosti od pH vrednosti*[11]

Zaključak

Rezultati ovih ispitivanja su pokazali da izluženi rezanci šećerne repe imaju mnogo bolje adsorpcione karakteristike za jone bakra u ispitanim opsezima pH u odnosu na jone drugih teških metala. Efikasnost adsorpcije jona Cu^{2+} je najniža na pH 3, dok je na pH 4 nešto viša i zadržava približno istu vrednost na svim ostalim ispitivanim pH vrednostima. Maksimalni kapacitet iznosi 6,50 mg/g, što odgovara efikasnosti uklanjanja ovih jona iz vode od 64,8%. Adsorpciju jona bakra je najbolje izvoditi na pH 4 zbog višeg adsorpcionog kapaciteta u odnosu na niže pH vrednosti i izbegavanja stvaranja hidroksida na višim pH, tako da će smanjenje koncentracije nakon adsorpcije biti posledica samo vezivanja jona na adsorbent. Makismalni adsorpcioni kapacitet jona Ni(II) pri početnoj koncentraciji od oko 50 mg/l je postignut na pH 5 i iznosi 2,12 mg/l. Adsorpcija jona Cd(II) je vrlo slaba u celom opsegu ispitanih pH vrednosti. Količina vezanih jona je svega 0,40 mg/g. Za jone hroma, najveći adsorpcioni kapacitet se postiže na najnižoj pH vrednosti, ali je zbog velikog utroška kiseline ipak pogodnije adsorpciju izvoditi na pH 2.

Zahvalnica: *Ovaj rad je deo projekta III 43005 finansiranog od strane Ministarstva prosvete, nauke i tehnološkog razvoja Republike Srbije.*

The influence of pH on the binding of heavy metal ions to the surface of lignocellulosic biosorbents

In this paper, the adsorption ability of sugar beet shreds to bond copper, nickel, chromium and cadmium ions at different pH values of water was studied. Results showed that sugar beet shreds have much better adsorption capacity for copper ions compared to other metal ions. Adsorption of these ions is best to performe at pH 4 because at lower pH amount of bound ions is less and at pH 5 and higher formation of hydroxide occurs. In that case, the decrease of residual concentration of metal ions is not only due to adsorption. For chromium

ions, the highest adsorption capacity is achieved at the lowest pH, but due to the high acid consumption it is recommended to perform it at pH 2.

Literatura

1. V. M. Nurchi, I.Villaescusa, *Coordination Chemistry Reviews,* **252** (2008) 1178.
2. T.A.H. Nguyen, H.H. Ngo, W.S. Guo, J. Zhang, S. Liang, Q.Y. Yue, Q. Li, T.V. Nguyen, *Bioresource Technology,* **148** (2013) 574.
3. A. E. Ofomaja, E. I. Unuabonah, N. A. Oladoja, *Bioresource Technology,* **101** (2010) 3844.
4. M. Iqbal, A. Saeed, S. I. Zafar, *Journal of Hazardous Materials,* **164 (1)** (2009) 161.
5. W. S. Wan Ngah, M. A. K. M. Hanafiah, *Journal of Environmental Sciences,* **20** (2008) 1168.
6. Z. Reddad, A. Y. Gérente, J.-F. Thubault, P. Le Cloirec, *Environmental Science & Technology,* **36** (2002) 2242.
7. X.-s. Wang, Y. Qin, *Process Biochemistry*, **40(2)** (2005) 677.
8. J. Choi, A. Ide, Y. B. Truong, I. L. Kyratzis, R. A. Caruso, *Journal of Materials Chemistry A,* **1** (2013) 5847.
9. P. Miretzky, A. Fernandez Cirelli, *Journal of Hazardous Materials,* **180** (2010) 1.
10. G. Blázquez, F. Hernáinz, M. Calero, M.A. Martín-Lara, G. Tenorio, *Chemical Engineering Journal,* **148** (2009) 473.
11. D. Duranoğlu, U. Beker, *Cr(VI) Adsorption Onto Biomass Waste Material-Derived Activated Carbon*,*Chapter 10*, in *Desalination Updates*, R.Y. Ning, inTechopen.com, 2015, (http://dx.doi.org/10.5772/60206)
12. M. Kobya, *Bioresource Technology*, **91(3)** (2004) 317.
13. Z. Reddad, A. Y. Gérente, J.-F. Thubault, P. Le Cloirec, *Environmental Science & Technology,* **36** (2002) 2067.

Simultaneous removal of selected pesticides from aqueos solutions by coconut shell activated carbon

Ksenija Kumrić, Marija Egerić, Radojka Vujasin, Đorđe Petrović, Aleksandar Devečerski, Ljiljana Matović
Vinča Institute of Nuclear Sciences, University of Belgrade,
P. O. Box 522, 1001 Belgrade, Serbia

Introduction

Pesticides are a diverse group of chemical compounds that are widely used in agricultures worldwide for the control of various types of pests, such as insects, fungi, bacteria, weeds, rodents and others. Although their use has offered significant economic benefits and provided a valuable aid to agricultural production, the extensive or inappropriate use of these chemicals has resulted in extensive contamination of the environment.[1] Pesticides released from agricultural practices are an important class of pollutants due to their toxicity, persistance, polar nature and water solubility. Therefore, pesticide contamination of water resources through agricultural activities is considered as a serious environmental problem which posed a direct threat to human health. The removal of these pollutants from the contaminted water has presently become the focus of many investigations.

Several methods, like photocatalytic degradation,[2] oxidation processes,[3] aerobic degradation,[4] nanofiltration membranes,[5] ozonozation,[6] coagulation[7] and adsorption,[8] have been applied to remediate pesticides from the aqueous environment. Adsorption is a well-known and efficient separation process for water decontamination. The process is superior to other pesticide removal methods in terms of costs, simplicity of design, flexibility, ease of operation and insensitivity to toxic pollutants.[9]

Adsorption process depends on the number of sites available, porosity and specific surface area of adsorbent, as well as various types of interactions. Adsorption of contaminants by activated carbons has been identified as one of the most effective and feasible technologies owing to activated carbons' microporous nature, favorable pore size distribution, high surface reactivity, large adsorption capacity, versatility and easy availability. Activated carbon may be prepared using a variety of raw materials. However, there has been an increasing interest in using lignocellulosic by-products including agricultural residues and coconut shells as raw materials.[10-12]

The aim of this study was to investigate the removal of the selected pesticides from aqueous solutions using coconut shell-derived activated carbon as adsorbent. Water was contaminated inside the lab with a pesticide mixture containing five pesticides of different polarities and different chemical structures (imidaclorid (Imi), acetamiprid (Ace), carbendazim (Car), simazine (Sim), linuron (Lin)) in order to simulate water contaminated by different agricultural pesticides. The effects of various experimental parameters, such as contact time, solution pH and initial pesticide concentration, were studied with respect to the removal efficiency of each pesticide. Moreover, experimental data were analyzed by Langmuir and Freundlich isotherms.

Experimental

Coconut shell activated carbon was obtained from Trayal corporation (Kruševac, Serbia), while pesticides Imi, Ace, Car, Sim and Lin were obtained from Fitofarmacija (Zemun,

Serbia). Stock solutions of the pesticides (100 mg/L) were prepared in methanol and stored in the dark at -18°C. Working solutions were prepared before each experiment by appropriate dilution of the stock solutions with deionized water.

Batch experiments were carried out at room temperature by mixing of 5 mg coconut shell activated carbon adsorbent and 50 mL of working multi-pesticide solution in closed polyethylene bottles. The total Imi, Ace, Car, Sim and Lin concentration in the working solution was 12.5 mg/L (2.5 mg/L each of the investigated pesticides) at pH 5.8. The samples were shaken on a laboratory shaker for 180 min at a stirring speed of 150 rpm. After that, the liquid phases were separated from the solid phases by filtration through a 0.45 µm microporous membrane filter. The initial and residual concentrations of pesticides in each aliqout were determined with an Agilent 1100 liquid chromatograph (Agilent Technologies, USA) with Zorbax XDB-C18 column (4.6 x 250 mm, 3.5 µm particle size) and DAD detector at 220 nm for Sim, 254 nm for Lin and 270 nm for Imi, Ace and Car. The mobile phase consisted of methanol (A) and deionized water (B), applying the following gradient profile: 0.0 min 43 % A and 57% B, 7 min 60% A and 40% B, 10 min 70 % A and 30 % B, 14 min 72 % A and 28 % B, and 20 min returned to the initial composition. The flow rate and sample volume were 0.7 mL/min and 20 µL.

The effects of different experimental parameters, such as contact time (0 – 24 h), solution pH (2 – 8) and initial total pesticide concentration (2.5 – 50 mg/L), were investigated with respect to the removal efficiency of pesticides. The concentrations of Imi, Ace, Car, Sim and Lin in multi-pesticide solution were set to be equal. All experiments were carried out in duplicate and the data obtained were used for analysis.

The equilibrium amount of pesticide adsorbed per unit mass of coconut shell activated carbon, q_e (mg/g) and the removal efficiency of particular pesticide, E / %, were evaluated using the equations:

$$q_e = \left(\frac{C_i - C_e}{W} \right) V \quad (1)$$

$$E = 100 \left(\frac{C_i - C_t}{C_i} \right) \quad (2)$$

where C_i is the initial pesticide concentration (mg/L), C_t is the pesticide concentration at time t (mg/L), C_e is the equilibrium concentration of pesticide (mg/L), V is the volume of the solution (L), and W is the mass of adsorbent (g).

Results and discussion

Five pesticides (Imi, Ace, Car, Sim, Lin) of different activity and polarity[13] were selected for study of their binding for coconut shell activated carbon. The effect of contact time on the adsorption of selected pesticides onto the coconut shell activated carbon was investigated at different contact times ranging from 1 min to 24 h. As can be seen in Fig. 1, adsorption occurred much faster at the beginning and slowed down gradually over time until reaching equilibrium due to the effects of the availability of the activated sites and the strength of the driving force. The equilibrium adsorption was established after 180 min of contact for all pesticides, except Lin for which equilibrium is attained much faster, after only 30 min. After equilibrium was reached, the contact time no longer had an influence on the pesticide

adsorption and the removal efficiences remained constant over the time period observed. Maximum removal, 95%, was obtained for Lin, while for the other four pesticides the removal efficiencies were in the range 80 – 89%. The adsorption time of 180 min was used for the rest of the study.

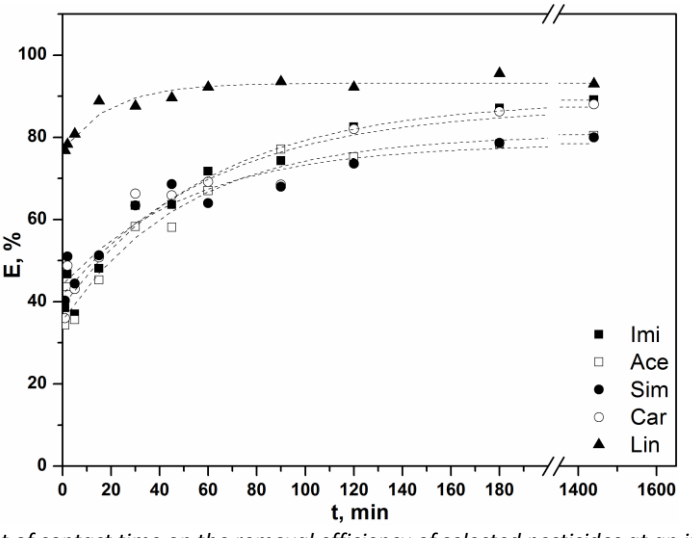

Fig. 1. *Effect of contact time on the removal efficiency of selected pesticides at an initial total pesticide concentration of 12.5 mg/L. Conditions: pH, 5.8; stirring speed, 150 rpm; concentration of adsorbent 0.1 g/L*

The removal of selected pesticides using the coconut shell activated carbon was studied over the pH range from 2 to 8 and the obtained results are shown in Fig. 2. According to the results of experiments, it was indicated that the maximum removal efficiencies of all pesticides were achieved at the initial solution pH values ranging from 3.5 to 6. The adsorption of pesticides at the pH < 3.5 or pH > 6 was lower than that at the pH range from 3.5 to 6, probably due to hydrolysis of these compounds.[14] Therefore, the pH of sample solutions was adjusted to 5 – 6 as the optimal for the removal of selected pesticides from aqueous solutions.

The effect of the initial pesticide concentration on the coconut shell activated carbon adsorption of Imi, Ace, Car, Sim and Lin was studied by varying the total pesticide concentration from 2.5 to 50 mg/L, that is, by varying the respective pesticide concentration from 0.5 to 10 mg/L in the multi-pesticide solution at pH 5.8, while keeping all other parameters constant. The removal efficiencies of the selected pesticides decreased with increasing initial pesticide concentration in the aqueous solution, because of the saturation of the available adsorption sites on the adsorbent. However, the equilibrium amount of pesticide adsorbed per unit mass of adsorbent, q_e, increased with increasing initial pesticide concentration (Fig. 3), because of the increase in the driving force of the pesticides toward the active sites on the adsorbent.

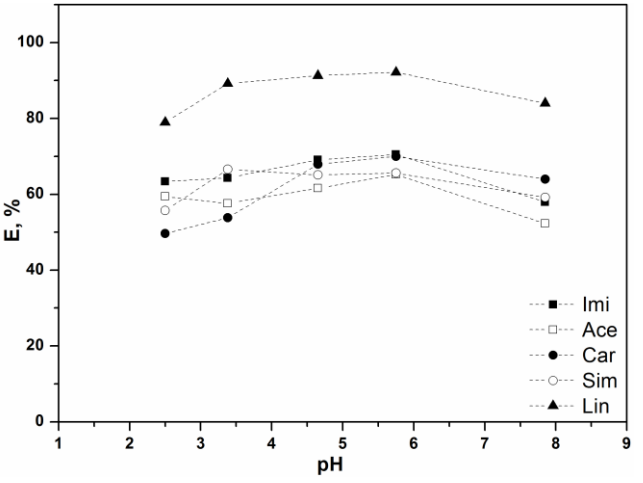

Fig. 2. *Effect of pH on the removal efficiency of selected pesticides at an initial total pesticide concentration of 12.5 mg/L. Conditions: contact time, 180 min; stirring speed, 150 rpm; concentration of adsorbent 0.1 g/L*

To determine the surface properties and the affinity of the adsorbent, the experimental data were analyzed using the Langmuir and Freundlich isotherm models. The corresponding Langmuir and Freundlich parameters and correlation coefficients for all the pesticides are reported in Table 1. It can be seen that the Langmuir plots have higher correlation coefficients than the Freundlich plots, suggesting that the Langmuir isotherm is a good model for the simultaneous sorption of all investigated pesticides. The Langmuir monolayer adsorption capacities of Imi, Ace, Car, Sim and Lin on the coconut shell activated carbon were estimated to be 46.4, 47.1, 59.9, 46.8 and 65.5, respectively. The investigated adsorbent has maximum affinity for linuron as indicated by *b* values.

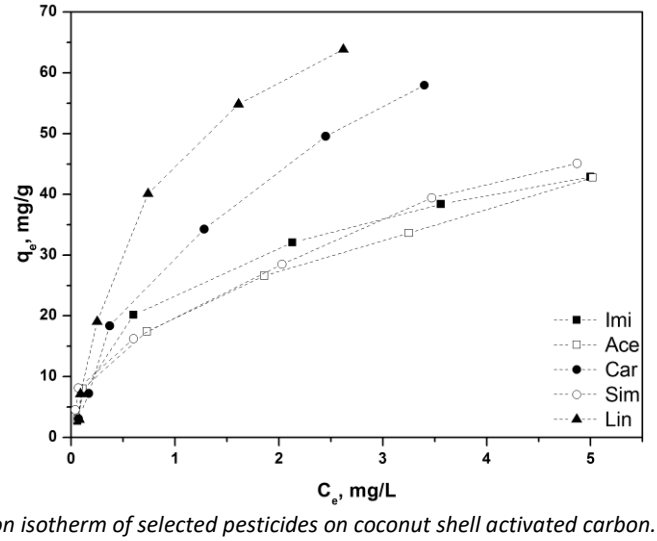

Fig. 3. *Adsorption isotherm of selected pesticides on coconut shell activated carbon. Conditions: pH, 5.8; contact time, 180 min;stirring speed, 150 rpm;concentration of adsorbent 0.1 g/L*

Table 1. *Langmuir and Freundlich parameters for the adsorption of Imi, Ace, Car, Sim and Lin onto coconut shell activated carbon.*

Pesticide	Langmuir fitting			Freundlich fitting		
	q_m / mg g^{-1}	K_L / L mg^{-1}	R^2	K_F	n	R^2
Imi	46.4	1.24	0.99	54.2	1.85	0.95
Ace	47.1	1.10	0.98	52.9	2.58	0.94
Car	59.9	1.39	0.988	39.5	1.42	0.97
Sim	46.8	1.21	0.98	41.8	3.17	0.95
Lin	65.5	1.70	0.99	52.3	3.29	0.95

Conclusion

Coconut shell activated carbon is an effective adsorbent for the simultaneous removal of selected pesticides from aqueous solutions. The maximum removal efficiencies and adsorption capacities of the selected pesticides were obtained at pH values between 3.5 and 6.0. The adsorption data for all pesticides on coconut shell activated carbon fit the Langmuir isotherm model. The study shows that the investigated adsorbent prepared from low-cost agricultural waste (coconut shell) has potential for application in the treatment of pesticide contaminated wastewaters.

Acknowledgement: *We acknowledge the support to this work provided by the Ministry of Education, Science and Technological Development of Serbia through the projects III 45006, III 45012 and III 43009.*

Istovremeno uklanjanje odabranih pesticida iz vode primenom ugljeničnog materijala dobijenog iz kokosove ljuske

U ovom radu ispitivana je mogućnost primene aktiviranog ugljeničnog materijala dobijenog iz kokosove ljuske kao adsorbensa za uklanjanje pesticida različite polarnosti (imidakloprid, acetamiprid, karbendazim, simazin, linuron) iz vode. Adsorpcija pesticida iz vodenog rastvora je rađena u šaržnom sistemu i ispitivan je uticaj različitih parametara na efikasnost uklanjanja pesticida u cilju optimizacije uslova za njihovo što efikasnije vezivanje za ispitivani adsorbens. Rezultati su pokazali da se ravnoteža uspostavlja nakon 180 min, a da je efikasnost uklanjanja najveća u intervalu pH-vrednosti od 3,5 do 6. Dobijeni podaci su fitovani pomoću dva ravnotežna adsorpciona modela - Lengmirovom i Frojndlihovom izotermom. Bolje slaganje je postignuto primenom Lengmirove izoterme, te su primenom ovog ravnotežnog modela određeni adsorpcioni kapaciteti za svaki pesticid posebno.Na osnovu dobijenih rezultata može se zaključiti da ugljenični materijal sintetisan iz kokosove ljuske ima dobar potencijal za primenu u prečišćavanju otpadnih voda zagađenih pesticidima.

References:

1. M. A. Kamboh, W. A. W. Ibrahim, H. R. Nodeh, M. M. Sanagi, S. T. H. Sherazi, *New J. Chem.*, **40** (2016) 3130.
2. L. Li, Q. Wu, Y. Guo, C. Hu, *Microporous Mesoporous Mater.*, **87** (2005) 1.
3. M. I. Badawi, M. Y. Ghali, T. A. Gad-Allah, *Desalination*, **194** (2006) 166.
4. M. Cycoń, M. Wójcik, Z. Piotrowska-Seget, *Chemosphere*, **76** (2009) 494.
5. A. L. Ahmad, L. S. Tan, S. R. A. Shukor, *J. Hazard. Mater.*, **151** (2008) 71.

6. J. Wu, C. Lan, G. Y. S. Chan, *Chemosphere*, **76** (2009) 1308.
7. Z. Jia, Y. Li, S. Lu, H. Peng, J. Ge, S. Chen, *J. Hazard. Mater.*, **129** (2006) 234.
8. M. Naushad, Z. A. Alothman, M. R. Khan, N. J. AL Qahtani, I. H. Alsohaimi, *J. Ind. Eng. Chem.*, **20** (2014) 4393.
9. T. Ahmad, M. Rafatullah, A. Ghazali, O. Sulaiman, R. Hashim, A. Ahmad, *J. Environ. Sci. Health*, **28** (2010) 231.
10. M. Kilic, E. Apaydin-Varol, A. E. Pütün, *J. Hazard. Mater.*, **189** (2011) 397.
11. Y. Zhu, P. Kolar, *J. Environ. Chem. Eng.*, **2** (2014) 2050.
12. A. Mohd Din, B. Hameed, A. Ahmad, *J. Hazard. Mater.*, **161** (2009) 1522.
13. T. Trtić-Petrović, J. Đorđević, N. Dujaković, K. Kumrić, T. Vasiljević, M. Laušević, *Anal. Bioanal. Chem.*, **397** (2010) 2233.
14. W. Zheng, W. Liu, *Pestic. Sci.*, **55** (1999) 482.

Biohemija

Biochemistry

Metaboličke promene tokom životnog ciklusa kukuruznog plamenca *Ostrinia nubilalis* (Hübner, 1796) – aktivnost citrat sintaze i laktat dehidrogenaze

Iva Uzelac, Miloš Avramov, Nikola Krivokuća, Snežana Gošić-Dondo*, Filip Franeta**, Elvira Vukašinović, Jelena Purać, Danijela Kojić, Željko D. Popović
Univerzitet u Novom Sadu, Prirodno-matematički fakultet, Departman za biologiju i ekologiju, Trg Dositeja Obradovića 2, 21000 Novi Sad, Srbija
**Institut za kukuruz „Zemun Polje“, Slobodana Bajića 1, 11185 Beograd, Srbija*
***Institut za ratarstvo i povrtarstvo „NS seme“, Maksima Gorkog 30, 21000 Novi Sad, Srbija*

Uvod

Tokom evolucije insekti su stekli brojne adaptacije na nepovoljne uslove staništa, kao što su niske i visoke temperature, ograničeni izvori hrane, visoke koncentracije soli, visok pritisak, nedostupna ili slabo dostupna voda i drugi. Jedna od takvih adaptacija je i dijapauza, kao period privremeno zaustavljenog razvoja u životnom ciklusu insekata, koji im omogućava da sinhronizuju svoju aktivnost sa sezonskom dostupnošću resursa, i tako kolonizuju umerene, tropske i polarne predele[1]. Dijapauza kod insekata može nastupiti na različitim razvojnim stadijumima – stadijumu embriona, larve, lutke ili odrasle jedinke, ali uvek tokom istog stadijuma karakterističnog za vrstu. Ulazak u dijapauzu može biti uslovljen i nestresnim faktorima poput fotoperioda ili je genetski kontrolisan i obavezan deo razvojnog ciklusa, pa tako organizam može mirovati i u najpovoljnijim uslovima za život[2-3]. Iako se dijapauza definiše kao faza mirovanja, ona nipošto nije pasivno stanje, već period tokom kojeg organizam prolazi kroz brojne promene, kako na morfoanatomskom i fiziološkom nivou, tako i na biohemijskom i molekulskom nivou. Pre svega, dolazi do snižavanja opšte stope metabolizma[4], smanjenja aktivnosti ili zaustavljanja metaboličkih puteva nižeg prioriteta i istovremenog preusmeravanja metabolizma ka sintezi specifičnih krioprotektivnih molekula[5-7], zatim do promena u masnokiselinskom sastavu membranskih i rezervnih lipida[8-10], kao i promena u ekspresiji karakterističnih grupa gena koji učestvuju u zaštiti od stresa, regulaciji ćelijskog ciklusa i ćelijske smrti[11-13].

Dijapauza kukuruznog plamenca *Ostrinia nubilalis* je adaptivna strategija koju je ova vrsta stekla tokom evolutivnog razvoja kao način preživljavanja nepovoljnih uslova tokom zime. Dijapauza kod ove vrste nastupa na stadijumu larve (gusenice) i neraskidivo je povezana sa sticanjem otpornosti na niske temperature, ali i otpornosti na dehidrataciju koja se postiže kontrolisanim mržnjenjem telesnih tečnosti. Biohemijski i molekulski mehanizmi koji to omogućavaju uključuju sintezu krioprotektora kao što su polihidroksilni alkoholi (glicerol, sorbitol i dr.) i ugljeni hidrati (trehaloza, glukoza i dr.), koji koligativno snižavaju tačku superhlađenja hemolimfe, dok nekoligativno stabilizuju proteine i ćelijske membrane[12,14]. U skladu sa tim, u prethodnim metabolomskim istraživanjima kod ove vrste, pomoću nuklearne magnetne rezonance (^{1}H-NMR), utvrđeno je da hemolimfa gusenica koje se aktivno razvijaju i hrane ima potpuno drugačiji „metabolomički otisak“ u odnosu na hemolimfu neaktivnih, dijapauzirajućih gusenica[15]. Naime, metabolički profil hemolimfe nedijapauzirajućih gusenica karakteriše se povećanim sadržajem laktata, acetata i sukcinata, što ukazuje na intenzivan katabolizam rezervnih lipida i ugljenih hidrata, u cilju

zadovoljenja visokih energetskih potreba. Sa druge strane, u hemolimfi dijapauzirajućih gusenica, inicijalno gajenih na 5°C, a potom postepeno hlađenih i u periodu od 10 dana izlaganih temperaturama od -3°C i -16°C, dominantni metaboliti su glicerol, prolin i alanin, koji imaju ulogu prirodnih krioprotektanata.

U cilju ispitivanja metaboličkih promena tokom dijapauze, tačnije pretpostavljenog prelaska sa aerobnog na anaerobni metabolizam, u ovom radu merene su aktivnosti dva metabolička enzima, citrat sintaze (CS) i laktat dehidrogenaze (LDH), u homogenatima celih lutki, nedijapauzirajućih gusenica i gusenica u sredini dijapauze koje su bile izlagane niskim temperaturama (od 5°C, -3°C i -16°C). Citrat sintaza (E.C. 2.3.3.1) katalizuje reakciju kondenzacije dvougljeničnog acetatnog ostatka acetil koenzima A i četvorougljeničnog molekula oksalacetata, pri čemu nastaje šestougljenični citrat (limunska kiselina). Citrat sintaza se nalazi u gotovo svim poznatim živim ćelijama i ima esencijalnu funkciju u centralnom metaboličkom putu aerobnih organizama, Krebsovom ciklusu. Često se koristi u istraživanjima specifičnih ćelijskih adaptacija onih organizama koji opstaju u staništima sa niskim temperaturama[16]. Laktat dehidrogenaza (EC 1.1.1.27) katalizuje reakciju oksidacije laktata u piruvat i obrnuto, reakciju redukcije piruvata u laktat, uz istovremenu oksidoredukciju koenzima NAD^+. Laktat dehidrogenaza je poslednji enzim anaerobne glikolize, koji produkcijom laktata i regeneracijom oksidovane forme koenzima NAD^+ omogućava kontinuiranu produkciju adenozin trifosfata (ATP) putem glikolize[17]. Visok nivo LDH se dovodi u vezu sa efikasnim anaerobnim sistemom, tako da kod insekata tkiva sa pretežno anaerobnim metabolizmom obiluju ovim enzimom, posebno mišići za koje je karakteristična brza i grčevita aktivnost[18].

Eksperimentalni deo

Dijapauzirajuće i nedijapauzirajuće gusenice kao i lutke sakupljene su na oglednim poljima Instituta za kukuruz „Zemun Polje“ i Instituta za ratarstvo i povrtarstvo „NS seme“ u Novom Sadu. Ukupno je formirano pet eksperimentalnih grupa: ND – kontrola – nedijapauzirajuće gusenice petog instara, uzorkovane u julu 2015. godine, D1 – gusenice u sredini dijapauze (januar 2015.) držane 10 dana na temperaturi od 5°C, D2 – gusenice u sredini dijapauze (januar – početak februara 2015.) držane 10 dana na temperaturi od -3°C, D3 – gusenice u sredini dijapauze (februar 2015.) držane 10 dana na temperaturi od -16°C i L – lutke, uzorkovane u avgustu 2015. godine. Svaku eksperimentalnu grupu činilo je pet bioloških ponavljanja (pulova), a svaki pul činilo je 10 gusenica ili 5 lutaka. Gusenice i lutke su homogenizovane u ledeno hladnom 50 mM fosfatnom puferu, pH 7, do formiranja 20 % w/v homogenata. Za određivanje koncentracije ukupnih proteina korišćen je komercijalni komplet Bradfordovog reagensa (Quick Start™ Bradford Protein Assay, Bio-Rad, cat no. 5000203), a prema uputstvu proizvođača za mikrotitar ploču od 250 µl.

Aktivnost CS je određena spektroskopski kontinualnom metodom[19]. Enzimski esej merenja aktivnosti citrat sintaze izveden je kuplovanjem osnovne enzimske reakcije sa drugim sistemom enzim-supstrat u kome se ditionitrobenzoeva kiselina (DTNB) konvertuje u 2-nitro-5-tiobenzoat (TNB), koji ima maksimum apsorpcije u ljubičastom delu spektra, na 412 nm talasne dužine. Stoga je u ovom sistemu porast apsorbance na 412 nm u pravilnim vremenskim intervalima proporcionalan aktivnosti citrat sintaze.

Aktivnost LDH je detektovana izmenjenom kontinualnom metodom[20], spektorskopskim očitavanjem apsorbance u realnom vremenu. Enzimski esej praćenja aktivnosti laktat

dehidrogenaze zasniva se na činjenici da apsorpcioni spektar redukovanog koenzima NADH poseduje maksimum apsorpcije na talasnoj dužini od 340 nm, što nije karakteristika oksidovane forme ovog koenzima (NAD^+). Stoga je, pri izvođenju eseja sa piruvatom kao supstratom i NADH kao koenzimom, pad apsorbance na talasnoj dužini od 340 nm u određenom vremenskom intervalu proporcionalan aktivnosti laktat dehidrogenaze koja prevodi piruvat u laktat, uz oksidaciju koenzima NADH.

Izmerene aktivnosti CS i LDH izražene su kao specifična aktivnost u internacionalnim milijedinicama aktivnosti enzima po miligramu proteina. Rezultati su statistički analizirani u programu Statistica 13.3 (StatSoft, Europe GmbH, Hamburg) i prikazani pomoću grafikona. Razlika između dobijenih vrednosti ispitivanih parametara kod različitih eksperimentalnih grupa testirana je jednofaktorskom analizom varijanse (ANOVA) i *post hoc* Fisherovim testom za nivo značajnosti od $p<0,05$.

Rezultati i diskusija

Najviša specifična aktivnost citrat sintaze izmerena je kod nedijapauzirajućih larvi (ND) i dostiže vrednosti oko 47 mIU/mg proteina, dok je kod dijapauzirajućih larvi izmerena statistički značajno niža specifična aktivnost (20–25 mIU/mg proteina), i pokazano je da se ta aktivnost razlikuje u zavisnosti od temperature na kojoj su larve aklimatizovane (Slika 1).

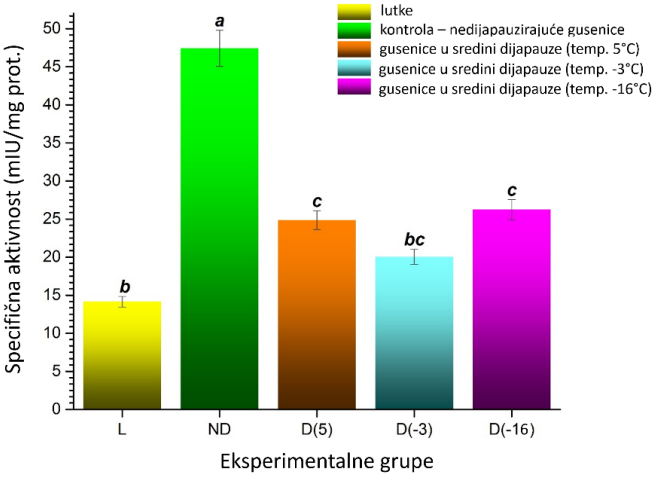

Slika 1. *Specifična aktivnost citrat sintaze izmerena u homogenatu celih gusenica i lutaka O. nubilalis. Rezultati su izraženi u broju nanomolova supstrata koji se transormiše u jednom minutu po miligramu proteina enzimskog preparata (mIU/mg prot.) ± standardna greška, dobijeni od 10 gusenica, odnosno 5 lutaka.*

Među dijapauzirajućim gusenicama, najniža vrednost specifične aktivnosti CS izmerena je kod eksperimentalne grupe aklimatizovane na temperaturi od -3°C (D-3), u odnosu na koju je specifična aktivnost citrat sintaze blago povišena kod preostale dve eksperimentalne grupe aklimatizovane na temperaturama od 5°C (D5) i -16°C (D-16) (Slika 1), ali ta razlika nije statistički značajna. Sa vrednošću od oko 14 mIU/mg proteina, najniža specifična aktivnost CS je izmerena kod lutaka (L) i ona je statistički značajno niža u odnosu na sve ostale grupe, izuzev dijapauzirajućih gusenica aklimatizovanih na -3°C (Slika 1).

Ovakvi rezultati mogu se objasniti u svetlu činjenice da je jedna od zajedničkih karakteristika organizama u hipometaboličkom stanju preusmeravanje metabolizma od aerobnog ka anaerobnom[21-22]. S obzirom na to da je Krebsov ciklus ključni metabolički put za oksidaciju ugljenih hidrata, lipida i aminokiselina kod aerobnih organizama, njegov intenzitet je najčešće smanjen tokom dijapauze, kao posledica opšte supresije inteziteta aerobnog metabolizma. Kako citrat sintaza katalizuje prvi korak Krebsovog ciklusa – reakciju kondezacije acetil-CoA i oksalacetata u citrat, ovaj enzim je jedan od ključnih elemenata koji kontrolišu stopu inteziteta ciklusa trikarboksilnih kiselina. U skladu sa tim, u ovom radu najviša aktivnost CS izmerena je kod grupe nedijapauzirajućih gusenica, koje imaju intezivan aerobni metabolizam, dok je kod lutki i dijapauzirajućih gusenica izlaganih niskim temperaturama aktivnost CS bila statistički značajno niža.

Dobijeni rezultati su u skladu sa prethodnim studijama na *O. nubilalis*, u kojima je potvrđena niža stopa oksidativnog metabolizma u dijapauzi, kao i zabeležena veća koncentracija laktata, acetata i sukcinata kod nedijapauzirajućih u odnosu na dijapauzirajuće gusenice[13,15,23]. Povećana količina navedenih metabolita ukazuje na intezivan oksidativni metabolizam lipida i ugljenih hidrata, koji je karakterističan za aktivni razvoj nedijapauzirajućih gusenica. Takođe, kod dijapauzirajućih larvi vrste muve *Eurosta solidaginis* i moljca *Epiblema scudderiana* aktivnost CS je snižena tokom sredine zime u poređenju sa vrednostima izmerenim tokom jeseni[24]. Kod *E. solidaginis* aktivnost CS se vraća na početne vrednosti do sredine aprila, a zatim se opet snižava krajem aprila, kada se larve ulutkavaju[24]. Slično, snižena aktivnost CS uočena je i kod dijapauzirajućih lutki muve *Sarcophaga crassipalpis*[25]. Rezultati pomenutih studija su u skladu sa izmerenom aktivnošću CS tokom životnog ciklusa kukuruznog plamenca, za koju je u ovom radu pokazano da je najviša kod nedijapauzirajućih larvi, a najniža kod lutki, verovatno kao posledica histolize larvalnih i istovremene histogeneze adultnih tkiva.

Kada je u pitanju enzim laktat dehidrogenaza, u zavisnosti od temperature na kojoj su aklimatizovane dijapauzirajuće larve, najviša specifična aktivnost LDH izmerena je u eksperimentalnoj grupi aklimatizovanoj na temperaturi od -3°C (D-3) i dostiže vrednosti od oko 1100 mIU/mg proteina (Slika 2). Kod preostale dve grupe dijapauzirajućih larvi aklimatizovanih na temperaturama od 5°C (D5) i -16°C (D-16), kao i kod nedijapauzirajućih larvi (ND), izmerena je statistički značajno niža aktivnost u odnosu na D(-3) (Slika 2). Međutim, sa izmerenim vrednostima u opsegu između 300 i 450 mIU/mg proteina, međusobna razlika u aktivnosti LDH između eksperimentalnih grupa ND, (D5) i (D-16) nije statistički značajna. Najniža specifična aktivnost LDH izmerena je, kao i kod CS, u eksperimentalnoj grupi lutaka i dostiže vrednosti od oko 100 mIU/mg proteina, što je statistički značajno niže u odnosu na sve ostale eksperimentalne grupe (Slika 2).

Kako citrat sintaza, sa jedne strane, može biti dobar pokazatelj aerobnog potencijala, tako LDH, sa druge strane, može biti dobar pokazatelj anaerobnog potencijala organizma, budući da ovaj enzim katališe poslednju u nizu reakcija procesa glikolize – interkonverziju piruvata i laktata. U slučaju nedostatka kiseonika, LDH pretvara piruvat u laktat kako bi se nesmetano nastavila glikoliza i sinteza ATP-a. U ovom radu izmeren je relativno nizak nivo aktivnosti LDH kod nedijapauzirajućih gusenica *O. nubilalis*, što na prvi pogled nije u skladu sa povećanom količinom laktata u hemolimfi ovih gusenica izmerenom u prethodno opisanoj metabolomičkoj studiji[15].

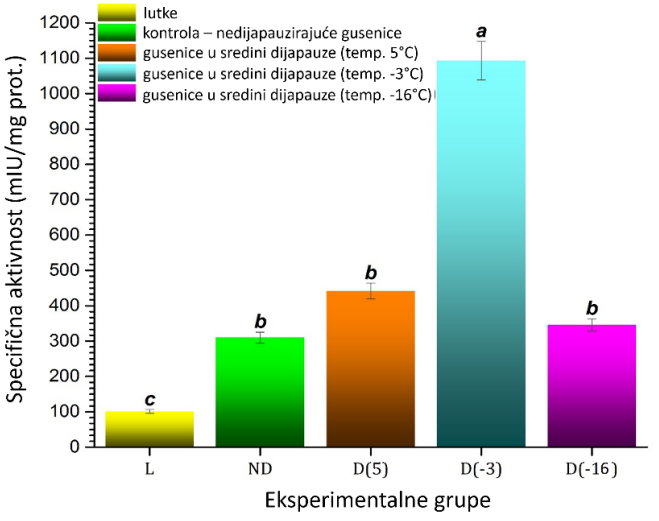

Slika 2. *Specifična aktivnost laktat dehidrogenaze (u smeru transformacije piruvata u laktat) izmerena u homogenatu celih gusenica i lutaka O. nubilalis. Rezultati su izraženi u broju nanomolova supstrata koji se transormiše u jednom minutu po miligramu proteina enzimskog preparata (mIU/mg prot.) ± standardna greška, dobijeni od 10 gusenica, odnosno 5 lutaka.*

Međutim, ovakav nalaz bi zapravo mogao da potvrdi aktivan katabolizam ugljenih hidrata i intenzivnu sintezu piruvata koji se nagomilava u ćeliji, te se njegov višak kratkoročno prevodi u laktat pre metamorfoze gusenica u lutke. Ovako nastali laktat bi se potom mogao oksidovati nazad do piruvata i trošiti tokom metamorfoze za podmirivanje visokih energetskih zahteva u procesu intenzivne histogeneze. Takođe, tom prilikom bi se regenerisala redukovana forma koenzima NADH, koji bi potom mogla služiti kao izvor redukcionih ekvivalenata u procesima antioksidativne zaštite, koja je dobro proučena kod ove vrste[6,7,13].

Sa druge strane, kod dijapauzirajućih gusenica izloženih temperaturi od 5˚C, aktivnost LDH je blago povišena, ali i dalje približnih vrednosti u odnosu na nedijapauzirajuće gusenice. Mada se radi o gusenicama u sredini dijapauze, na osnovu povećanja količine glicerola i smanjenja količine laktata pri izlaganju larvi temperaturi od 5˚C[15], može se pretpostaviti da se, sa postepenim snižavanjem temperature, pokreće adaptivni odgovor sticanja otpornosti na niske temperature. Najzad, izlaganjem dijapauzirajućih gusenica temperaturi od -3˚C, aktivnost LDH dostiže maksimalne vrednosti i raste za preko 70% u odnosu na nedijapauzirajuće gusenice. Istovremeno, nivo glicerola u hemolimfi gusenica u sredini dijapauze statistički značajno raste sa hlađenjem na -3˚C, kao i nivo alanina, dok nivo laktata opada[15]. Uočena negativna korelacija između aktivnosti LDH izmerene u ovom radu i količine laktata u prethodnim metabolomičkim studijama može ukazivati na to da organizam pri izlaganju temperaturi od -3˚C pojačano oksiduje laktat, prethodno nagomilan visokom aktivnošću LDH, do piruvata. Međutim, piruvat je kao metabolit veoma reaktivan i stoga nije pogodan za čuvanje, te se reakcijom transaminacije najverovatnije prevodi u L-alanin, koji je povoljniji metabolit za čuvanje i može da deluje krioprotektivno[26].

Niža aktivnost LDH kod dijapauzirajućih larvi *O. nubilalis* izlaganih temperaturi od -16˚C, u odnosu na aktivnost kod onih izlaganih temperaturi od -3˚C, izmerena u ovoj studiji, naizgled je u skladu sa sniženom aktivnošću LDH kod dijapauzirajućih larvi muve *Eurosta solidaginis* izlaganih temperaturi od -10˚C u odnosu na aktivnost kod onih izlaganih temperaturi od 0˚C[27]. Međutim, snižena aktivnost glikolitičkih enzima, uključujući i LDH, kod muve *E. solidaginis* rezultat je inhibicije fosfofruktokinaze na temperaturama izrazito ispod nule, kada dolazi do prekidanja procesa glikolize i usmeravanja metabolita ka sintezi sorbitola[27]. Budući da je nivo sorbitola kod dijapauzirajućih i nedijapauzirajućih larvi *O. nubilalis* sličan, a da njegova koncentracija čak i opada pri izlaganju dijapauzirajućih larvi u sredini dijapauze niskim temperaturama[28], najverovatnije je da kod kukuruznog plamenca pri temperaturama izrazito ispod nule dolazi do sveopšte supresije metaboličkih procesa. Naposletku, najniži nivo aktivnosti LDH u ovom radu izmeren je kod lutki *O. nubilalis,* što može biti u skladu sa dubokom supresijom metabolizma, kao karakteristikom primećenom kod mnogih vrsta na stadijumu lutke, kada su veoma intenzivne histoliza larvalnih i histogeneza adultnih tkiva[29]. Vrednosti dobijene merenjem aktivnosti oba enzima podvrgnute su analizi glavnih komponenti (PCA, *engl*. Principal Component Analysis) sa ciljem rasvetljavanja opšteg obrasca aktivnosti enzima u odgovoru na razvojni stadijum i temperaturu na kojoj su aklimatizovane dijapauzirajuće larve. Prve dve komponente izvedene pomoću PCA obuhvataju 98,26 % varijanse podataka (Slika 3). Prva komponenta (K1) čini 65,65 % ukupne varijanse i budući da se njome jasno razdvajaju dijapauzirajuće larve aklimatizovane na temperaturama od 5°C i -16°C (negativne vrednosti) od onih aklimatizovanih na temperaturi od -3°C (pozitivne vrednosti), ova dimenzija najverovatnije razdvaja eksperimentalne grupe prema temperaturi aklimatizacije (Slika 3A). Aktivnost laktat dehidrogenaze je u pozitivnoj korelaciji sa K1, dok je aktivnost citrat sintaze u gotovo zanemarljivoj negativnoj korelaciji sa K1 (Slika 3B).

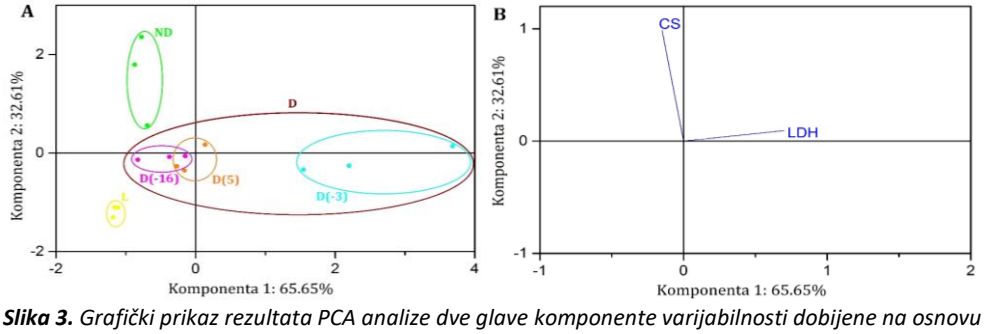

Slika 3. *Grafički prikaz rezultata PCA analize dve glave komponente varijabilnosti dobijene na osnovu merenja specifične aktivnosti citrat sintaze i laktat dehidrogenaze.*

Druga komponenta (K2), iako manje značajna, čini 32,61% ukupne varijanse, i jasno razdvaja eksperimentalne grupe prema razvojnom stadijumu na kom se nalaze jedinke (Slika 3A). Može se uočiti da vrednosti K2 postepeno prelaze iz pozitivnih, kod nedijapauzirajućih larvi, preko vrednosti oko nule kod dijapauzirajućih larvi, do negativnih vrednosti kod lutaka. Prema tome, druga komponenta mogla bi da oslikava aktivnost CS i LDH u zavisnosti od razvojnog stadijuma na kome se jedinka *O. nubilalis* nalazi. Pritom je aktivnost oba enzima u pozitivnoj korelaciji sa K2, s tim da je ta korelacija veoma izražena kod citrat sintaze, dok je kod laktat dehidrogenaze gotovo zanemarljivo mala (Slika 3B). Kada se uzmu u obzir obe

komponente, može se zaključiti da je aktivnost citrat sintaze više pod uticajem razvojnog stadijuma u kome se jedinka nalazi, dok na aktivnost laktat dehidrogenaze u većoj meri utiče temperatura.

Zaključak

Rezultati izneti u ovom radu ukazuju da je dijapauza period dinamičnih metaboličkih, ali postepenih promena, koje su u tesnoj vezi sa izlaganjem gusenica niskim temperaturama. Utvrđeno je da aktivnost citrat sintaze značajno opada tokom dijapauze, što je u skladu sa tim da je dijapauza hipometabolička faza mirovanja. Sa druge strane, aktivnost laktat dehidrogenaze je značajno povećana tokom dijapauze, što ukazuje na preusmeravanje metabolita ka anaerobnom metabolizmu i intezivnoj sintezi krioprotektivnih jedinjenja. Međutim, iako se aktivnosti oba analizirana enzima – CS i LDH, razlikuju u različitim razvojnim stadijumima i nakon izlaganja niskim temperaturama, one nisu uvek bile u suprotnosti jedna sa drugom, kao „lik i predmet u ogledalu“, kako je to bilo očekivano na osnovu funkcije koju ovi enzimi imaju u aerobnom i anaerobnom metabolizmu. To ukazuje na činjenicu da se tokom dijapauze aktivnost metaboličkih enzima neprestano održava u stanju dinamičke ravnoteže, pri čemu često koncentracija odgovarajućih metabolita, koji su supstrati ili proizvodi za date enzime, određuje smer i intenzitet energetskog metabolizma. Stoga bi u budućim istraživanjima trebalo ispitati aktivnost laktat dehidrogenaze u smeru oksidacije laktata u piruvat, a takođe i povratnu aktivnost drugih metaboličkih enzima čiji se produkti mogu dovesti u vezu sa citrat sintazom i laktat dehidrogenazom, pre svega, alanin-aminostransferaze i aspartat-aminotransferaze, kako bi se dobila kompletna slika energetskog metabolizma *O. nubilalis*, u uslovima dijapauze i izloženosti niskim temperaturama.

Zahvalnica: *Ovaj rad je finansiran od strane Ministarstva prosvete, nauke i tehnološkog razvoja, kroz projekat osnovnih istraživanja “Molekularni mehanizmi redoks signalinga u homeostazi, adaptaciji i patologiji”, br. 173014.*

Metabolic changes during the life cycle of the European corn borer *Ostrinia nubilalis* (Hübner, 1796) – the activity of citrate synthase and lactate dehydrogenase

Diapause is a complex resting phase which enables organisms to cope with harsh environmental conditions. Winter diapause of the European corn borer Ostrinia nubilalis is tightly connected with the development of the cold hardiness during which diapausing caterpillars undergo numerous metabolic changes. In order to further explore metabolism during diapause, we measured activities of two essential enzymes – citrate synthase (CS), as a reliable marker of aerobic metabolism, and lactate dehydrogenase (LDH), as a good indicator of anaerobic metabolism. Spectrophotometrical measurements were performed in the whole body homogenates of pupae (P), non-diapausing (ND), and diapausing larvae (D). Furthermore, diapausing larvae were also exposed to low temperatures (5°C, -3°C, -16°C). The highest activity of CS was measured in the group of non-diapausing caterpillars, while the activity of LDH was low in this group. This is in agreement with the initial assumption that the intensity of Krebs cycle, a key metabolic pathway for oxidation carbon hydrates, lipids and amino acids in aerobic organisms, is especially elevated in non-diapausing caterpillars due to their high energy demands caused by an active life and metabolic

preparations ahead of the metamorphosis. Measured CS activity was significantly lower in diapausing caterpillars exposed to low temperatures, while LDH activity was increased, especially after the exposure to temperatures slightly below zero (-3°C). This is in accordance with the less intensive catabolism of carbohydrates and synthesis of pyruvate in more anaerobic, hypometabolic conditions of diapause. Both enzymes, CS and LDH had the lowest activities in homogenates of pupae, most likely as a consequence of simultaneous processes of histolysis of larval and histogenesis of adult tissues.

Literatura

1. V. Koštál, *J Insect Physiol*. **52** (2006) 113–127.
2. J. L. Nation, Insect physiology and biochemistry, RC Press, Taylor & Francis Group, New York (2008).
3. M. Watanabe, *App Entomol Zool*. **41** (2006) 15–31.
4. D. A. Hahn, D. L. Denlinger, *Annu Rev Entomol*. **56** (2011) 103–121.
5. G. Grubor-Lajšić, W. Block, V. Palanački, S. Glumac, *CryoLett*. **12** (1991) 177–182.
6. A. Jovanović-Galović, D. Blagojević, G. Grubor-Lajšić, M. R. Worland, M. B. Spasić, *Arch Insect Biochem Pysiol*. **64** (2007) 111-119.
7. D. Kojić, I. Spasojević, M. Mojović, D. Blagojević, M. R. Worland, G. Grubor-Lajšić, M. B. Spasić, *Eur J Entomol*. **106** (2009) 451-454.
8. L. E. Vukašinović, W. D. Pond, M. R. Worland, D. Kojić, J. Purać, P. D. Blagojević, G. Grubor-Lajšić, *Comp Biochem and Physiol*. **165** (2013) 219-225.
9. L. E. Vukašinović, W. D. Pond, M. R. Worland, D. Kojić, J. Purać, D. Ž. Popović, G. Grubor-Lajšić, *Comp Biochem and Physiol B – Biochem & Mol Biol*. **184** (2015) 36-43.
10. L. E. Vukašinović, W. D. Pond, G. Grubor-Lajšić, M. R. Worland, D. Kojić, J. Purać, D. Ž. Popović, P. D. Blagojević, *Journal of Comparative Physiology B* **188** (2018) 27-36.
11. D. L. Denlinger, *Ann Rev Entom*. **478** (2002) 93-122.
12. T. H. MacRae, *Cell Mol Life Sci*. **67** (2010) 2405-2424.
13. D. Ž. Popović, A. Subotić, V. T. Nikolić, R. Radojičić, P. D. Blagojević, G. Grubor-Lajšić, V. Koštál, *Comp Biochem and Physio*. **186** (2015) 1-7.
14. K. B. Storey, J. M. Storey, *Can J Zool*. **90** (2012) 456-470.
15. J. Purać, D. Kojić, D. Ž. Popović, E. Vukašinović, S. Tiziani, U. L. Gunter, G. Grubor-Lajšić, *Acta Chimica Slovenica*, **62** (2015) 761-767.
16. J. M. R. Russell, U. Gerike, J. M. Danson, W. D. Hough, L. G. Taylor, *Structure* **6** (1998) 351-361.
17. K. B. Storey, *Comp Biochem Physiol B*. **199** (2016) 13-20.
18. S. Friedman, Intermediary metabolism. In: Fundamentals of Insect Physiology (M. S. Blum, editor). J. Wiley & Sons (1985) 467-505.
19. P. A. Srere, *Methods Enzymol*. **13** (1969) 3-11.
20. R. J. Henry, N. Chiamoru, O. J. Golub, S. Berkman, *Amer J Clin Pathol*. **34** (1960) 381-398.
21. M. Guppy, P. Withers, *Biol Rev Camb Philos Soc*. **74** (1999) 1-40.
22. K. B. Storey, *Comp Biochem Physiol A*. **133** (2002) 733-754.
23. S. D. Beck, W. Hanec, *Journal of Insect Physiology*, **4** (1960) 304-318.
24. K. B. Storey, R. D. Joanisse, *Insect Biochem Molec Biol*. **24** (1994) 145-150.
25. M. R. Michaud, D. L. Denlinger, *J Comp Physiol B*. **177** (2007) 753-763.
26. G. Košanin, završni rad, Univerzitet u Novom Sadu, Prirodno-matematički fakultet, 2017.
27. K. B. Storey, *Insect Bioche*. **12** (1982) 501-505.
28. D. Kojić, doktorska disertacija, Univerzitet u Novom Sadu, Prirodno-matematički fakultet, 2009.
29. H. V. Danks, Insect Dormancy: An Ecological Perspective, Biological Survey of Canada Press, Ottawa (1987).

Hemija i tehnologija makromolekula

Chemistry and Technology
of Macromolecules

Chitosan-based films for application in food industry

Marija Lučić Škorić, Melina Kalagasidis Krušić*, Aleksandra Nešić**, Sanja Šešlija***, Gabriella Santagata****, Mario Malinconico****
Innovation Center of Faculty of Technology and Metallurgy, Belgrade, Serbia
**University of Belgrade, Faculty of Technology and Metallurgy, Belgrade, Serbia*
***University of Belgrade, Vinča Institute for Nuclear Sciences, Belgrade, Serbia*
****University of Belgrade, Institute of Chemistry, Technology and Metallurgy, Belgrade, Serbia*
*****Institute for Polymers, Composites and Biomaterials, National Research Council, Pozzuoli, Italy*

Introduction

Food packaging is an essential part of the food industry, since food safety and its quality directly depend on used material for packaging. If food is exposed to moisture, which is a good environment for the growth of bacteria and mold, and inadequate storage temperature, it can be easily spoiled; therefore, in order to maintain food quality for longer periods it is necessary to have adequate protection from external effects and factors[1]. Variety of different materials is currently used for food packaging, but polymers are usually the main choice because of the satisfactory characteristics and low-cost. Polyolefins, polyesters, polystyrene, polyamides are currently most widely used for food packaging and, despite all the advantages, these materials are not biodegradable and cause serious environmental problems when disposed[2].

Therefore, market demands are redirected to the use of biodegradable "green materials" that are derived from renewable sources, which reduces the negative impact on the environment. There are a large number of current researches on food packaging materials are focused on natural polymers, and most of all to polysaccharides[3]. Among them, chitosan proved to be a very interesting material for use in food packaging due to the ability to form films with good barrier properties against the transport of gases such as oxygen and carbon dioxide. Since chitosan-based films generally do not meet all the necessary food packaging requirements, they are often changed and/or combined with other polymers, plasticizers or reinforced with nanofillers[4].

In this study, chitosan-based films with the potential application for food packaging were prepared. The aim of the study was to investigate the effect of poly(vinyl alcohol) addition to chitosan film in terms of thermal, mechanical, morphological, and barrier properties. Although PVA is synthetic water-soluble polymer, it is often used for biomedical and pharmaceutical purposes, due to its biocompatibility, biodegradability, and non-toxicity. Also, the structural changes of prepared films were examined by FTIR.

Experimental part

Materials: low-viscous chitosan (Ch, Sigma-Aldrich, M_w~653 kg mol^{-1}); poly(vinyl alcohol) (PVA, Acros Organics, M_w~67000 kg mol^{-1}); itaconic acid (IA, Fluka); acidic acid (Zorka); glycerol (G, Zorka);

Film preparation: All films were prepared by solvent-casting method. Ch solution was prepared by dissolving Ch in IA (2 wt.%) with constant stirring for 24 h. PVA was dissolved in distilled water at 50 ℃. When both polymers were completely dissolved, PVA solution

was added to Ch and stirred until homogenized and casted in PTFE mold with diameter of 11 cm. The films were dried to constant weight at 37 °C. The dried films were carefully removed from the molds and stored until further use. Two series of film with and without glycerol were prepared (Tab. 1). Glycerol content in all films was 10 wt.% calculated to the total weight of polymers.

Table 1. Chitosan, poly(vinyl alcohol) and glycerol content in prepared films

Sample	Ch to PVA ratio	Glycerol
Ch/0PVA	1 : 0	/
Ch/0.5PVA	1 : 0.5	
Ch/1PVA	1 : 1	
Ch/1.5PVA	1 : 1.5	
Ch/2PVA	1 : 2	
Ch/0.5PVA/G	1 : 0.5	10 wt.%
Ch/1PVA/G	1 : 1	
Ch/1.5PVA/G	1 : 1.5	
Ch/2PVA/G	1 : 2	

Films characterization: The Fourier-transform infrared (ATR-FTIR) spectra were analyzed using the Perkin Elmer Spektrum 100 spectrometer equipped with diamond crystal Perkin Elmer Universal ATR. The spectra were collected at 25 ℃ in the range of 4000 cm^{-1} – 400 cm^{-1} with the resolution of 4 cm^{-1}.

Mechanical properties were performed using Instron dynamometer model 1185, equipped with a 1 kN load cell, according to the ASTM D638 (2010) standard test method. Dumbbell-shaped films (4 mm wide, 26.73 mm long and 0.05 mm thick) were used and tested at a crosshead speed of 2 mm min^{-1}. Prior to measurements, all the films were conditioned at 25 °C and 50% RH for 48 h.

Thermogravimetric analysis (TGA) was performed by means of a Mettler-Toledo TG-SDTA 851, under nominal nitrogen flow of 30 mL min^{-1}, in the temperature range from 25 to 600 °C and at the heating rate of 20 °C min^{-1}. The measurements were performed on 5 mg of samples, placed in ceramic crucibles and for each sample, thermogravimetric tests were performed in triplicate.

Water vapor permeability (WVP) tests were conducted according to ASTM E96 standard method. The samples with exposed area of 6.54 cm^2 were sealed over a circular opening of permeation cells filled with distilled water. These cells were kept in oven at 25 °C under 50 % RH. After the system reached steady state conditions, the weight change of the cell was measured every 2 h. All measurements were performed in triplicate. The standard deviation was ±10 %. For calculation of water vapor permeability, Equation (1) was used:

$$WVP = L\ WVTR/(A \cdot \Delta p) \quad (1)$$

where WVTR is the water vapor transmission rate of films (g s^{-1}), L is average thickness of the film (mm), A is the permeation area (mm^2), Δp is the difference in water vapor pressure between the two exposed sides of the film (Pa)[5].

Results and discussion

Appearance of the prepared films:

The average thickness of the films prepared by solvent/casting method is given in Tab. 2. It can be seen that thickness depended on the content of polymers in the films, but not on the presence of glycerol.

Table 2. *Average thickness of prepared films*

Film	Thickness, μm	
	With G	Without G
Ch/0PVA/G	50.0±1.0	
Ch/0.5PVA/G	75.0±1.0	72.0±1.0
Ch/1PVA/G	69.0±1.0	76.2±1.0
Ch/2PVA/G	88.0±1.0	81.6±1.0

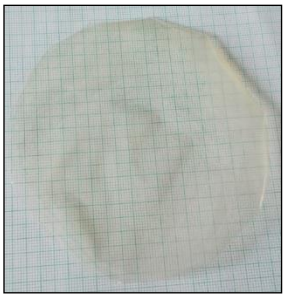

Figure 1. *Appearance of Ch/1PVA/G film*

Prepared films were transparent and colorless, which is desired and favorable for the suggested application (Fig. 1). It has been observed that the films with PVA and plasticizer glycerol are more soft and elastic than pure chitosan film. For that reason, further experiments were performed with samples that contained glycerol.

ATR-FTIR analysis

Fig. 2 and Tab. 3 show the ATR-FTIR spectra of the film Ch/1PVA/G. Characteristic peaks for both Ch and PVA appear in the spectra of the prepared films, indicating that both components are successfully incorporated in the films[6].

Table 3. *Peaks in ATR-FTIR spectra of Ch/1PVA/G*

Peak position, cm^{-1}	**Origin**
3700-3000	Stretching vibration of O-H and/or N-H in Ch and PVA
Around 2920	Vibration of CH_2 group
1630	Complexation between Ch and IA
1423 and 1376	Symmetric deformation of CH_2 and CH_3
1071 and 1025	C-O stretch vibration in Ch
1155 and 896	Asymmetric stretching of the C-O-C bridge

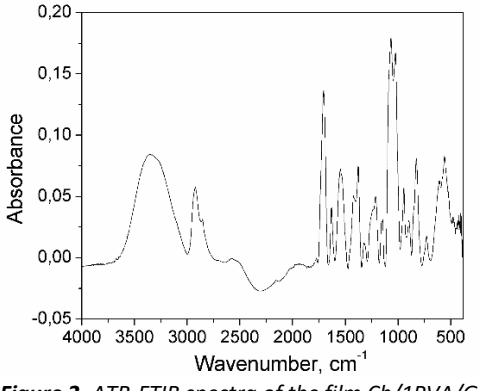

Figure 2. *ATR-FTIR spectra of the film Ch/1PVA/G*

Mechanical analysis

Mechanical parameters such as tensile strength (TS) and elongation at break are reliable indicators for the cracks formation in polymeric films used for packaging (Table 4).

Table 4. *Tensile strength (TS) and elongation at break for the Ch/PVA films with and without glycerol*

Film	TS, MPa		Elongation at break, %	
	With G	Without G	With G	Without G
Ch/0PVA	-	132.2	-	4.68
Ch/0.5PVA	9.15	86.2	55.7	12.8
Ch/1PVA	5.09	70.0	87.6	13.5
Ch/2PVA	4.51	56.2	91.9	23.1

The highest TS value, 132.2 MPa, was obtained for a neat chitosan film, while the addition of PVA and glycerol reduced TS. With an increase in the PVA content from 0.5 to 2 wt.%, TS decreased from 86.2 to 56.2 MPa indicating that PVA reduces film's strength. Also, the addition of glycerol significantly reduced TS value (~ 80%) in all films. On the other hand, with an increase of PVA in films the percentage of elongation increased together with the flexibility particularly in the case of films where glycerol was added.

Thermal analysis

Thermal stability of pure polymers, chitosan and PVA, as well as Ch and PVA films, was tested via thermogravimetric analysis. Fig. 3 shows the TGA and DTG curves of the neat chitosan and poly(vinyl alcohol) powder and Ch/1PVA/G film.

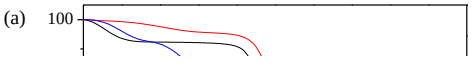

Figure 3. *The TGA (a) and DTG (b) curves of neat chitosan, poly(vinyl alcohol) powder and Ch/1PVA/G film*

Thermal degradation of chitosan occurs in two steps (Fig. 3). The first step starts at 30 °C and ends at 80 °C with a loss of mass of 7 wt.% due to water loss. The second phase begins at 220 °C and reaches a maximum at 300 °C with a weight loss of 55 wt.%. The observed behavior is the result of degradation (thermal and oxidative) of chitosan, evaporation and elimination of volatile products.

It can be seen that PVA degradation takes place in two stages. There is no significant loss in mass until 250 °C when degradation starts. Degradation ends at 500 °C, with a maximum at 335 °C (with a weight loss of 60% and 430 °C).

On the other hand, the degradation process of the Ch/1PVA/G film exhibited three degradation stages: a) elimination of free water (to 200 °C); b) evaporation of bound water

(from 200 to 320 °C) and c) degradation of Ch/PVA films above 320 °C. Temperatures at which a weight loss of 5 wt.% and 50 wt. % of Ch/1PVA/G film occurs are 90 °C and 346 °C, and temperature with the highest degradation rate (T_{maxDTG}) is 339 °C. Since significant changes in film occur after 100 °C due to the influence of elevated temperatures, Ch/PVA could be used for food packaging.

Water vapor permeability

In order to reduce or prevent the transfer of moisture between the food and the surrounding environment, the permeability of the packaging materials to the water vapor should be minimized.

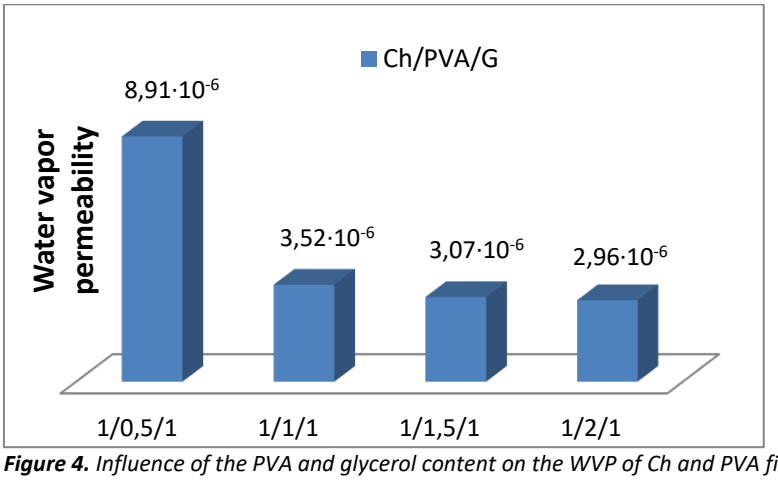

Figure 4. *Influence of the PVA and glycerol content on the WVP of Ch and PVA films*

Fig. 4 shows influence of the PVA and glycerol content on the WVP of Ch and PVA films. It can be observed that the WVP decreased with the increase of PVA content in the chitosan films, which could be explained with the formation of hydrogen bonds between-OH groups of PVA and -OH or $-NH_2$ groups in chitosan. The obtained values of WVP were higher by several orders of magnitude than those reported for the films made from PS, LDPE, HDPE, and PP as shown in Table 5[7]. Ch/PVA films have relatively high WVP, but it is still acceptable for the food packaging application. Still, focus in further research should be pointed towards reduction of WVP by crosslinking of Ch and PVA in films.

Table 5. *The WVP parameters of the Ch/PVA films and some of the food packaging materials*

Film	WVP, g·(mm^2 h Pa)$^{-1}$	Reference
Ch/0PVA/G	$8.91 \cdot 10^{-6}$	This work
Ch/0.5PVA/G	$3.52 \cdot 10^{-6}$	
Ch/1PVA/G	$3.07 \cdot 10^{-6}$	
Ch/2PVA/G	$2.96 \cdot 10^{-6}$	
LDPE	$2.40–3.13 \cdot 10^{-10}$	[7]
HDPE	$0.63–1.25 \cdot 10^{-10}$	
PP	$0.83–1.67 \cdot 10^{-10}$	
PS	$4.07–16.3 \cdot 10^{-11}$	

Conclusion

Films based on chitosan and poly(vinyl alcohol) were successfully prepared by solvent-casting method. Mechanical analysis showed that films had acceptable values of tensile strength, while elongation at break increased with addition of plasticizer. Thermal analysis revealed that all films were stable until 100 °C giving them potential to be used food packaging. Furthermore, water vapor permeability was tested and its values were still acceptable for the proposed application. However, properties of the prepared films have been found to be satisfactory for the use as an edible food packaging materials, but additional efforts, such as crosslinking, have to be made in order to satisfy all requirements demanded for food packaging materials.

Primena filmova na bazi hitozana u prehrambenoj industriji

Prekomerna upotreba sintetskih polimera za pakovanje hrane je dovela do ozbiljnog ekološkog problema, jer takva pakovanja nisu biorazgradiva. Samim tim, dnevno se stvaraju velike količine otpada koji ugrožava životnu sredinu. Upravo iz tog razloga, pažnja naučnika je usmerena na razvoj biorazgradivih filmova na bazi polisaharida.

U ovom radu pripremljeni su filmovi hitozana (Ch) i poli(vinil alkohola) (PVA) metodom izlivanja iz rastvora i otparavanjem rastvarača. Iako je PVA sintetski polimer, on je biokompatibilan, biodegradabilan i netoksičan, a njegova primena dovodi do poboljšanja svojstava Ch filmova. Utvrđeno je da se sa povećanjem sadržaja PVA smanjuje zatezna čvrstoća filmova i povećava izduženje pri kidanju, dok sadržaj PVA nema značajan uticaj na termička svojstva. Takođe, Ch/PVA filmovi imaju relativno visoku propustljivost vodene pare. Navedena svojstva ukazuju da se ovi filmovi mogu koristiti kao jestivi, ali da je neophodna dalja modifikacija kako bi se zadovoljili svi kriterijumi za pakovanje hrane.

References:

1. C.E. Realini, B. Marcos, Active and intelligent packaging systems for a modern society, *Meat Science*, **98** (2014) 404-419
2. S. Lambert, C. Sinclair, A. Boxall, Occurrence, Degradation, and Effect of Polymer-Based Materials in the Environment, in: D.M. Whitacre (Ed.) Reviews of Environmental Contamination and Toxicology, 227, Springer International Publishing, Cham, 2014, pp. 1-53
3. C.G. Otoni, P.J.P. Espitia, R.J. Avena-Bustillos, T.H. McHugh, Trends in antimicrobial food packaging systems: Emitting sachets and absorbent pads, *Food Res Int*, **83** (2016) 60-73
4. B.W.S. Souza, M.A. Cerqueira, J.T. Martins, A. Casariego, J.A. Teixeira, A.A. Vicente, *Food Hydrocolloid*, **24** (2010) 330-335
5. A. Gennadios, M.A. Hanna, L.B. Kurth, , *LWT - Food Sci Techn*, **30** (1997) 337-350
6. Y. Boonsongrit, B.W. Mueller, A. Mitrevej, *Eur J Pharm Biopharm*, **69** (2008) 388-395
7. S.-Y. Sung, L.T. Sin, T.-T. Tee, S.-T. Bee, A.R. Rahmat, W.A.W.A. Rahman, A.-C. Tan, M. Vikhraman, *Trends Food Sci Techn*, **33** (2013) 110-123

Glucose-sensitive chitosan/PVA microbeads with the potential application for the controlled release of insulin

Marija Lučić Škorić, Nikola Pavlović*, Antonije Mitrović*, Melina Kalagasidis Krušić*
Innovation Center of Faculty of Technology and Metallurgy, Belgrade, Serbia
**University of Belgrade, Faculty of Technology and Metallurgy, Belgrade, Serbia*

Introduction

Diabetes mellitus is a metabolic disorder where glucose regulation fails as a result of (1) insufficient production and secretion of insulin from the body due to an autoimmune destruction of pancreatic β-cells (type 1 diabetes) or (2) a combination of impaired insulin resistance and insulin secretion (type 2 diabetes)[1]. Diabetes is a global burden affecting over 400 million people across the world, with most diabetics suffering from type 2 diabetes[2]. Multiple subcutaneous injections of insulin and regular monitoring of blood glucose levels are essential for patients. However, such self-administration is uncomfortable, painful and requires substantial patient compliance. For tight control of hyperglycemia and prevention of the resulting complications in diabetic patients, it is highly desirable to develop a simple, effective, and continuous self-regulated delivery systems[3].

Glucose-sensitive hydrogel is considered as an ideal system for site-specific controlled drug delivery, because it can adapt the rate of drug release in response to changes in glucose concentration in order to keep the blood glucose levels within the normal range[4]. For synthesis of such hydrogel, chitosan could be used in combination with poly(vinyl alcohol) (PVA), which is a water-soluble polymer broadly applied in pharmaceutical and biomedical fields due to its biocompatible, gelation and non-toxic properties [3].

The goal of this research was synthesis of glucose-sensitive hydrogel which would be used for controlled insulin delivery. Chitosan/PVA hydrogels crosslinked with boric acid and sodium-tripolyphosphate were synthesized in the form of spherical particles. The effects of chitosan content, temperature and time of crosslinking on hydrogel properties were studied. Swelling behavior of these hydrogels was investigated in the distilled water, phosphate buffer saline (PBS) and glucose solutions in PBS in order to determine their glucose-sensitivity. Also, preliminary insulin release tests were performed.

Experimental part

Materials: middle viscous chitosan (MVCh, Sigma A.G, 200-400 mPa·s), M_w~1537 kg mol^{-1}; low viscous chitosan (LVCh, Sigma A.G, <200 mPa·s), M_w~653 kg mol^{-1}; poly(vinyl alcohol) (PVA, Sigma A.G), M_w~67000 g mol^{-1}; D(+)-glucose (Kemika); boric acid (Analar); sodium-tripolyphosphate (TPP, Acros Organics); acidic acid (Zorka Pharma); sodium chloride (Zorka Pharma); sodium dihydrogen phosphate (Analytika), disodium hydrogen phosphate (Sigma A.G); sodium hydroxide (Lach:ner); distilled water.

Hydrogel synthesis: The hydrogels were synthesized in the form of spherical microbeads (Fig. 1) by dropping of polymer solution into a crosslinker solution. Before synthesis, the following polymers solutions were prepared: (a) LVCh solution (2, 3 and 5 wt.%) in 2 wt.% acetic acid solution; (b) 2wt.% MVCh solution in 2 wt.% acetic acid solution; (c) 10 wt.% PVA solution in distilled water at 50 °C. Polymer solutions were mixed and homogenized in an appropriate ratio (Tab. 1) after which they were added to the crosslinker solutions in a drop-wise manner using a pump (New Era Pump Systems Inc., Model: NE-1000). Two different

crosslinker solutions were used during the synthesis: (a) 1 wt.% boric acid and 1 wt.% TPP solution and (b) 5 wt.% boric acid solution.

Table 1. *Ch:PVA ration in the synthetized hydrogels*

Sample	Ch content, %	PVA content, %
LVCh2	66.7	33.3
LVCh3	75.0	25.0
LVCh5	83.3	16.7
MVCh2	66.7	33.3

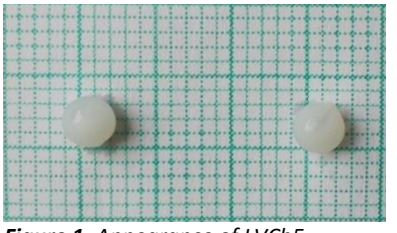

Figure 1. *Appearance of LVCh5 hydrogel microbeads*

After dropping of polymer was completed, the obtained hydrogels were kept in a crosslinker solution for 24 h at 25 ℃ and then washed with distilled water. The hydrogels were then subjected to freeze-thawing cycles three times for 24 h. When freeze-thawing cycles were finished, hydrogels were rinsed with 0.1 M NaOH solution to remove excess acetic acid and dried to a constant weight at 37 °C.

Swelling behavior of Ch/PVA hydrogels: Swelling studies were performed using dry samples, which were immersed in excess of four different swelling media: (1) distilled water; (2) PBS buffer; (3) glucose solution in PBS buffer, concentration 100 mg dL^{-1}; (4) glucose solution in PBS buffer, concentration 400 mg dL^{-1}. Swelling process was monitored gravimetrically until equilibrium was reached. Swelling degree (SD) was calculated according to following equation (1):

$$SD=((w_t-w_0)/w_0)\ 100 \quad (1)$$

where w_0 and w_t present the initial weight of the dry sample and weight of the swollen hydrogel at time *t*.

Insulin release tests: Release of insulin was monitored in preliminary test in glucose/PBS solution with concentration of 400 mg dL^{-1}. Prior to release, 0.2 g of LVCh5 sample was immersed in 3 mL of insulin solution (Mixtard® 30, 100 i.u./ml of insulin) after which they were rinsed with water. Release was measured in glucose solution at 37 °C, at indicated time intervals (5–180 min, 24 and 48 h) by UV/VIS spectrophotometer at λ_{max} 270 nm (UV-1800, Shimadzu).

Results and discussion

Ch/PVA hydrogel appearance

Samples obtained by dropping the Ch/PVA solution in 5 wt.% boric acid solution did not form the hydrogel with defined spherical shape. Firstly, irregular beads were observed, but after several hours complete dissolution of beads occurred. Hence, it was impossible to obtain hydrogels if boric acid is the only crosslinker used and it is necessary to introduce secondary crosslinking with TPP in ordered to achieve desired mechanical properties.

When crosslinking solution contained boric acid and TPP, hydrogels were successfully synthetized. All samples, except in the case of the LVCh3, were in the form of spherical microbeads (Fig. 1). The sample LVCh3 was irregular in shape and agglomeration of particles was noticed, so this sample was not used in the further experiments. Also, it was observed

that diameter of the samples decreased after each freeze-thawing cycle, while the diameter of completely dried microbeads was 2±0,2mm.

Swelling behavior of the Ch/PVA hydrogels

Swelling behavior of the Ch/PVA hydrogel microbeads was investigated in referent media and in the solutions that imitate normoglicemia and hyperglycaemic concentration of glucose (100 mg dL^{-1} and 400 mg dL^{-1} glucose in PBS buffer). The obtained results are presented in Fig. 2.

Figure 2. *Swelling behavior (a) LVCh2, (b) LVCh5 and (c) MVCh2*

In the first half an hour, the fastest swelling rate of sample LVCh2 is observed in both glucose/PBS solutions (100 and 400 mg dL^{-1}). In terms of proposed application, this could be favorable behavior because certain amount of insulin can be quickly released to lower blood sugar level (Fig. 2a). Also, this confirms that sample LVCh2 is glucose-sensitive. Concentration of glucose had significant influence on the swelling degree of LVCh2, but not in the way expected. It has been observed that these hydrogels have higher degree of swelling in a solution with lower concentration of glucose. This would lead to a higher insulin release when glucose concentration is normal than when it is elevated, causing lowering of blood sugar level from normal to hypoglycaemic and endangering the health of patients.

Similar behavior was observed for the sample MVCh2, which also exhibited glucose-sensitivity. However, this sample is also considered to be unfavorable for controlled release of insulin, since the sample reached a higher swelling degree in solutions with lower glucose concentration (Fig. 2c).
In the case of sample LVCh5, different results were achieved. Just like previous two samples, LVCh5 also swells faster in the solutions containing glucose compared to swelling in water and PBS. It is also noticed that equilibrium swelling degree of this sample is higher compared to LVCh2 and MVCh2. However, the most significant difference was observed through the influence of glucose concentration on the degree of swelling. While LVCh2 and MVCh2 hydrogels have a higher degree of swelling in solutions with normoglycemic concentration of glucose, it was found that swelling degree of sample LVCh5 is higher in solutions with hyperglycaemic glucose concentrations. The obtained results indicate that LVCh5 hydrogel could be potentially used to treat diabetes because its swelling rate is proportional to glucose concentrations, and greater amounts of insulin will be released at high blood sugar levels.

Release of insulin from LVCh5
Preliminary insulin release tests were performed from the sample LVCh5 which exhibited the most suitable behavior during swelling experiments. Insulin was incorporated in hydrogel by swelling from the solution containing 100 i.u./ml. Release was investigated in the solution with the hyperglycaemic glucose concentrations (400 mg/dL^{-1}) and UV/VIS spectra of insulin release in the time interval of 2 days are given in Fig. 3.

Figure 3. *Release of insulin from LVCh5*

Characteristic peak for the insulin was observed at wavelength of 270 nm which is in good correlation with data in literature [5]. It was found that absorbance increased with time through 24 h indicating continuous release of insulin. The highest absorbance value was achieved after 48 h (Fig. 3). These results indicate that insulin could be release from LVCh5 hydrogel, but further experiments have to be performed in order to determine its concentration.

Conclusion

Glucose-sensitive chitosan and poly(vinyl alcohol) (PVA) hydrogels were successfully synthetized in the form of spherical microbeads. It was found that use of TPP is necessary in order to obtain microbeads. Shape of the microbeads is dependent on the polymer ratio in reaction mixture.

In order to investigate potential application of synthetized hydrogels for release of insulin, their swelling behavior was evaluated in distilled water, PBS buffer and 100 and 400 mg dL^{-1} glucose/PBS solution (normoglycemic and hyperglycaemic glucose concentration). It was found that all prepared samples were glucose-sensitive. However, influence of glucose concentration of the hydrogels swelling is important. Two samples exhibited higher swelling degree in solution with lower glucose concentration and one sample had favorable higher swelling degree in solution with higher glucose concentration. That sample was further selected for the preliminary insulin release test. In the UV/VIS spectra, absorbance at maximal wavelength corresponding to insulin increased as the release continued. These results are indicating that Ch/PVA hydrogel has potential to be used for controlled release of insulin and the treatment of *Diabetes mellitus*.

Mikrogelovi hitozana i PVA osetljivi na glukozu sa potencijalnom primenom za kontrolisano otpuštanje insulina

Predmet ovog rada je sinteza hidrogelova osetljivih na glukozu koji mogu da kontrolisano otpuste glukozu i na taj način imitiraju funkciju pankreasa u kontroli nivoa glukoze. Hidrogelovi hitozana (Ch) i poli(vinil alkohola) (PVA) su sintetisani u obliku sfernih čestica umreženih bornom kiselinom i natrijum-tripolifosfatom. Ispitano je bubrenje dobijenih hidrogelova u destilovanoj vodi, fosfatnom puferu (PBS) i rastvoru glukoze u PBS-u, pri čemu je koncentracija glukoze varirana od normoglikemijske (100 mg dl^{-1}), do izrazito hiperglikemijskih koncentracija (400 mg dl^{-1}).

Utvrđeno je da su Ch/PVA hidrogelovi osetljivi na glukozu, ali pojedini su nepovoljni za kontrolisano otpuštanje insulina jer dostižu veći stepen bubrenja u rastvorima glukoze niže koncentracije. Kao najbolji za upotrebu u kontrolisanom otpuštanju insulina pokazao se uzorak sa odnosom Ch:PVA=5:1 zahvajujući većem stepenu bubrenja sa porastom koncentracije glukoze, pa je on korišćen za preliminarno ispitivanje otpuštanja insulina. UV/VIS spektrofotometrijom je utvrđeno da se insulin otpušta tokom 48 h, što ukazuje da se ovi hidrogelovi potencijalno mogu koristiti za lečenje Diabetes mellitus *i da je neophodno sprovesti dalja istraživanja u toj oblasti.*

Reference:

1. [1] Z. Gu, T.T. Dang, M. Ma, B.C. Tang, H. Cheng, S. Jiang, Y. Dong, Y. Zhang, D.G. Anderson, *ACS Nano*, **7** (2013) 6758-6766.
2. [2] Y. Xiao, T. Gong, Y. Jiang, Y. Wang, Z.T. Wen, S. Zhou, C. Bao, X. Xu, *Polymer*, **82** (2016) 1-10.
3. [3] M.A. Abureesh, A.A. Oladipo, M. Gazi, *Int J Biolog Macromol*, **90** (2016) 75-80.
4. [4] X. Zou, X. Zhao, L. Ye, *Chem Eng J*, **273** (2015) 92-100.
5. [5] M. Correia, M.T. Neves-Petersen, P.B. Jeppesen, S. Gregersen, S.B. Petersen, *PLoS ONE*, **7** (2012), https://doi.org/10.1371/journal.pone.0050733.